A HYPOTHESIS-GENERATING CHEMICAL PROTEOMICS APPROACH REVEALS

PHOSPHOTYROSINE PATHWAYS IN THE AFRICAN TRYPANOSOME

by

RANJAN KUMAR BEHERA

(Under the Direction of Kojo Mensa-Wilmot)

ABSTRACT

New drugs are needed for human African trypanosomiasis (HAT) caused by subspecies of *Trypanosoma brucei* as drug resistance and toxic side effects plague current therapies. The phosphotyrosine signaling in trypanosome could be a drug target because it is unique and divergent from the mammalian system. The 4-anilinoquinazoline class of tyrosine kinase inhibitors have been successfully developed as anticancer drugs. From a focused screen of 4-anilinoquinazolines, we discovered GW572016 that kills *T. brucei* at low micromolar concentrations. We developed a chemical biology approach with GW572016 to gain insight into the phosphotyrosine signaling pathways in the African trypanosome. We also performed a structure-activity relationship study to optimize 4-aninlinoquinazoline scaffold for antitrypanosmal lead drug discovery. Finally, efficacy of select tyrosine kinase inhibitors was tested in a mouse model of acute HAT.

GW572016 as a tool inhibits tyrosine phosphorylation of trypanosome proteins. Subsequently, thirty-nine proteins were identified as a part of the GW572016-susceptible phosphotyrosine-signaling pathway. Predicted functions of these proteins include (i) endocytosis (*e.g.* actin A), (ii) cytoskeleton and cell morphogenesis (*e.g.* beta-tubulin), and (iii) flagellum

biogenesis (*e.g.* PFR-1/PFR-C). We studied the effects of GW572016 on these three pathways. GW572016 inhibited transferrin endocytosis. Further, the drug causes loss of trypanosome polarity evident from (i) changes in the intracellular localization of beta-tubulin, (ii) redistribution of tyrosylated alpha-tubulin, and (iii) retraction of the flagellum into the cell body. From the 4-anilinoquinazoline scaffold optimization study, we discovered many compounds better (GI_{50}) than GW572016. The *in vivo* study with tyrosine kinase inhibitors revealed that these compounds could control parasitemia, and they improved mean survival of the treated group. Also, GW572016 could cure the infection in 25% of mice. We propose that 4-anilinoquinazoline is a lead chemical scaffold for antitrypanosome drug discovery.

INDEX WORDS: *Trypanosoma brucei (T. brucei)*, Human African trypanosomiasis (HAT), Phosphotyrosine signaling, 4-anilinoquinazolines, GW572016 (lapatinib).

A HYPOTHESIS-GENERATING CHEMICAL PROTEOMICS APPROACH REVEALS

PHOSPHOTYROSINE PATHWAYS IN THE AFRICAN TRYPANOSOME

by

RANJAN KUMAR BEHERA

B.V.Sc. & A.H., Orissa University of Agriculture and Technology, India, 2004

M.S., The University of Georgia, Athens, GA, 2009

A Dissertation Submitted to the Graduate Faculty of The University of Georgia in Partial

Fulfillment of the Requirements for the Degree

DOCTOR OF PHILOSOPHY

ATHENS, GEORGIA

2013

A HYPOTHESIS-GENERATING CHEMICAL PROTEOMICS APPROACH REVEALS

PHOSPHOTYROSINE PATHWAYS IN THE AFRICAN TRYPANOSOME

By

RANJAN KUMAR BEHERA

Major Professor:	Kojo Mensa-Wilmot	
Committee:	Stephen L. Hajduk	
	Cordula Schulz	
	Eileen J. Kennedy	

DEDICATION

I dedicate this dissertation to…

My Lord

Paramapremamaya Sri Sri Thakur Anukulchandra and

Acharyadev Paramapujyapada Sri Sri Dada

For the blessings to know you and love you

My Parents

Lakshyapati Behera and Tapaswini Behera

For the blessings to know life and love you

My Mentor

Kojo Mensa-Wilmot

For the blessings to know science and love you

ACKNOWLEDGEMENTS

support, and help during the initial years. The inspiration from Dr. Fechheimer has been a motivation to successfully complete the interdisciplinary teaching certificate. I sincerely thank Drs. DeLoris Wenzel Hesse and William Said for their tremendous support of my teaching and educational research.

I also take the opportunity to thank the amazing Cellular Biology staff for their co-operation and help.

I am indebted to many friends and their families in and around Athens for making my life relaxing and eventful on various occasions. Thanks to Dr. Animesh Dhara for being with me as my best pal at UGA.

Finally, I would like to acknowledge my parents whose love, sacrifice, and support have made me the person I am today. Last but not least, I would like to thank my wife Rebati and my son Rohan for they have enriched my life with love, dedication, and service. It is because of them that I feel strong, and every event of my life special and meaningful.

.

TABLE OF CONTENTS

LIST OF TABLES

LIST OF FIGURES

CHAPTER I

INTRODUCTION AND LITERATURE REVIEW

1.1 Human African Trypanosomiasis-A Deadly But Neglected Parasitic Disease

1.1.1 Overview

Trypanosoma brucei causes human African trypanosomiasis (sleeping sickness), a "neglected tropical disease" **[1, 2]**. Transmission of HAT occurs primarily through biting of trypanosome-infected tsetse fly (*Glossina spp.*). Depending on the sub-species of *T. brucei* involved HAT could be acute*, Trypanosoma brucei rhodesiense,* or chronic, *Trypanosoma brucei gambiense* **[3, 4]**. The disease in general manifests with an early (hemolymphatic) stage, which in untreated cases proceeds to the late (encephalitic) stage when the parasites cross the blood-brain barrier and affect the central nervous system **[5]**. Death could be the ultimate outcome without proper medication.

Approximately 60 million people in 36 sub-Saharan African countries are potentially at risk of acquiring the *T. brucei* infection, and nearly 10,000 people die from HAT every year **[6]**. Global burden of parasitic disease ranks HAT as the third most significant parasitic disease next to malaria and schistosomiasis **[7].** As reported, the incidence of new cases of sleeping sickness between 1980-2000 in the African subcontinent follows a strong re-emerging trend that can be attributed to the lack of control and surveillance measures in endemic countries **[5, 8].** The acute form of HAT is immuno-suppressive and predisposes the patients to a higher risk to HIV type 2 infections **[9]**.

1.1.2 Life cycle of *Trypanosoma brucei*

T. brucei completes its life cycle between human hosts and the insect vector **(Fig 1.1)**. The insect form parasites are called procyclic and that found in the human host are called bloodstream form. Further, *T. brucei* goes through three developmental stages in the insect: (1) the procyclic trypomastigote form, (2) the epimastigote form and (3) the metacyclic trypomastigote form. The metacyclic trypomastigote are the only infective form in human that in the bloodstream can develop into the actively dividing long slender (LS) forms and the non-replicating short stumpy forms (SS). The population density triggers the formation of SS from LS, a phenomenon described as quorum sensing **[10, 11]**. The LS form of *T. brucei* is responsible for pathogenesis in the vertebrate host. The bloodstream form parasites are covered by a variant surface glycoprotein (VSG) coat that helps them to evade the host immune system by a mechanism called "antigenic variation" **[12, 13]**.

1.1.3 Clinical Manifestation

HAT can be manifested in two forms depending on the sub-species of *T. brucei* involved **[14-16]**. The main difference between these two forms is how quickly the disease progresses from early to late stage.

(i) Acute form of HAT: The acute form of the disease, endemic to eastern and southern Africa, is caused by *T. b. rhodesiense*. It takes only a few weeks or months post infection for the symptoms to develop in this form of HAT, and the infection quickly progresses to late stage. Although, acute form is more virulent, it accounts for only 5% of the detected cases.

(ii) Chronic form of HAT: *Trypanosoma brucei gambiense* is responsible for the chronic form that is prevalent in west and central Africa. In this form of infection the patient

might remain asymptomatic for several months or years. By the time, the symptoms are detected in chronic form the disease is already in an advanced stage, and the central nervous system is also affected. The chronic form of infection constitutes as many as 95% of reported cases.

Parasites are inoculated with salivary secretion into bloodstream of the host while the infected Tsetse fly takes a blood meal [125, 126]. At first the parasites proliferate in the circulation (blood and lymph) of the host; this stage of infection is called the early or hemolymphatic stage. Later, the parasites cross the blood-brain-barrier and invade the central nervous system leading to the second or late or encephalitic stage infection [4, 7, 127-129]. The clinical manifestation of trypanosomiasis occurs as early as during the early stage which, in most cases, is not very severe. The patient might have episodic fever, headaches, joint pains, malaise, vomiting and pruritis [130, 131]. The characteristic features of first stage are lymphadenopathy and sometimes hepato-splenomegaly. But, the symptoms are more apparent during the late stage disease and along with severe headache and prolonged fever neurological symptoms like dementia, uncoordinated gait, sleep disorder and abnormal behavior might be observed [132, 133]. When not treated, the conditions of the patient worsen followed by coma and death [134].

1.2 Chemotherapy Of Human African Trypanosomiasis

1.2.1 Overview

Treatment of human African trypanosomiasis relies only on chemotherapy. Current therapy for HAT employs four main drugs (suramin, pentamidine, melarsoprol, and eflornithine), all of which are toxic and cannot be taken orally [17-21]. Administration of these drugs is cumbersome and requires hospitalization. All drugs produce adverse side effects and are not well tolerated (except pentamidine) by many patients. To summarize, the

current therapy fails to meet the safety standard to deal with the severity of sleeping sickness. There is a critical need for novel orally active drugs for treatment of HAT.

1.2.2 Current Chemotherapy

The choice of drug for treatment of HAT depends on the stage of the disease. It is easier to control the infection in early stage when the toxicity issue of chemotherapy is lower. However, for the late stage the drug should be able to cross the blood-brain barrier. Therefore, an optimum level of drug should be maintained in the circulation that makes the patient amenable to higher level of toxicity.

(i) Suramin: Suramin **(Fig-1.2.A)** is a colorless and water-soluble polysuphonated naphthalene derivative of urea **[22, 23]**. The clinical use of suramin started in early 1920s and found to be effective against early stage of *T. b. rhodesiense* infection. Because of its anionic charge suramin cannot enter into the CNS. Although suramin is in use for a long time no issue of drug resistance has been reported. The patient receives the drug by intravenous injection which might produce immediate or delayed side effects that can be fatal **[18]**. The long half life of suramin in circulation is because of tight binding to serum albumin and low-density lipoprotein (LDL). The mechanism of suramin action on trypanosomes is not known. It is expected that suramin might have multiple target in the cell.

(ii) Pentamidine: Pentamidine **(Fig. 1.2.B)**, an aromatic diamidine analog, was first introduced in 1941 **[21, 23]**. It is the choice of drug for early stage of *T. b. gambiense* infection. Pentamidine is preferably given by intramuscular injection to avoid hypertensive reaction by intravenous administration; it is less active by oral route as it gets protonated at physiological pH. It also has toxic effect that might damage vital organs like the pancreas, liver, and the kidney. Pentamidine binds to serum proteins and cannot diffuse into the CNS **[24]**. The half life

4

is short because the drug is metabolized by the mammalian P450 cytochrome system and excreted in urine [25-27]. Three transporters have been suggested for uptake of pentamidine by trypanosomes [28, 29]. The exact mode of action is not well understood. Pentamidine inhibits the mitochondrial topoisomerase II and disrupt the kDNA (mitochondrial DNA) structure leading to loss of kDNA in trypanosome (dyskinetoplastic) [30-32]. However, the loss of kDNA is not enough to explain the trypanocidal effect of the drug [33]. Therefore, other possible mechanism like inhibition of S-adenosylmethionine decarboxylase (AdoMetDC) [34] or plasma membrane Ca^{+2}-ATPase activity [35], or disruption of mitochondrial membrane potential [36] have been proposed.

(iii) Eflornithine: Eflornithine **(Fig-1.2.C)** was developed in early 1990, and it is in front line use for the late-stage HAT caused by *T. b. gambiense* [37, 38]. The drug has a complex intravenous dosing regimen such as 400 mg/kg/day, four times (2h each) daily for 7 days [18]. The reason for such a high dose to cure the infection could be that the drug is poorly transported across the blood-brain-barrier [39]. Eflornithine inhibits ornithine decarboxylase (ODC), which catalyzes the first committed step of the polyamine biosynthesis pathway [40, 41]. Recently, eflornithine has been used in combination therapy with nifurtimox, which is only effective for the acute stage infection [42].

(iv) Melarsoprol: Melarsoprol **(Fig-1.2.D),** a melaminophenyl arsenical, was introduced in 1949. It still remains the only drug for the treatment of late-stage HAT in both acute and chronic forms of infection. Melarsoprol is delivered intravenously with propylene glycol solvent that causes tissue irritation. The drug is toxic and induces a fatal reactive encephalopathy in 5-10% the patients [43, 44]. Other drug related side effects like convulsion, fever, rashes, nausea, and unconsciousness. P2-purine transporter in trypanosomes is responsible for uptake of

melarsoprol into the cell **[45]**. Once inside the cell, the drug caused rapid lysis of bloodstream trypanosomes, which has been attributed to depletion of trypanothione and inhibition of trypanothione reductase **[46-48]**.

1.2.3 Drug Discovery Challenges

Treatment and prevention of *T. brucei* infection has been very challenging for two reasons. First, it's hard to find out safe drug targets because both human and the parasite share many common metabolic pathways. Second, the parasite changes its glycoprotein surface coat (antigenic variation) frequently, which preclude the development of an effective vaccine. The discovery of a novel chemical entity for chemotherapy is a tedious process. It involves huge expenditure and takes a long time (more than 15 years) from the point of target validation to the ultimate clinical approval **[49-51]**. Studies indicate that the overall costs ranges from $500 million to $ 2 billion to make a new drug available in the market. The pharmaceutical companies lack interest in developing drugs for a less profitable disease like HAT **[52]**. Therefore, no new drugs have been developed for treatment of HAT in recent decades.

1.2.4 Recent Advances

Several research projects are now in progress for drug discovery against neglected parasitic diseases **[53]**. In an effort to optimize diamidine scaffold against HAT, the orally active DB289 was discovered for the early stage infection with support from Bill and Melinda Gates Foundation **[4, 54]**. However, subsequent clinical trials revealed hepatic and renal toxicity effects, and the project was discontinued **[54]**. Two other diamidine analogs, DB75 and DB820, have demonstrated good trypanocidal activity with ability to cross the blood-brain barrier and kill trypanosomes in brain **[55]**. Nitroheterocycles targeting reductase enzymes have been tested on trypanosomes with high trypanocidal activity *in vitro* and in animal models; fexinidazole a

member of the group is now in clinical trial **[56-59]**. SCYX-7158 has been identified as an orally active preclinical drug for the late stage **[59, 60]**.

Several groups have screened potential inhibitors by purifying recombinant target proteins expressed in heterologous systems. Some of these protein targets include glycogen synthase kinase 3 **[61]**, hexokinase **[62]**, trypanothione synthetase and reductase **[63-65]**, 6-phosphogluconate dehydrogenase **[66]**. DDD85646 targets N-myristoyl transferase in *T. brucei* **[67, 68]**. In parallel, computer-assisted drug design (CADD) approach is being used to study the structure-activity-relationship, physiochemical parameters, and anti-trypanosomal properties of different classes of inhibitors **[69, 70]**.

1.3. Protein Kinase Signaling

1.3.1 Overview

Protein kinases (PKs) catalyze phosphorylation of proteins. PKs can be classified into three major groups based on the amino acids they can phosphorylate, and include protein tyrosine kinases (PTKs), serine/threonine protein kinases and dual specificity kinases. PTKs phosphorylate tyrosine residues (*e.g.* EGFR and SRC) and the serine/threonine kinases phosphorylate the serine/threonine residues (*e.g.* MAP Kinase and Protein Kinase A). However, dual specificity kinases are capable of phosphorylating both tyrosine as well as serine/threonine residues (*e.g.* DYRK, CLK). All three types of protein kinases share significant structural similarities that are characterized by the presence of a N-terminal ATP-binding pocket and a catalytic core having a conserved aspartic acid residue **[71, 72]**.

1.3.2 Protein Tyrosine Kinases in eukaryotes

Protein tyrosine kinases participate in a wide variety of cellular processes such as cell

growth, differentiation, proliferation, signal transduction, morphogenesis in eukaryotes [73, 74]. There are approximately 2000 different types of kinases encoded by the human genome of which 90 are tyrosine kinases [75]. Based on the cellular localization these tyrosine kinases can be either (i) receptor tyrosine kinases (58 RTKs in human) or (ii) cytoplasmic or non-receptor tyrosine kinases (32 NRTKs in human) [76]. It is important to mention that RTKs are found only in vertebrates and choanoflagellates where as NRTKs are found in all eukaryotes [77, 78]. Based on the kinase regulatory domains and phosphorylation pattern these are many subgroups of PTKs under these two groups.

There are nearly 20 different families of RTKs identified like the epidermal growth factor receptor (EGFR) family, vascular endothelial growth factor receptor (VEGFR) family and insulin receptor family. Structurally, all RTKs have an extracellular N-terminal ligand-binding domain, a transmembrane domain and an intracellular C-terminal catalytic domain (Fig 1.3) [71, 72]. A representative ribbon diagram of the tyrosine kinase domain of the insulin receptor is presented (Fig-1.4) [79]. RTKs are generally monomeric receptors, but can form a multimeric complex as in the case of insulin receptor. Activation of tyrosine kinase activity in RTKs follows an event of extracellular ligand binding that leads to the receptor dimerization and subsequent autophosphorylation of the cytoplasmic domain. The phosphorylation of tyrosine residues in RTKs facilitates binding of adapter proteins containing Src homology 2 (SH2) or phosphotyrosine binding (PTB) domains [80-82]. These adapter proteins links the RTKs to downstream signaling pathways in the cell associated with cellular processes like growth, differentiation, and apoptosis [83].

Non-receptor tyrosine kinase class includes several families of kinase such as the ABL family, SRC family, and JAK family. NRTKs are found in the cytoplasm, but sometimes they

are attached to plasma membrane through N-terminal modification (myristoylation and palmitoylation) [72, 84]. The extracellular domain and the transmembrane domains are absent in NRTKs. However, NRTKs have a catalytic tyrosine kinase domain and another domain for interaction with other proteins, lipids, or DNA **[72]**. The SH2 and SH3 domains are the common protein-protein interaction domains in NRTKs.

The tyrosine kinases have a typical two lobed kinase domain **(Fig 1.4)**, which catalyzes the transfer of the terminal γ-phosphate from ATP to the hydroxyl group of a specific tyrosine residue in the target protein. There is a cleft in between the two lobes (N-terminal lobe and C-terminal lobe) of the kinase domain, which is the site for ATP-biding **[72, 85]**. The ATP-binding sites are significantly different in different tyrosine kinases. This feature allows specific binding of small molecule inhibitors to a particular type of PTK. The small molecule ATP-mimics compete with the cellular ATP for the binding site and can inhibit the kinase activity upon binding.

1.3.3 Tyrosine Kinase Signaling in Trypanosomes

The conventional protein tyrosine kinases are absent in the genome of *T. brucei* **[78]**. However, bioinformatics analysis suggests that many genome-encoded proteins in *T. brucei* have kinase domains similar to those of EGFR **[86]**. There are several lines of evidences, which support tyrosine kinase activity in *T. brucei*. Diacylglycerol-stimulated endocytosis of transferrin in *T. brucei* depends on tyrosine kinase activity, which is inhibited by Tyrphostin A47, a tyrosine kinase inhibitor **[87]**. Whole cell extracts of *T. brucei* can phosphorylate tyrosine residues utilizing a synthetic polypeptide substrate and inhibitor like genistein can reduce the phosphorylation level **[88, 89]**. Western blotting and mass-spectrometry analysis in the bloodstream form *T. brucei* have detected tyrosine phosphorylated proteins **[90-92]**. Tyrosine-

phosphorylated proteins have also been localized in the nucleolus in procyclic trypanosomes **[93]**. Interferon-γ, an activator of mammalian tyrosine kinases **[94, 95]**, enhances tyrosine phosphorylation of proteins in *T. brucei* **[96]**.

1.4 Tyrosine Kinase Inhibitors

1.4.1 Overview

Tyrosine kinases regulate essential cellular pathways that require tight regulation of their activation. Constitutive activation of tyrosine kinase activity has been implicated in development of different types of cancers **[97, 98]**. Therefore, an important aspect of drug discovery for cancer chemotherapy is through identification of small molecule tyrosine kinase inhibitors. These small molecules target the ATP binding site of specific tyrosine kinase and competitively inhibit the kinase activity **[99-102]**. Several classes of small molecule ATP mimics have been developed for oncology studies such as anilinoquinazolines, anilinoquinolines and pyrrolopyrimidine.

1.4.2 4-Anilinoquinazolines

The epidermal growth factor receptor (EGFR), a member of the RTK subfamily, is overexpressed in wide varieties of mammalian cancers **[103, 104]**. 4-anilinoquinazolines are an important group of tyrosine kinase inhibitors optimized against EGFR and developed into drugs (*e.g.* lapatinib, gefitinib, and erlotininb) **[105, 106]**. Structure-activity relationship study indicates that this class of inhibitors displays a high level of selectivity for the ATP binding site **[107, 108]**. Given that the intracellular ATP concentration is high and the ATP-binding site is conserved among kinases**[109]**, a strong selectively is crucial. Homology modeling suggests that the quinazoline ring binds into the adenine binding pocket is required for activity; the 4-anilino

head group fits into a deep hydrophobic pocket that provides selectivity **[110]**. Subsequently, the binding chemistry of 4-anilinoquinazoline with EGFR **[111]** as well as serine/threonine kinases (CKD2 and p38) **[112]** was resolved by X-ray crystallography.

GW572016 (lapatinib) is a 4-anilinoquinazoline derivative first approved by FDA for treatment of breast cancer along with capecitabine. It is a dual inhibitor of both epidermal growth factor receptor (EGFR) and human epidermal growth factor receptor 2 (HER2) **[113, 114]**. It inhibits the kinase by reversibly binding to the ATP biding site. Crystal structure of EGFR has been resolved with lapatinib and erlotinib at the inhibition sites **(Fig 1.5) [111])**.

GW572016 is an orally bioavailable drug given at a dose of 1250 mg daily **[115]**. In the body, the drug is metabolized mainly by cytochrome P450 3A4 isozyme with a half life of 24 hours **[116]**. Minor clinical toxicities like diarrhea, nausea, and rash have been reported. AG1478 is also a potent EGFR inhibitor, but because of poor solubility at physiological pH it could not succeed as a drug **[117, 118]**. Gefitinib (Iressa) and erlotinib (OSI-774) are analogs of AG1478 developed into drugs subsequently **[119, 120]**. Chemical structures of some 4-anilinoquinazolines have been shown **(Fig 1.6)**.

Figure 1.1: The life cycle of *T. brucei.* Adapted from **[121]**. In the salivary glands of the tsetse fly vector, the trypanosomes are blocked in the G0/G1 phase of their cell cycle. These forms, termed metacyclics, are competent for cellular differentiation into proliferative slender bloodstream forms soon after being injected in mammalian blood following insect bite. Both metacyclic and slender forms are completely covered by a coat of VSG, whose continuous antigenic variation allows the parasite to sustain long-lasting chronic infection. The LS forms progressively transform into cell-cycle-arrested SS forms, which are competent for differentiation into procyclic forms soon after being taken up back in the fly. Procyclic forms actively proliferate in the insect midgut. Their surface coat is characterized by the replacement of VSG by another major surface protein termed procyclin. After a complex journey in the fly, the trypanosomes eventually differentiate into infective metacyclic forms.

Figure 1.1

Metacyclic form (quiescent)

Procyclin

Salivary glands

Tsetse fly

Slender bloodstream form (proliferative)

Blood

VSG

Digestive tract

Mammal

Procyclic form (proliferative)

Stumpy bloodstream form (quiescent)

Current Opinion in Immunology
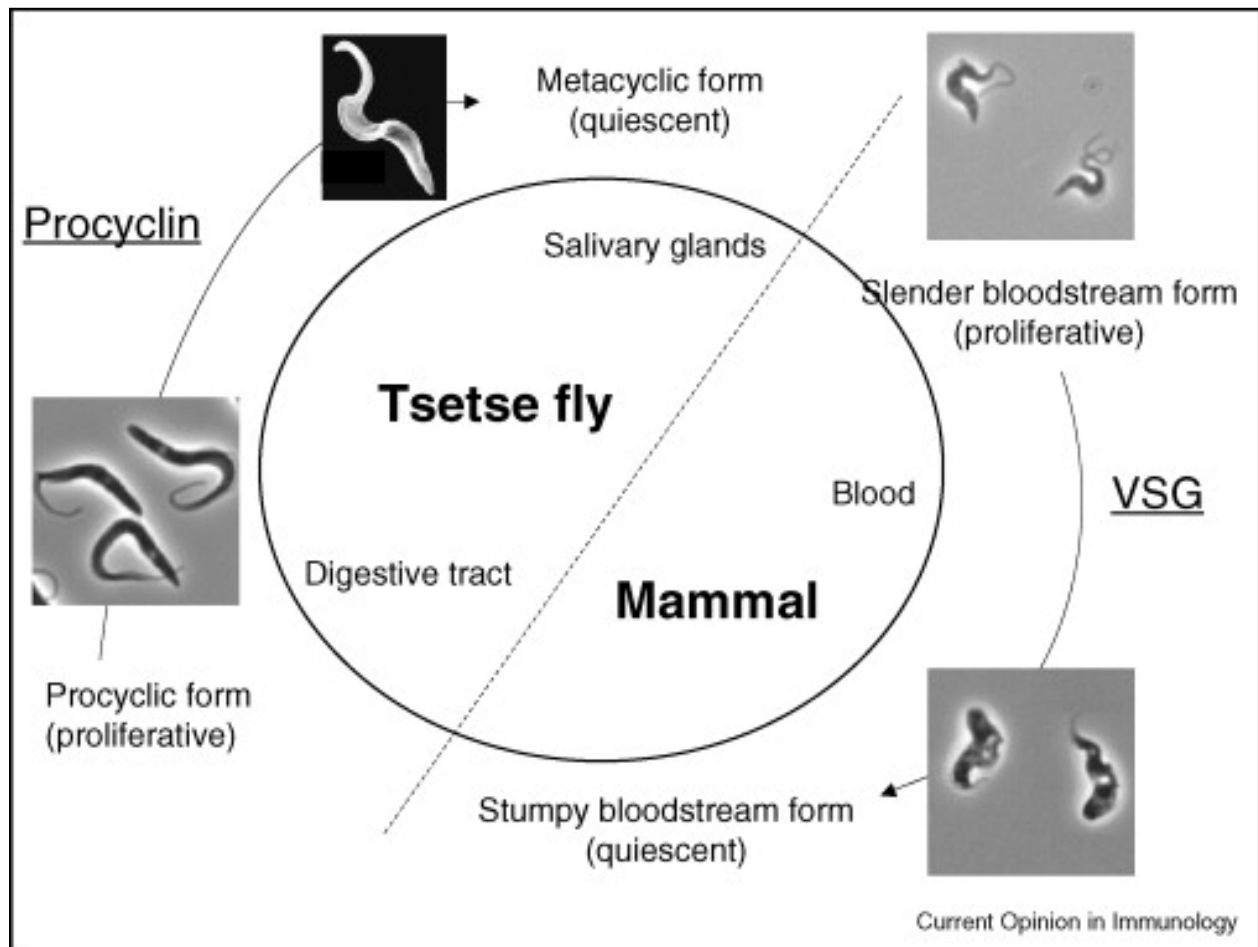
Figure 1.2: Drugs registered for human African trypanosomiasis. Adapted from **[122]**.
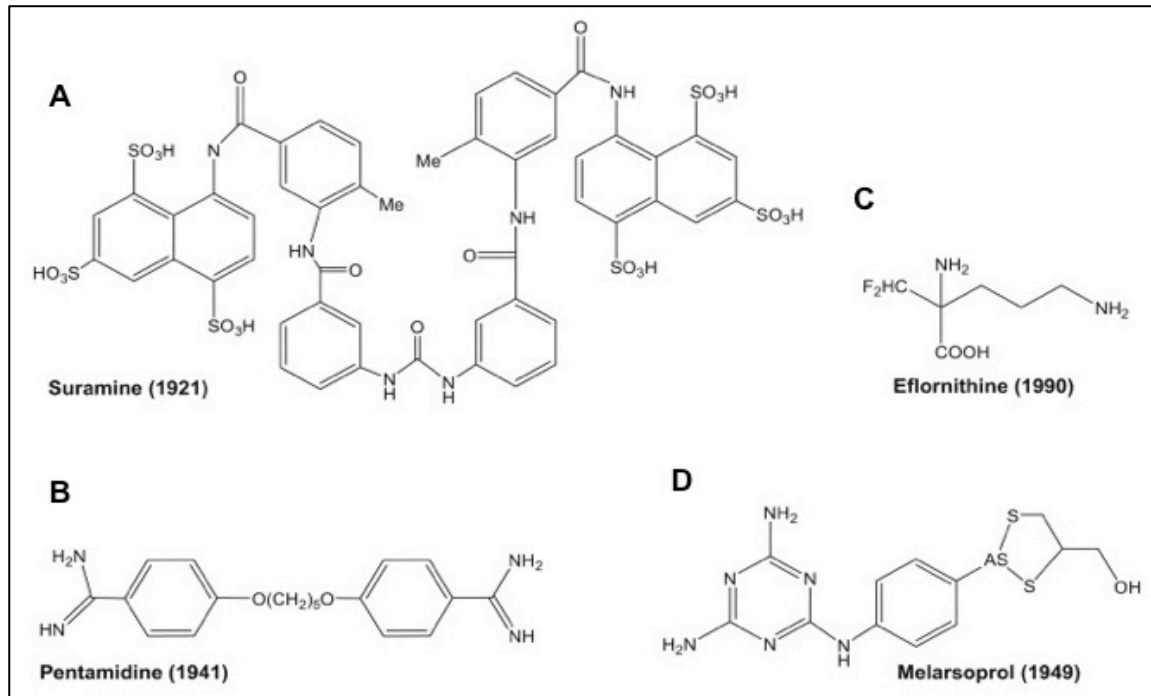
Figure 1.3: Epidermal grow factor (EGF) receptor signaling overview. Adapted from **[123]**. The EGFR family members share a common architecture: an extracellular ligand-binding region, a single transmembrane helix, an intracellular tyrosine kinase domain and a C-terminal tail. The well accepted mechanism for EGFR activation is that ligand-engagement induces dimerization of the receptor and activation of the intracellular kinase domain, which then phosphorylates several tyrosine residues in the C-terminal tail. These phospho-tyrosines in the C-terminal tail recruit downstream PTB- or SH2-containing signaling molecules, which relay the signal to downstream pathways.

Figure 1.3
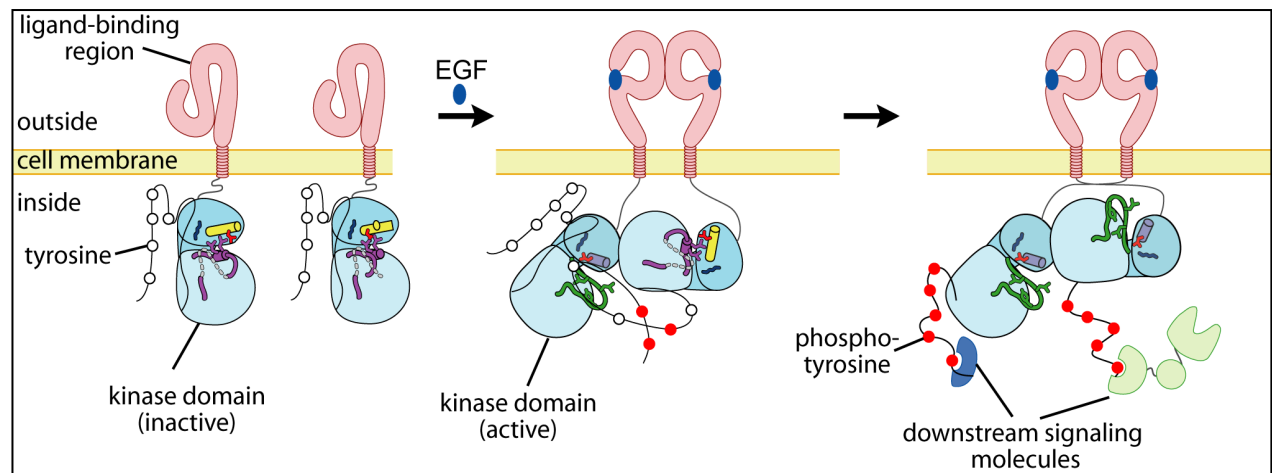
Figure 1.4: Ribbon diagram of the tyrosine kinase domain of the insulin receptor. Adapted from **[79]**. The alpha helices are shown in *red*, the beta-strands in *blue*, the nucleotide-binding loop in *yellow*, the catalytic loop in *orange*, the activation loop in *green*, and the tyrosine-containing peptide substrate in *pink*. The ATP analog (AMP-PNP) is shown in *black ball-and-stick* representation. The amino and carboxy termini are denoted by N and C.

Figure 1.4
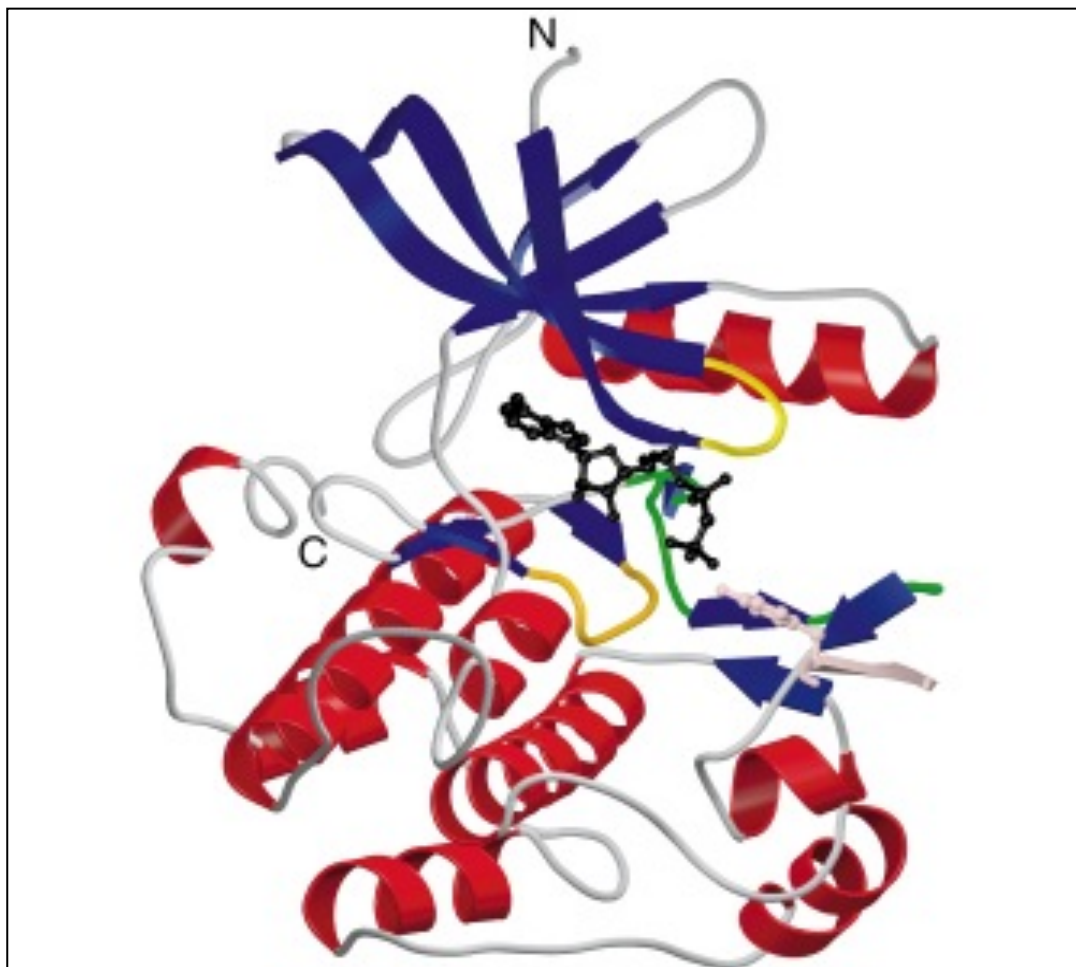
Figure 1.5: Crystal structures of epidermal growth factor receptor (EGFR) tyrosine kinase.
Adapted and modified from **[111]**. **(A)** Illustration of the active-state locations of the major structural regions of EGFR-TK. The position of an adenosine triphosphate (ATP) analog AMP-PNP in the catalytic cleft is shown and the locations of the catalytic glutamic acid (Glu) and lysine (Lys) residues are shown (PDB accession code of structure used: 1ITW). **(B and C)** Ribbon representation of the two crystallized conformations of EGFR-TK. **(B)** Crystal structure of EGFR-TK in complex with erlotinib (Protein Data Bank [PDB] accession code 1M17). **(C)** Crystal structure of EGFR-TK in complex with lapatinib (PDB accession code 1XKK). The kinase N- and C-lobes and C-helix are indicated, the activation loop is colored in gold and the glycine rich P-loop, blue. EGFR-TK inhibitors erlotinib and lapatinib are shown as space-filling spheres. Locations of activating leucine-747 to glutamic acid-749 LRE deletion and leucine-858 to arginine (L858R) point mutation are shown in stick format in red and are labeled. The conformation of the two crystal structures differs with the activation loop of the erlotinib-bound structure seen in an active-like conformation and the activation loop of the lapatinib-bound crystal structure trapped in an inactive conformation.

Figure 1.5
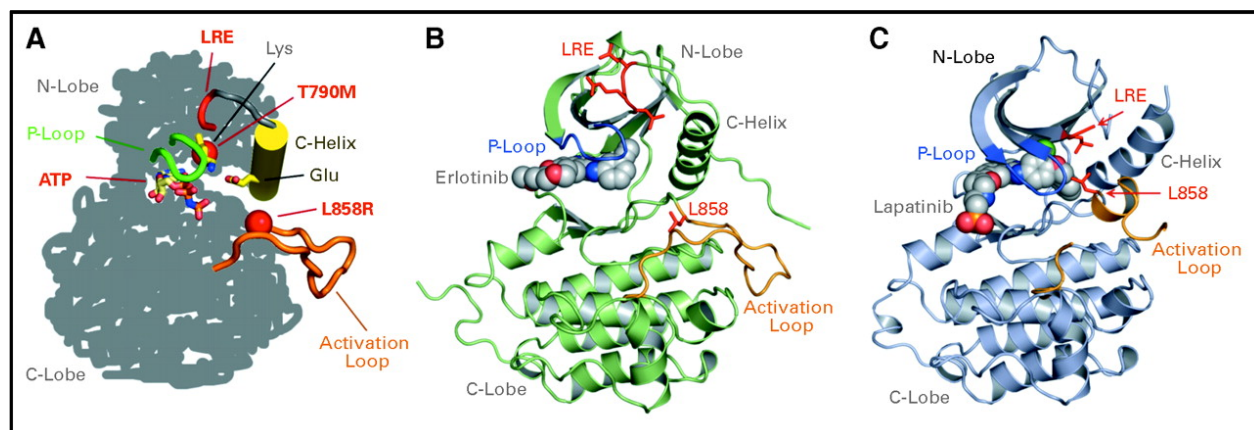
Figure 1.6: Structures of some tyrosine kinase inhibitors. Adapted from **[124]**. The 4-anilinoquinazoline backbone is highlighted in red.
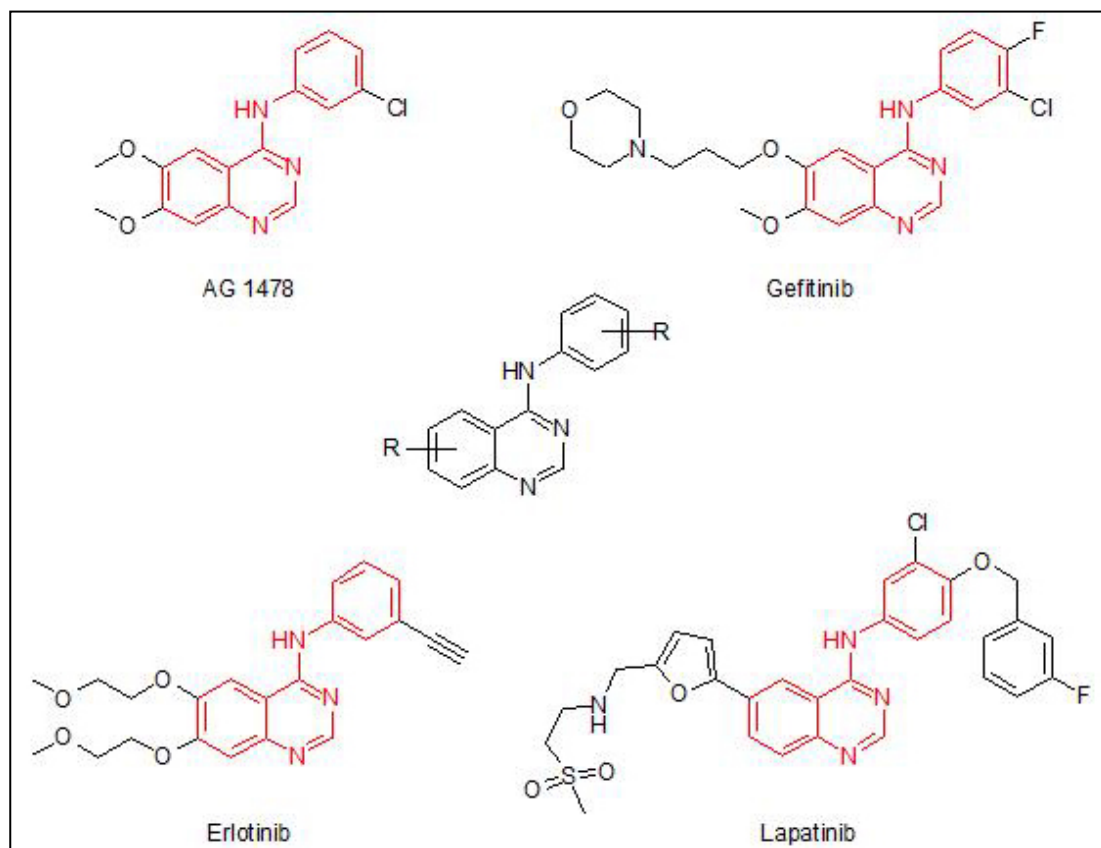
References

1.   O'Connell, D., *Neglected Diseases.* Nature, 2007. 449(7159): p. 157-157.

2.   Hotez, P.J., et al., *Control of neglected tropical diseases.* The New England journal of medicine, 2007. 357(10): p. 1018-27.

3.   Barrett, M.P., et al., *Human African trypanosomiasis: pharmacological re-engagement with a neglected disease.* British Journal of Pharmacology, 2007. 152(8): p. 1155-1171.

4.   Kennedy, P.G., *Human African trypanosomiasis of the CNS: current issues and challenges.* J Clin Invest, 2004. 113(4): p. 496-504.

5.   Simarro, P.P., J. Jannin, and P. Cattand, *Eliminating human African trypanosomiasis: where do we stand and what comes next?* PLoS Med, 2008. 5(2): p. e55.

6.   Simarro, P.P., et al., *The human African trypanosomiasis control and surveillance programme of the World Health Organization 2000-2009: the way forward.* PLoS Negl Trop Dis, 2011. 5(2): p. e1007.

7.   Kennedy, P.G., *The continuing problem of human African trypanosomiasis (sleeping sickness).* Ann Neurol, 2008. 64(2): p. 116-26.

8.   Courtin, F., et al., *Sleeping sickness in West Africa (1906-2006): changes in spatial repartition and lessons from the past.* Tropical medicine & international health : TM & IH, 2008. 13(3): p. 334-44.

9.   Matete, G.O. and O.A. Kajejo, *Human African trypanosomiasis and human immunodeficiency virus co-infection in Western Kenya.* East Afr Med J, 2005. 82(1): p. 20-3.

10.   Seed, J.R. and S.J. Black, *A proposed density-dependent model of long slender to short stumpy transformation in the African trypanosomes.* J Parasitol, 1997. 83(4): p. 656-62.

11.   Seed, J.R. and S.J. Black, *A revised arithmetic model of long slender to short stumpy transformation in the African trypanosomes.* J Parasitol, 1999. 85(5): p. 850-4.

12.   Stockdale, C., et al., *Antigenic variation in Trypanosoma brucei: joining the DOTs.* PLoS Biol, 2008. 6(7): p. e185.

13.   Morrison, L.J., L. Marcello, and R. McCulloch, *Antigenic variation in the African trypanosome: molecular mechanisms and phenotypic complexity.* Cell Microbiol, 2009. 11(12): p. 1724-34.

14.   MacLean, L., et al., *Severity of human african trypanosomiasis in East Africa is associated with geographic location, parasite genotype, and host inflammatory cytokine response profile.* Infect Immun, 2004. 72(12): p. 7040-4.

15. Blum, J.A., A.L. Neumayr, and C.F. Hatz, *Human African trypanosomiasis in endemic populations and travellers.* Eur J Clin Microbiol Infect Dis, 2012. 31(6): p. 905-13.

16. Barrett, M.P., et al., *The trypanosomiases.* Lancet, 2003. 362(9394): p. 1469-80.

17. Barrett, M.P., *The fall and rise of sleeping sickness.* Lancet, 1999. 353(9159): p. 1113-4.

18. Legros, D., et al., *Treatment of human African trypanosomiasis--present situation and needs for research and development.* Lancet Infect Dis, 2002. 2(7): p. 437-40.

19. Fairlamb, A.H., *Chemotherapy of human African trypanosomiasis: current and future prospects.* Trends Parasitol, 2003. 19(11): p. 488-94.

20. Burchmore, R.J., et al., *Chemotherapy of human African trypanosomiasis.* Curr Pharm Des, 2002. 8(4): p. 256-67.

21. Docampo, R. and S.N. Moreno, *Current chemotherapy of human African trypanosomiasis.* Parasitol Res, 2003. 90 Supp 1: p. S10-3.

22. Wilkinson, S.R. and J.M. Kelly, *Trypanocidal drugs: mechanisms, resistance and new targets.* Expert Rev Mol Med, 2009. 11: p. e31.

23. Nok, A.J., *Arsenicals (melarsoprol), pentamidine and suramin in the treatment of human African trypanosomiasis.* Parasitol Res, 2003. 90(1): p. 71-9.

24. Sanderson, L., et al., *Pentamidine movement across the murine blood-brain and blood-cerebrospinal fluid barriers: effect of trypanosome infection, combination therapy, P-glycoprotein, and multidrug resistance-associated protein.* J Pharmacol Exp Ther, 2009. 329(3): p. 967-77.

25. Conte, J.E., Jr., R.A. Upton, and E.T. Lin, *Pentamidine pharmacokinetics in patients with AIDS with impaired renal function.* J Infect Dis, 1987. 156(6): p. 885-90.

26. Berger, B.J., et al., *Primary and secondary metabolism of pentamidine by rats.* Antimicrob Agents Chemother, 1992. 36(9): p. 1825-31.

27. Berger, B.J. and A.H. Fairlamb, *Cytochrome P450 in trypanosomatids.* Biochem Pharmacol, 1993. 46(1): p. 149-57.

28. Carter, N.S., B.J. Berger, and A.H. Fairlamb, *Uptake of diamidine drugs by the P2 nucleoside transporter in melarsen-sensitive and -resistant Trypanosoma brucei brucei.* J Biol Chem, 1995. 270(47): p. 28153-7.

29. De Koning, H.P., *Uptake of pentamidine in Trypanosoma brucei brucei is mediated by three distinct transporters: implications for cross-resistance with arsenicals.* Mol Pharmacol, 2001. 59(3): p. 586-92.

30. Shapiro, T.A. and P.T. Englund, *Selective cleavage of kinetoplast DNA minicircles promoted by antitrypanosomal drugs.* Proc Natl Acad Sci U S A, 1990. 87(3): p. 950-4.

31. Wilson, W.D., et al., *Antiparasitic compounds that target DNA.* Biochimie, 2008. 90(7): p. 999-1014.

32. Wang, C.C., *Molecular mechanisms and therapeutic approaches to the treatment of African trypanosomiasis.* Annu Rev Pharmacol Toxicol, 1995. 35: p. 93-127.

33. Lai, D.H., et al., *Adaptations of Trypanosoma brucei to gradual loss of kinetoplast DNA: Trypanosoma equiperdum and Trypanosoma evansi are petite mutants of T. brucei.* Proc Natl Acad Sci U S A, 2008. 105(6): p. 1999-2004.

34. Bitonti, A.J., J.A. Dumont, and P.P. McCann, *Characterization of Trypanosoma brucei brucei S-adenosyl-L-methionine decarboxylase and its inhibition by Berenil, pentamidine and methylglyoxal bis(guanylhydrazone).* Biochem J, 1986. 237(3): p. 685-9.

35. Benaim, G., et al., *A calmodulin-stimulated Ca2+ pump in plasma-membrane vesicles from Trypanosoma brucei; selective inhibition by pentamidine.* Biochem J, 1993. 296 (Pt 3): p. 759-63.

36. Vercesi, A.E. and R. Docampo, *Ca2+ transport by digitonin-permeabilized Leishmania donovani. Effects of Ca2+, pentamidine and WR-6026 on mitochondrial membrane potential in situ.* Biochem J, 1992. 284 (Pt 2): p. 463-7.

37. Robays, J., et al., *Eflornithine is a cost-effective alternative to melarsoprol for the treatment of second-stage human West African trypanosomiasis in Caxito, Angola.* Trop Med Int Health, 2008. 13(2): p. 265-71.

38. Balasegaram, M., et al., *Effectiveness of melarsoprol and eflornithine as first-line regimens for gambiense sleeping sickness in nine Medecins Sans Frontieres programmes.* Trans R Soc Trop Med Hyg, 2009. 103(3): p. 280-90.

39. Sanderson, L., et al., *The blood-brain barrier significantly limits eflornithine entry into Trypanosoma brucei brucei infected mouse brain.* J Neurochem, 2008. 107(4): p. 1136-46.

40. Berger, B.J., N.S. Carter, and A.H. Fairlamb, *Polyamine and pentamidine metabolism in African trypanosomes.* Acta Trop, 1993. 54(3-4): p. 215-24.

41. Heby, O., S.C. Roberts, and B. Ullman, *Polyamine biosynthetic enzymes as drug targets in parasitic protozoa.* Biochem Soc Trans, 2003. 31(2): p. 415-9.

42. Priotto, G., et al., *Nifurtimox-eflornithine combination therapy for second-stage African Trypanosoma brucei gambiense trypanosomiasis: a multicentre, randomised, phase III, non-inferiority trial.* Lancet, 2009. 374(9683): p. 56-64.

43. Pepin J Fau - Milord, F. and F. Milord, *The treatment of human African trypanosomiasis.* Adv. Parasitol., 1994. 33(0065-308X): p. 1-47.

44. Enanga, B., et al., *Sleeping sickness and the brain.* Cell Mol Life Sci, 2002. 59(5): p. 845-58.

45. Carter, N.S. and A.H. Fairlamb, *Arsenical-resistant trypanosomes lack an unusual adenosine transporter.* Nature, 1993. 361(6408): p. 173-6.

46. Fairlamb, A.H., G.B. Henderson, and A. Cerami, *Trypanothione is the primary target for arsenical drugs against African trypanosomes.* Proc Natl Acad Sci U S A, 1989. 86(8): p. 2607-11.

47. Fairlamb, A.H. and A. Cerami, *Metabolism and functions of trypanothione in the Kinetoplastida.* Annu Rev Microbiol, 1992. 46: p. 695-729.

48. Krieger, S., et al., *Trypanosomes lacking trypanothione reductase are avirulent and show increased sensitivity to oxidative stress.* Mol Microbiol, 2000. 35(3): p. 542-52.

49. Adams, C.P. and V.V. Brantner, *Estimating The Cost Of New Drug Development: Is It Really $802 Million?* Health Affairs, 2006. 25(2): p. 420-428.

50. DiMasi, J.A., *The value of improving the productivity of the drug development process: faster times and better decisions.* Pharmacoeconomics 2002. 20(1170-7690): p. 1-10.

51. DiMasi Ja Fau - Hansen, R.W., H.G. Hansen Rw Fau - Grabowski, and H.G. Grabowski, *The price of innovation: new estimates of drug development costs.* J Health Econ., 2003. 22(2): p. 151-185.

52. Fairlamb, A.H., *Future prospects for the chemotherapy of human trypanosomiasis. 1. Novel approaches to the chemotherapy of trypanosomiasis.* Trans R Soc Trop Med Hyg, 1990. 84(5): p. 613-7.

53. da Cunha, E.F.F., et al., *New Approaches to the Development of Anti-Protozoan Drug Candidates: a Review of Patents.* Journal of the Brazilian Chemical Society, 2010. 21(10): p. 1787-1806.

54. Wenzler, T., et al., *New treatment option for second-stage African sleeping sickness: in vitro and in vivo efficacy of aza analogs of DB289.* Antimicrob Agents Chemother, 2009. 53(10): p. 4185-92.

55. Mathis, A.M., et al., *Accumulation and intracellular distribution of antitrypanosomal diamidine compounds DB75 and DB820 in African trypanosomes.* Antimicrob Agents Chemother, 2006. 50(6): p. 2185-91.

56. Jennings, F.W. and G.M. Urquhart, *The use of the 2 substituted 5-nitroimidazole, Fexinidazole (Hoe 239) in the treatment of chronic T. brucei infections in mice.* Z Parasitenkd, 1983. 69(5): p. 577-81.

57.   Baliani, A., et al., *Design and synthesis of a series of melamine-based nitroheterocycles with activity against Trypanosomatid parasites.* J Med Chem, 2005. 48(17): p. 5570-9.

58.   Hall, B.S., et al., *Exploiting the drug-activating properties of a novel trypanosomal nitroreductase.* Antimicrob Agents Chemother, 2010. 54(3): p. 1193-9.

59.   Nare, B., et al., *Discovery of novel orally bioavailable oxaborole 6-carboxamides that demonstrate cure in a murine model of late-stage central nervous system african trypanosomiasis.* Antimicrobial agents and chemotherapy, 2010. 54(10): p. 4379-88.

60.   Jacobs, R.T., et al., *SCYX-7158, an orally-active benzoxaborole for the treatment of stage 2 human African trypanosomiasis.* PLoS Negl Trop Dis, 2011. 5(6): p. e1151.

61.   Oduor, R.O., et al., *Trypanosoma brucei glycogen synthase kinase-3, a target for anti-trypanosomal drug development: a public-private partnership to identify novel leads.* PLoS neglected tropical diseases, 2011. 5(4): p. e1017.

62.   Sharlow, E.R., et al., *A target-based high throughput screen yields Trypanosoma brucei hexokinase small molecule inhibitors with antiparasitic activity.* PLoS neglected tropical diseases, 2010. 4(4): p. e659.

63.   Comini, M.A., et al., *Validation of Trypanosoma brucei trypanothione synthetase as drug target.* Free Radical Biology and Medicine, 2004. 36(10): p. 1289-1302.

64.   Torrie, L.S., et al., *Chemical validation of trypanothione synthetase: a potential drug target for human trypanosomiasis.* The Journal of biological chemistry, 2009. 284(52): p. 36137-45.

65.   Spinks, D., et al., *Investigation of Trypanothione Reductase as a Drug Target in Trypanosoma brucei.* ChemMedChem, 2009. 4(12): p. 2060-2069.

66.   Ruda, G.F., et al., *Virtual fragment screening for novel inhibitors of 6-phosphogluconate dehydrogenase.* Bioorganic & medicinal chemistry, 2010. 18(14): p. 5056-62.

67.   Price, H.P., et al., *Myristoyl-CoA:protein N-myristoyltransferase, an essential enzyme and potential drug target in kinetoplastid parasites.* The Journal of biological chemistry, 2003. 278(9): p. 7206-14.

68.   Frearson, J.A., et al., *N-myristoyltransferase inhibitors as new leads to treat sleeping sickness.* Nature, 2010. 464(7289): p. 728-U100.

69.   Paliwal, S., A. Narayan, and S. Paliwal, *Quantitative Structure Activity Relationship Analysis of Dicationic Diphenylisoxazole as Potent Anti-Trypanosomal Agents.* Qsar & Combinatorial Science, 2009. 28(11-12): p. 1367-1375.

70.   Paliwal, S.K., A.N. Verma, and S. Paliwal, *Neglected disease - african sleeping sickness: recent synthetic and modeling advances.* Scientia pharmaceutica, 2011. 79(3): p. 389-428.

71.   Cowan-Jacob, S.W., *Structural biology of protein tyrosine kinases.* Cell Mol Life Sci, 2006. 63(22): p. 2608-25.

72.   Hubbard, S.R., et al., *Crystal structure of the tyrosine kinase domain of the human insulin receptor.* Nature, 1994. 372(6508): p. 746-54.

73.   Hunter, T., *The Croonian Lecture 1997. The phosphorylation of proteins on tyrosine: its role in cell growth and disease.* Philos Trans R Soc Lond B Biol Sci, 1998. 353(1368): p. 583-605.

74.   Jordan, J.D., E.M. Landau, and R. Iyengar, *Signaling networks: the origins of cellular multitasking.* Cell, 2000. 103(2): p. 193-200.

75.   Manning, G., et al., *The protein kinase complement of the human genome.* Science, 2002. 298(5600): p. 1912-34.

76.   Robinson, D.R., Y.M. Wu, and S.F. Lin, *The protein tyrosine kinase family of the human genome.* Oncogene, 2000. 19(49): p. 5548-57.

77.   King, N. and S.B. Carroll, *A receptor tyrosine kinase from choanoflagellates: molecular insights into early animal evolution.* Proceedings of the National Academy of Sciences of the United States of America, 2001. 98(26): p. 15032-7.

78.   Parsons, M., et al., *Comparative analysis of the kinomes of three pathogenic trypanosomatids: Leishmania major, Trypanosoma brucei and Trypanosoma cruzi.* BMC Genomics, 2005. 6: p. 127.

79.   Hubbard, S.R. and J.H. Till, *Protein tyrosine kinase structure and function.* Annual Review of Biochemistry, 2000. 69: p. 373-398.

80.   Carpenter, C.L., et al., *Phosphoinositide 3-Kinase Is Activated by Phosphopeptides That Bind to the Sh2 Domains of the 85-Kda Subunit.* Journal of Biological Chemistry, 1993. 268(13): p. 9478-9483.

81.   Myers, M.G., et al., *Irs-1 Activates Phosphatidylinositol 3'-Kinase by Associating with Src Homology-2 Domains of P85.* Proceedings of the National Academy of Sciences of the United States of America, 1992. 89(21): p. 10350-10354.

82.   Anderson, D., et al., *Binding of Sh2 Domains of Phospholipase-C-Gamma-1, Gap, and Src to Activated Growth-Factor Receptors.* Science, 1990. 250(4983): p. 979-982.

83.   Schlessinger, J., *Cell signaling by receptor tyrosine kinases.* Cell, 2000. 103(2): p. 211-225.

84.   Neet, K. and T. Hunter, *Vertebrate non-receptor protein-tyrosine kinase families.* Genes to Cells, 1996. 1(2): p. 147-169.

85. Johnson, L.N., *Protein kinase inhibitors: contributions from structure to clinical compounds.* Quarterly Reviews of Biophysics, 2009. 42(1): p. 1-40.

86. Hardin, C.F., *A GPI-Phospholipase C and and Protein Tyrosine Kinases in Trypanosoma brucei*, in *Cellular Biology*. 2009, University of Georgia: Athens.

87. Subramanya, S. and K. Mensa-Wilmot, *Diacylglycerol-stimulated endocytosis of transferrin in trypanosomatids is dependent on tyrosine kinase activity.* PLoS One, 2010. 5(1): p. e8538.

88. Wheeler-Alm, E. and S.Z. Shapiro, *Evidence of tyrosine kinase activity in the protozoan parasite Trypanosoma brucei.* J Protozool, 1992. 39(3): p. 413-6.

89. Akiyama, T., et al., *Genistein, a specific inhibitor of tyrosine-specific protein kinases.* J Biol Chem, 1987. 262(12): p. 5592-5.

90. Nett, I.R., et al., *The phosphoproteome of bloodstream form Trypanosoma brucei, causative agent of African sleeping sickness.* Mol Cell Proteomics, 2009. 8(7): p. 1527-38.

91. Wheeler-Alm, E. and S.Z. Shapiro, *Glycosome-associated tyrosine-phosphorylated protein in Trypanosoma brucei.* Trop Med Parasitol, 1993. 44(4): p. 281-4.

92. Parsons, M., et al., *Trypanosoma congolense: developmental regulation of protein kinases and tyrosine phosphorylation during the life cycle.* Exp Parasitol, 1995. 80(3): p. 507-14.

93. Nett, I.R.E., et al., *Identification and Specific Localization of Tyrosine-Phosphorylated Proteins in Trypanosoma brucei.* Eukaryotic Cell, 2009. 8(4): p. 617-626.

94. Mustafa, E., et al., *Tyrosine kinases are required for interferon-gamma-stimulated proliferation of Trypanosoma brucei brucei.* J Infect Dis, 1997. 175(3): p. 669-73.

95. Hamadien, M., M. Bakhiet, and R.A. Harris, *Interferon-gamma induces secretion of trypanosome lymphocyte triggering factor via tyrosine protein kinases.* Parasitology, 2000. 120 (Pt 3): p. 281-7.

96. Mustafa, E., et al., *Tyrosine kinases are required for interferon-gamma-stimulated proliferation of Trypanosoma brucei brucei.* Journal of Infectious Diseases, 1997. 175(3): p. 669-673.

97. Krause, D.S. and R.A. Van Etten, *Tyrosine kinases as targets for cancer therapy.* New England Journal of Medicine, 2005. 353(2): p. 172-187.

98. Madhusudan, S. and T.S. Ganesan, *Tyrosine kinase inhibitors in cancer therapy.* Clinical Biochemistry, 2004. 37(7): p. 618-635.

99.   Levitzki, A. and E. Mishani, *Tyrphostins and other tyrosine kinase inhibitors.* Annu Rev Biochem, 2006. 75: p. 93-109.

100.   Levitzki, A. and A. Gazit, *Tyrosine kinase inhibition: an approach to drug development.* Science, 1995. 267(5205): p. 1782-8.

101.   Ellis, A.G., et al., *Preclinical analysis of the analinoquinazoline AG1478, a specific small molecule inhibitor of EGF receptor tyrosine kinase.* Biochem Pharmacol, 2006. 71(10): p. 1422-34.

102.   Levitzki, A., *Tyrosine kinase inhibitors: views of selectivity, sensitivity, and clinical performance.* Annu Rev Pharmacol Toxicol, 2013. 53: p. 161-85.

103.   Borg, J.P., et al., *ERBIN: a basolateral PDZ protein that interacts with the mammalian ERBB2/HER2 receptor.* Nature Cell Biology, 2000. 2(7): p. 407-414.

104.   Vlahovic, G. and J. Crawford, *Activation of tyrosine kinases in cancer.* Oncologist, 2003. 8(6): p. 531-538.

105.   Tiseo, M., M. Loprevite, and A. Ardizzoni, *Epidermal growth factor receptor inhibitors: a new prospective in the treatment of lung cancer.* Curr Med Chem Anticancer Agents, 2004. 4(2): p. 139-48.

106.   Cockerill, G.S. and K.E. Lackey, *Small molecule inhibitors of the class 1 receptor tyrosine kinase family.* Curr Top Med Chem, 2002. 2(9): p. 1001-10.

107.   Denny, W.A., et al., *Structure-activity relationships for 4-anilinoquinazolines as potent inhibitors at the ATP binding site of the epidermal growth factor receptor in vitro.* Clinical and Experimental Pharmacology and Physiology, 1996. 23(5): p. 424-427.

108.   Smaill, J.B., et al., *Tyrosine kinase inhibitors. 18. 6-substituted 4-anilinoquinazolines and 4-anilinopyrido [3,4-d]pyrimidines as soluble, irreversible inhibitors of the epidermal growth factor receptor.* Journal of Medicinal Chemistry, 2001. 44(3): p. 429-440.

109.   Bridges, A.J., *The epidermal growth factor receptor family of tyrosine kinases and cancer: Can an atypical exemplar be a sound therapeutic target?* Current Medicinal Chemistry, 1996. 3(3): p. 167-194.

110.   Palmer, B.D., et al., *Tyrosine kinase inhibitors .11. Soluble analogues of pyrrolo- and pyrazoloquinazolines as epidermal growth factor receptor inhibitors: Synthesis, biological evaluation, and modeling of the mode of binding.* Journal of Medicinal Chemistry, 1997. 40(10): p. 1519-1529.

111.   Wood, E.R., et al., *A unique structure for epidermal growth factor receptor bound to GW572016 (Lapatinib): Relationships among protein conformation, inhibitor off-rate, and receptor activity in tumor cells.* Cancer Research, 2004. 64(18): p. 6652-6659.

112.   Shewchuk, L., et al., *Binding mode of the 4-anilinoquinazoline class of protein kinase inhibitor: X-ray crystallographic studies of 4-anilinoquinazolines bound to cyclin-dependent kinase 2 and p38 kinase.* J Med Chem, 2000. 43(1): p. 133-8.

113.   Spector, N.L., et al., *Study of the biologic effects of lapatinib, a reversible inhibitor of ErbB1 and ErbB2 tyrosine kinases, on tumor growth and survival pathways in patients with advanced malignancies.* Journal of Clinical Oncology, 2005. 23(11): p. 2502-2512.

114.   Lackey, K.E., *Lessons from the drug discovery of lapatinib, a dual ErbB1/2 tyrosine kinase inhibitor.* Curr Top Med Chem, 2006. 6(5): p. 435-60.

115.   Medina, P.J. and S. Goodin, *Lapatinib: A dual inhibitor of human epidermal growth factor receptor tyrosine kinases.* Clinical Therapeutics, 2008. 30(8): p. 1426-1447.

116.   Burris, H.A., et al., *Phase I safety, pharmacokinetics, and clinical activity study of lapatinib (GW572016), a reversible dual inhibitor of epidermal growth factor receptor tyrosine kinases, in heavily pretreated patients with metastatic carcinomas.* Journal of Clinical Oncology, 2005. 23(23): p. 5305-5313.

117.   Clayton, A.H., et al., *Fluorescence and analytical ultracentrifugation analyses of the interaction of the tyrosine kinase inhibitor, tyrphostin AG 1478-mesylate, with albumin.* Anal Biochem, 2005. 342(2): p. 292-9.

118.   Lichtner, R.B., et al., *Signaling-inactive epidermal growth factor receptor/ligand complexes in intact carcinoma cells by quinazoline tyrosine kinase inhibitors.* Cancer Research, 2001. 61(15): p. 5790-5795.

119.   Cohen, M.H., et al., *FDA drug approval summary: Gefitinib (ZD1839) (Iressa (R)) tablets.* Oncologist, 2003. 8(4): p. 303-306.

120.   Cohen, M.H., et al., *FDA drug approval summary: Erlotinib (Tarceva (R)) tablets.* Oncologist, 2005. 10(7): p. 461-466.

121.   Pays, E. and B. Vanhollebeke, *Human innate immunity against African trypanosomes.* Curr Opin Immunol, 2009. 21(5): p. 493-8.

122.   Abdel-Sattar, E., et al., *Antitrypanosomal activity of some pregnane glycosides isolated from Caralluma species.* Phytomedicine, 2009. 16(6-7): p. 659-664.

123.   Lab, K., *Structural Biology of Cell Signaling and DNA Replication.* 2013: Unversityof California, Berkeley.

124.   Colabufo, N.A., et al., *EGFR tyrosine kinase inhibitors and multidrug resistance: perspectives.* Frontiers in Bioscience-Landmark, 2011. 16: p. 1811-1823.

125.   Van Den Abbeele, J., et al., *Trypanosoma brucei modifies the tsetse salivary composition, altering the fly feeding behavior that favors parasite transmission.* PLoS Pathog, 2010. 6(6): p. e1000926.

126.   Caljon, G., et al., *Tsetse fly saliva accelerates the onset of Trypanosoma brucei infection in a mouse model associated with a reduced host inflammatory response.* Infect Immun, 2006. 74(11): p. 6324-30.

127.   Schultzberg, M., et al., *Spread of Trypanosoma brucei to the nervous system: early attack on circumventricular organs and sensory ganglia.* J Neurosci Res, 1988. 21(1): p. 56-61.

128.   Enanga, B., et al., *Sleeping sickness and the brain.* Cell Mol Life Sci, 2002. 59(5): p. 845-58.

129.   Pentreath, V.W., *Royal Society of Tropical Medicine and Hygiene Meeting at Manson House, London, 19 May 1994. Trypanosomiasis and the nervous system. Pathology and immunology.* Trans R Soc Trop Med Hyg, 1995. 89(1): p. 9-15.

130.   Krampitz, H.E., *[Symptoms, pathogenesis and diagnostic value of the primary reaction in African sleeping sickness].* Z Tropenmed Parasitol, 1967. 18(3): p. 273-9.

131.   Greenwood, B.M. and H.C. Whittle, *The pathogenesis of sleeping sickness.* Trans R Soc Trop Med Hyg, 1980. 74(6): p. 716-25.

132.   MacLean, L., et al., *Stage progression and neurological symptoms in Trypanosoma brucei rhodesiense sleeping sickness: role of the CNS inflammatory response.* PLoS Negl Trop Dis, 2012. 6(10): p. e1857.

133.   Blum, J. and C. Burri, *Treatment of late stage sleeping sickness caused by T.b. gambiense: a new approach to the use of an old drug.* Swiss Med Wkly, 2002. 132(5-6): p. 51-6.

134.   Dumas, M., Bouteille. B, Buguet A, *Progress in human African trypanosomiasis, sleeping sickness.* 1999, Paris: Springer-Verlag.

CHAPTER II

CHEMICAL BIOLOGY OF PHOSPHOTYROSINE PATHWAYS

IN THE AFRICAN TRYPANOSOME WITH A SMALL MOLECULE TYROSINE

KINASE INHIBITOR GW572016 (LAPATINIB)[1]

Abstract

Trypanosoma brucei has a divergent phospho-tyrosine signaling that is not well understood. The classical receptor tyrosine kinases are absent in the parasite. However, the EGFR-like kinase domains and tyrosine-phosphorylated peptides in the parasite are reported. In this study, we have used a small molecule GW572016 (lapatinib) as a tool chemical to explore cellular pathways regulated by tyrosine phosphorylation in the trypanosome. GW572016 inhibited tyrosine phosphorylation of select proteins. We identified 39 potential effector proteins in the GW572016-inhibitable phospho-tyrosine (pTyr) signaling pathway by proteomic analysis. These proteins provide a molecular explanation of the biological pathways regulated by the pTyr signaling in *T. brucei*. We focused on three pathways predicted from this data: (i) cell morphology (*e.g.,* BILBO-1), (ii) flagellum biogenesis (*e.g.,* PFR-1), and (iii) endocytosis (*e.g.,* actin A). The drug alters cell morphology and causes loss of trypanosome polarity evident from (i) changes in the intracellular localization of β-tubulin, (ii) redistribution of tyrosylated α-tubulin, and (iii) retraction of the flagellum into the cell body. Also, the receptor mediated transferrin endocytosis was blocked upon pretreatment of the cells with the drug. These effects of the GW572016 on the trypanosome could be explained as loss-of-function of effector proteins. We hereby present GW572016 as a novel chemical tool that established the link between phosphotyrosine signaling and the three important cellular pathways in the African trypanosome.

2.1 Introduction

Trypanosoma brucei, an extracellular blood protozoan, causes Human African Trypanosomiasis (HAT) for which the choice of treatment is unsatisfactory. In an attempt to develop novel therapeutics for HAT it is important to understand cellular pathways that can be

targeted in the parasite; the target pathway should be biologically essential but systematically different from the host. Phosphotyrosine signaling is a molecular pathway that is not well understood in trypanosomes unlike the much-studied mammalian systems [1, 2]. *T. brucei* has a divergent pTyr signaling system characterized by the absence of conventional receptor Tyr kinases (RTKs) [3, 4] and pTyr-binding domains (*e.g.,* SH2) [2]. However, phosphorylated Tyr residues are detected in the parasite [5-7]. This suggests that dual-specificity kinases might be involved in the phosphorylation of tyrosine residues [3].

Iron is essential for survival of *T. brucei*. Transferrin receptors are present on the cell surface, which facilitates iron uptake by a receptor-mediated endocytic process [8]. Inhibition of transferrin endocytosis by a tyrosine kinase inhibitor Tyrphostin A-47 indicates that protein tyrosine kinase activity in the parasite is present [9, 10]. Also, a tyrosine kinase dependent pathway in *T. brucei* induces interferon-gamma (IFN-γ) production [11]. Because trypanosomes have a unique Tyr-phosphorylation system, further studies will provide a detailed insight into the enzymes, substrates and associated cellular pathways. Further, small molecule inhibitors of the pTyr signaling may be developed for discovery of new lead drugs against HAT.

Small molecules based chemical biology has been a powerful tool in cell biology, and the strategy has been employed to trace the relevant signaling pathways [12, 13]. In trypanosomes, however, such an approach has not been reported. In order to investigate the phospho-tyrosine signaling in *T. brucei*, we searched for small chemical entities that can affect Tyr-phosphorylation of proteins. We identified GW572016 from a "focused screen" of ten compounds that we used as a chemical tool. In a target profiling study, four GW572016 -binding protein kinases were identified [14].

We hereby report 39 trypanosome proteins that are present in a "GW572016-inhibitable

pTyr signaling pathway". These proteins are involved in a number of cellular pathways; some of, the pathways that we studied are (i) cell morphology, (ii) flagellum biogenesis, and (iii) endocytosis. We found that GW572016 blocked Tyr-phosphorylation of select trypanosome proteins. Within the trypanosome, the overall morphology was altered from long slender to round with retraction of flagellum in to the cell body. The intracellular distribution of tyrosinated α-tubulin was changed. The drug inhibited endocytosis of transferrin. We conclude from this study that pTyr signaling is involved in the cellular pathways of flagellum biogenesis, intracellular localization of tyrosinated α-tubulin, trypanosome morphology, and transferrin endocytosis.

2.2 Materials And Methods

2.2.1 Parasites and cell culture

The blood stream form *Trypanosoma brucei* (Lister 427 strain) was obtained from Dr. C. C. Wang (University of California, San Francisco) and routinely cultured in HMI-9 medium **[15]** containing 10% fetal bovine serum (Atlanta Biologicals, Lawrenceville, GA), 10% Serum Plus (SAFC Biosciences, Lenexa, KS), and 1% antibiotics-antimycotic solution (Cellgro, Manassas, VA) at 37 ºC, 5% CO_2.

2.2.2 Materials

GW572016 was a gift from GlaxoSmithKline (Durham, NC) and Tyrphostin A47 was purchased from Santa Cruz Biotechnology (Santa Cruz, CA). Dimethyl Sulfoxide (DMSO) was from Fisher Scientific (Fair Lawn, NJ). AcrylaGel and Bis-AcrylaGel were purchased from National Diagnostics (Atlanta, GA). Immobilon P membrane was from Millipore (Bedford, MA). Sodium dodecyl sulfate (SDS), 5-bromo-4-chloro-indoyl phosphate (BCIP), p-nitroblue

tetrazolium chloride (NBT), and N,N,N',N'- tetramethylenediamine (TEMED) were from BioRad (Melville, NY). GelCode blue dye and Pierce Silver stain kit were from Thermo Scientific (Rockford, IL). Aprotinin, leupeptin, phenylmethanesulfonylfluoride (PMSF), N^α-Tosyl-Lys-chloromethylketone (TLCK), and sodium orthovanadate were purchased from Sigma (Saint Louis, MO). 4, 6-Diamidino-2-phenylindole (DAPI) and propidium iodide were from Invitrogen (Eugene, OR) and Sigma (Saint Louis, MO) respectively. VectaShield mounting medium was from Vector Laboratories (Burlingame, CA). Tween 20, Triton X-100, and glutaraldehyde were from Fisher Scientific (Fair Lawn, NJ). Sepharose CL4B, digitonin, paraformaldehyde, poly-L-lysine, and bovine serum albumin (BSA) were from Sigma (Saint Louis, MO). All other reagents were analytical grade or better.

2.2.3 Antibodies

P-Tyr-100 (anti-phosphotyrosine mouse monoclonal antibody) and immobilized P-Tyr-100 were from Cell Signaling Technology, Inc. (Danvers, MA). IgG-alkaline phosphatase conjugated goat anti-mouse was from Sigma (Saint Louis, MO). 12G10 (anti-alpha-tubulin mouse monoclonal antibody) was from Developmental Studies Hybridoma Bank (University of Iowa); KMX-1 (anti-beta-tubulin mouse monoclonal antibody) was from Millipore (Temecula, CA), and YL1/2 (anti-tyrosylated-alpha-tubulin rat monoclonal antibody) was from Chemicon International (Temecula, CA). L8C4 (anti-PFR2 mouse monoclonal antibody) was a gift from Dr. K. Gull (University of Oxford) [16]. Transferrin-AlexaFluor 488 (Tf-AF488) was purchased from Invitrogen (Eugene, OR).

2.2.4 GW572016 treatment of *T. brucei*

For western blotting, immunofluorescence, and scanning electron microscopy (SEM) approximately 10^7 *T. brucei* were harvested in late log phase (8 x 10^5/ml) and resuspended in

HMI-9 at either 10^7/ ml (western blotting) or 5 x 10^5/ml (immunofluorescence and SEM) for treatment with DMSO (control) or GW572016 (10 µM) for 2 h at 37 ºC and 5% CO_2.

2.2.5 Western blotting

Phosphotyrosine (pTyr) in *T. brucei* was detected by western blot using P-Tyr-100 antibody following a modified version of the manufacture's protocol. In brief, GW572016-treated and control cells were washed twice in bicine-buffered saline supplemented with 1% glucose (BBS/G) and lysed in 2X SDS-PAGE sample buffer. Total proteins (7.5 x 10^6 cells equivalent per lane) were resolved by 10% SDS-PAGE and transferred to Immobilon P membrane using a semi-dry electrophoretic transfer cell **[17]**. The membrane was blocked for an hour at room temperature with 1x Tris buffered saline (TBS) containing 0.1% Tween-20 (TBST) and 5% w/v nonfat dry milk, and then incubated overnight at 4 °C with P-Tyr-100 antibody (1:500 dilution). After withdrawing the solution containing P-Tyr-100 a one-hour incubation with alkaline phosphatase conjugated secondary antibody (1:1000 dilution) was carried out at room temperature prior to color development with BCIP/ NBT. All antibodies were diluted in the blocking buffer. After every incubation step, the membrane was washed four times (5 min each) with 1x TBST. In a parallel experiment, alpha-tubulin in *T. brucei* was detected with 12G10 antibody (1: 10,000 dilution) as a loading control (2.5 x 10^6 cells equivalent per lane).

2.2.6 Immunofluorescence microscopy

For immunofluorescence assay, parasites were treated with GW572016 or DMSO as mentioned above, and washed twice in 1 ml of PBS/G (pH-7.4). Cells were fixed with 4% paraformaldehyde and adhered to poly-L-lysine-coated coverslips for 30 min, permeabilized in 0.1 % Triton X-100 for 25 min at room temperature, washed once in PBS, and blocked with 1% bovine serum albumin (BSA) in PBS. Cells on the cover slips were incubated for 1 h at room

temperature with one primary antibody at a time (at different dilutions), such as P-Tyr-100 (1: 400); 12G10 (1: 1000); KMX-1 (1:250); YL1/2 (1:400); and L8C4 (undiluted). The cells were thoroughly rinsed three times with 500 µl PBS for 5 min each time and incubated with Alexa Fluor-594 (red) or Alexa Fluor-488 (green)-coupled goat anti-mouse or goat anti-rat secondary antibody (1:1000 dilution) for 1 h at room temperature. All antibodies were diluted in the 1% bovine serum albumin (BSA) in PBS blocking buffer. In one set of controls, fixed cells were incubated with the secondary antibodies only. Following antibody incubation, cells were washed in PBS five times and mounted on glass slides with anti-fade Vectashield containing 4, 6-Diamidino-2-phenylindole (DAPI). DIC (differential interference contrast) and fluorescence images were captured and analyzed using an Axio Observer Z1 (inverted fluorescence microscope) fitted with an AxioCam MRm operated by AxioVision 4.6 software.

2.2.7 Scanning electron microscopy (SEM)

After treatment of *T. brucei* in DMSO or drug, cells were fixed in 2% glutaraldehyde at room temperature for 1 h, washed twice in 1 ml PBS, and transferred to poly-L-lysine-coated coverslips as described earlier. The cells on the coverslips were fixed with 1% osmium tetraoxide for 30 min and dehydrated in increasing concentrations of ethanol (25% -100%; 5 min each). All of these steps were performed at room temperature. The samples were dried at critical point with a Tousimis Critical Point Dryer (Samdri-780 A), and sputter coated (gold) with SPI Module Sputter Coater following standard protocols. Using a Zeiss 1450EP variable pressure scanning electron microscope, samples were viewed and images captured.

2.2.8 Anti-phosphotyrosine antibody affinity column chromatography and LC MS-MS

Approximately 2×10^8 blood stream *T. brucei* cells were harvested and each 1×10^8 cells, resuspended at a density of 5×10^5/ ml, was treated with either DMSO (solvent) or GW572016

(10 μM) for 3 h in HMI-9. Cells were pelleted post treatment separately, washed twice in ice-cold phosphate buffer saline with 1% glucose (PBS/G), and lysed in 1 ml lysis buffer (20mM Tris-HCl pH 7.4, 60 mM $MgCl_2$, 60 mM KCl, 1 mM DTT, 1% Triton-X, 1mM sodium vanadate) containing the protease inhibitors [1mM phenylmethanesulfonylfluoride (PMSF), 2 μg/ mL aprotinin, 5 μg/ mM leupeptin, 37 μg/ ml N^α-Tosyl-Lys- chloromethylketone (TLCK), 2 μM FMKO24]. From each treatment, 500 μl of the cell lysate was incubated with 24 μl of either Sepharose CL4B (control) or immobilized anti-phosphotyrosine antibody (Sepharose P-Tyr-100) columns for 4 h at 4 ºC. The beads were recovered by centrifugation at 13,000 xg for 10 min at 4 ºC and washed thrice (5 min each) in 500 μl lysis buffer containing 1M KCl. Proteins were eluted sequentially from the columns three times with (i) 50 μl of 200 μM Tyrphostin A47 in PBS, (ii) 200 mM phenyl phosphate in PBS, and pooled separately (150 μl total volume). After eluting with one solvent the columns were washed with 500 μl lysis buffer to avoid carryover of the eluted proteins to subsequent elution. Samples were kept on ice-water during the entire procedure.

The pooled eluates were precipitated with 6% trichloroacetic acid (TCA), and heated in 1X SDS-PAGE loading buffer after neutralization of acidic pH with ammonia vapor. Proteins were separated on 10% SDS-PAGE mini gel, and silver stained per manufacturer's instructions. Each SDS-polyacrylamide gel lane containing proteins of interest were cut into five pieces, each of which was further cut into 4 mm^2 pieces, destained with the silver stain destaining solution, and dehydrated with acetonitrile for trypsin digestion. Proteins digestion and LC MS-MS were performed as described [14].

2.2.9 Transferrin endocytosis assay

Trypanosomes were harvested from culture medium, washed in serum-free HMI-9

medium and resuspended at a density of 10^4/ ml in 1 ml serum-free medium containing either DMSO or 1 μM GW572016. Next, 25 μg of transferrin-AlexaFluor 488 (Tf-AF488) was added and samples were incubated for 15 min at 37 $^{\circ}$C, 5% CO_2. Separately, 10^4 cells in 1ml of HMI-9 media were incubated with 1.5 μM digitonin (final concentration) for 10 min at room temperature. All samples were centrifuged at 2000 xg for 5 min at 4 $^{\circ}$C, washed once with 1 ml cold 1X PBS containing 1% glucose (PBS/G) and resuspended in 400 μl of cold buffer B (10 mM HEPES, 140 mM NaCl, 2.5 mM $CaCl_2$, 10 mM glucose, pH 7.4). Next, propidium iodide was added to a final concentration of 3 μM, and samples were incubated for 15 min on ice protected from light. Data was collected on a CyAn ADP Analyzer (Beckman Coulter; Hialeah); and analyzed by FlowJo software (Tree Star; Ashland, OR). Experiments were performed at least twice and a representative experiment is shown.

2.3 Results

2.3.1 GW572016 (Lapatinib) inhibits tyrosine phosphorylation of proteins in *T. brucei*

GW572016 (Fig. 2.1A) is one of the most selective mammalian EGFR-tyrosine kinase inhibitors developed so far **[18]**. GW572016 inhibits Tyr-phosphorylation by epidermal growth factor receptor EGFR/Her2 in human cells **[19, 20]**. Therefore, we first investigated whether GW572016 was able to inhibit tyrosine phosphorylation of proteins in *T. brucei*. We used P-Tyr-100, an anti pTyr monoclonal antibody, **[21, 22]** to detect tyrosine-phosphorylated proteins in the total cell lysate by (i) western blotting and (ii) in single cell by fluorescence microscopy.

In western blot assays, the intensity of the phospho-Tyr signal decreased in cells treated with GW572016 (lane-2, Fig. 2.1B) when compared to the control (DMSO treated; lane-1, Fig. 2.1B). Certain protein bands that remain unaltered (two of them marked by diamond symbols) serve as internal loading controls affirming that GW572016 inhibits tyrosine-phosphorylation

only of select proteins. In another control experiment, anti-tubulin was used in a western blot of cells to show that equal amount of proteins were loaded in each lane of the gel. An immunofluorescence assay (Fig. 2.1C) revealed the effect of GW572016 at a single cell level, and confirmed that a decrease in the intensity of phospho-Tyr signal is associated with addition of GW572016 to the parasite. These finding suggests that GW572016 has a specific effect on tyrosine phosphorylation in *T. brucei*.

2.3.2 Discovery of proteins in the GW572016-susceptible phosphotyrosine pathways

Recently, four possible protein kinase targets for GW572016 have been reported **[14]**. However, the cellular pathways, regulated by tyrosine kinase signaling, that are affected by GW572016 in *T. brucei* are not known. A possible way of identifying these functional pathways is by looking for the proteins downstream of the GW572016-binding protein kinases. We used an affinity chromatography-shotgun proteomic approach (Fig. 2.2A; see material and methods for details and) to investigate the tyrosine-phosphorylated proteins inhibited by GW572016, and subsequently identify the pathways they regulate. The purpose of using Tyrphostin A47 and phenyl phosphate to elute proteins from the P-Tyr-100 column is that they have similar chemical structures as Tyr and pTyr respectively. The representative protein profiles eluted with Tyrphostin A47, phenyl phosphate, SDS sample buffer are shown in Fig. 2.2B. Lanes 1, 4, 7 represent proteins eluted from the Sepharose CL4B. Proteins in the anti-pTyr antibody affinity column are in lanes 2, 5, 8 (from cells not treated with GW572016) and lanes 3, 6, 9 (cells treated with GW572016). It is found that pre-treatment of cells with GW572016 significantly reduced binding of proteins to the anti-pTyr columns. This could be due to dephosphorylation of proteins upon treatment with the drug. The proteins from the MS analysis were classified into

three groups as described below. Representative proteins from the three classes are shown in Fig. 2.2C.

Class I (14 proteins, Table 2.1)**:** This class includes the proteins that bound nonspecifically to both Sepharose CL4B and the anti-pTyr antibody columns.

Class II (6 proteins, Table 2.2): These polypeptides preferentially bound to the anti-pTyr antibody column as compared to the Sepharose CL4B, but were not affected by pretreatment of *T. brucei* with GW572016. Therefore, these proteins are not present in a GW572016-inhibitable pTyr pathway.

Class III (39 proteins, Table 2.3 and Table 2.4): These proteins bound to the anti-pTyr antibody column with greater affinity as compared to the Sepharose CL4B. Also, the binding was decreased when the cells were treated with GW572016 which suggests that these group are involved in the GW572016-susceptible pTyr-signaling pathway in *T. brucei*.

2.3.3 *T. brucei* shape is altered after GW572016 treatment

While studying the effects of GW572016 on *T. brucei* growth **[14]**, we observed progressive swelling of the parasite at the posterior end, apparently cumulating with a round morphology possessing limited motility. In order to quantitate the relative distribution of unaffected (like normal), swollen and rounded cells in the population, we treated *T. brucei* with GW572016 (10 μM) for variable time periods and analyzed them by differential interface contrast (DIC) microscopy (Fig. 2.3A). Sixty five percent of the cells were showing posterior swelling in first 30 min of treatment with GW572016. By 2 h, similar population of both hypertrophied and rounded cells (40% each) was observed. In 3 h more than 55% of cells were rounded (Fig. 2.3B). This data suggests that GW572016 alters the appearance of bloodstream

trypanosomes. DAPI staining further reveals that the DNA material diffuses out and fills the interior of the rounded cell.

2.3.4 Intracellular distribution of β-tubulin and tyrosylated α-tubulin is affected by GW572016

Trypanosomes are highly polarized cells whose shape is maintained, at least partly, by a complex of subpellicular microtubules beneath the plasma membrane [23-25]. A change in the shape of the trypanosomes (Fig. 2.3A) is likely to be accompanied by turnover of microtubule components. We therefore performed immunofluorescence assay to study the effect of GW572016 on tubulin distribution. GW572016 did not affect the distribution pattern of alpha-tubulin content (Fig. 2.4A) [26]. However, the intracellular localization of tyrosylated alpha-tubulin, a subset of alpha-tubulin, is altered (Fig. 2.4C). Generally tyrosinated alpha-tubulins are present in the newly made microtubule [27]. In case of trypanosomes they are located in the basal body, emergent flagellum, and posterior end of the cell in *T. brucei* depending upon the stage of the cell cycle [16, 28]. We observed that after treatment with GW572016, the tyrosylated alpha-tubulins no longer remain localized to these structures; instead it filled up the cell interior (Fig. 2.4C). Beta-tubulin, present between the nucleus and the kinetoplast in normal cells, was relocalized to the cell periphery in rounded cells (Fig. 2.4B) [16].

2.3.5 Effect of GW572016 on the flagellum of *T. brucei*

T. brucei has a single flagellum. From light microscopy experiments (Fig. 2.4A), GW572016-treated trypanosomes appear to lack flagella. To investigate the effect of GW572016 on the flagellum, further we performed immunofluorescence assay with antibody (L8C4) against the paraflagellar rod protein PFR 2 [9, 29, 30]. The paraflagellar rod (PFR) is a para-crystalline structure that runs along the axonemal microtubule of the flagellum, and the PFR proteins are

essential for flagellum biogenesis [31, 32]. We observed that the flagellum is localized to the cell periphery in rounded cells (Fig. 2.5A). To confirm this data further we used scanning electron microscopy and observed that the flagellum is being withdrawn into the cell body (Fig. 2.5B).

2.3.6 GW572016 inhibits transferrin endocytosis

Iron is essential for viability of bloodstream form *T. brucei* [33, 34]. Transferrin receptors, present on the surface of the parasite, facilitate internalization of iron from host blood by endocytosis. Diacylglycerol (DAG), a second messenger in the glycosyl-phosphatidylinositol (GPI) signaling pathway, stimulates transferrin endocytosis in *T. brucei* [9]. Further, studies with tyrphostin A47, a tyrosine kinase inhibitor, indicates that tyrosine kinases are the effectors for DAG-mediated endocytosis in trypanosomatids [10]. Based on these data we hypothesized that GW572016, a tyrosine kinase inhibitor, would inhibit transferrin endocytosis in *T. brucei*.

Cells treated with GW572016 (1 μM) had decreased Alexa Fluor 488 fluorescent-transferrin (from uptake of transferrin-Alexa 488) compared to a DMSO control (Fig. 2.6A). Propidium iodide (PI) signal of cells treated with GW572016 was not different from cells treated with DMSO. The digitonin control produced a strong PI signal compared to either DMSO or GW572016 treated cells (Fig. 2.6B). This was expected because digitonin permeabilizes the plasma membrane and allows efficient intracellular accumulation of PI. Therefore, the decreased AF488 fluorescence observed was not a result of cell death, but from inhibition of transferrin endocytosis with GW572016 treatment.

2.4 Discussion

Phosphotyrosine signaling is known to regulate important cellular pathways in vertebrates [1, 2]. Although Tyr-phosphorylated proteins and tyrosine kinase activity have been

reported in trypanosomes, the signal transduction pathways are poorly understood **[5]**. The classic mammalian-type receptor Tyr kinases (RTKs) are not expressed in *T. brucei* **[3]**. Therefore, it is implicated that dual-specificity kinases are responsible for tyrosine phosphorylation in trypanosome **[3].** Also, mammalian-type pTyr-binding domains such as SH2 are not present. Because the pTyr signaling in trypanosome has deeply diverged from the vertebrate system, a similar approach such as looking for homologous genes that are studied in the other systems cannot be carried out. As an alternative strategy, chemical biology that employs small molecule inhibitors of pTyr-signaling pathway like GW572016 (Fig. 2.1B) can be used to investigate into the divergent pathway in the parasite. At first, GW572016 was used in a discovery proteomics approach and four protein kinases that bind the drug (TbLBPKs) were identified **[14]**. These four TbLBPKs share significant similarity and identity with kinase homologs from different species **[14]**.

We showed that GW572016 inhibits Tyr-phosphorylation of select trypanosome proteins (Fig. 1B). In the next step we were able to identify candidate proteins, which are present in the GW572016-susceptible pTyr pathway and grouped as Class III proteins. These are the proteins whose binding to the anti-pTyr affinity column decreased when the cells were treated with GW572016 (Table 2.3, 2.4 and Fig. 2.2). However, there are proteins, which showed nonselective biding to the anti-pTyr affinity column (Table-2.1) and the proteins whose binding to the anti-pTyr affinity column was not affected by GW572016 treatment. An explanation for the class III proteins is that GW572016 treatment inhibited phosphorylation of these proteins that resulted in decreased binding to the affinity column. As mentioned in the table-2.3 and 2.4 these proteins fall into several cellular pathways. To understand the anti-pTyr pathways in trypanosome, we focused on studying three important pathways that are indicated.

Effect of GW572016 on *T. brucei* can be explained by the "loss-of-function" of the Class III proteins. For example, RNAi of BILBO-1 (Table 2.3), a class III protein, produced a round phenotype similar to what we observed after GW572016 treatment of cells (Fig. 2.3) **[35]**. It is worth discussing here that we noticed alteration in the localization pattern of (i) β-tubulin, (ii) tyrosinated α-tubulin and (iii) flagellum topology upon treatment with GW572016 (Fig. 2.4 and Fig. 2.5). However, the effects of BILBO-1 knock down on these pathways are not known yet. The cell shape in trypanosomes is maintained by the tubulin cytoskeleton. We consider that possible inhibition of tyrosine phosphorylation of tubulin and another cytoskeleton component actin, a class III protein, might be leading to the rounding up of cells. The paraflagellar rod (PFR) is essential for motility and polarized cell shape in trypanosome. Although there are more than twenty PFR proteins known, the understanding on their posttranslational regulation has been inadequate **[36]**.

Based on our proteomic data and localization of phosphotyrosine foci along the flagellum of procyclic form *T. brucei,* we believe that Par4, PFC 19 might be tyrosine phosphorylated (Table 2.3). However, further experiments are required to validate this hypothesis.

Endocytosis of transferrin is important for viability of trypanosome that is regulated by Tyr kinase activity **[10, 37]**. We demonstrated that GW572016 inhibits transferrin endocytosis (Fig. 2.6) and kills the parasite [14]. Actin is required for endocytosis of transferrin in bloodstream form *T. brucei* **[38]**. Because actin is tyrosine phosphorylated in other eukaryotes **[39]**, we think that effect of GW572016 on endocytosis could be due to inhibition of tyrosine phosphorylation on actin.

To summarize, we adopted a chemical biology approach to understand the pathways regulated by phosphotyrosine signaling in the African trypanosome. At first, we showed that the

46

small molecule GW572016 inhibited tyrosine phosphorylation of specific proteins (Fig. 2.1B and Fig. 1C). In the next step, we identified 39 proteins that are affected by GW572016 (Fig. 2.2A, Table 2.3 and Table 2.4). We hypothesize that the phosphotyrosine signal transduction pathway in trypanosome is linked to cell morphology, flagellum biogenesis, and endocytosis. This strategy can be successfully used in other organisms like plants and yeasts that have divergent phosphotyrosine pathway.

Figure 2.1: GW572016 inhibits tyrosine phosphorylation of proteins in *T. brucei*. (A) Chemical structure of GW572016**. (B)** Western blot detection of tyrosine-phosphorylated proteins using P-Tyr-100 antibody. Bloodstream *T. brucei* (10^7 cells/ml) were treated with either DMSO (0 μM control) or GW572016 (10 μM) in HMI-9 medium for 2 h at 37 °C. Cells were pelleted, lysed in 1X SDS-PAGE sample buffer, and proteins resolved on 10% polyacrylamide gel. Proteins were transferred to PVDF membrane for western blotting. Lane 1 and 2 represent the DMSO and GW572016 treated samples respectively. Anti α-tubulin blot is a control for the total protein loading. An asterisk (*) indicates a decrease in the protein level after treatment with GW572016; (♦) indicates protein that remains unaffected. **(C)** Single cell immunofluorescence assay: effect of GW572016 on tyrosine-phosphorylated proteins. *T. brucei* cells were treated as described in panel B, fixed in 4% paraformaldehyde, and pTyr on proteins detected with anti-pTyr antibody P-Tyr-100. DAPI staining of the nucleus (n) and the kinetoplast (k) (mitochondrial DNA disk) are shown. Scale bar in the differential interference contrast (DIC) panel is 10 μm.

Figure 2.1

A

B

C
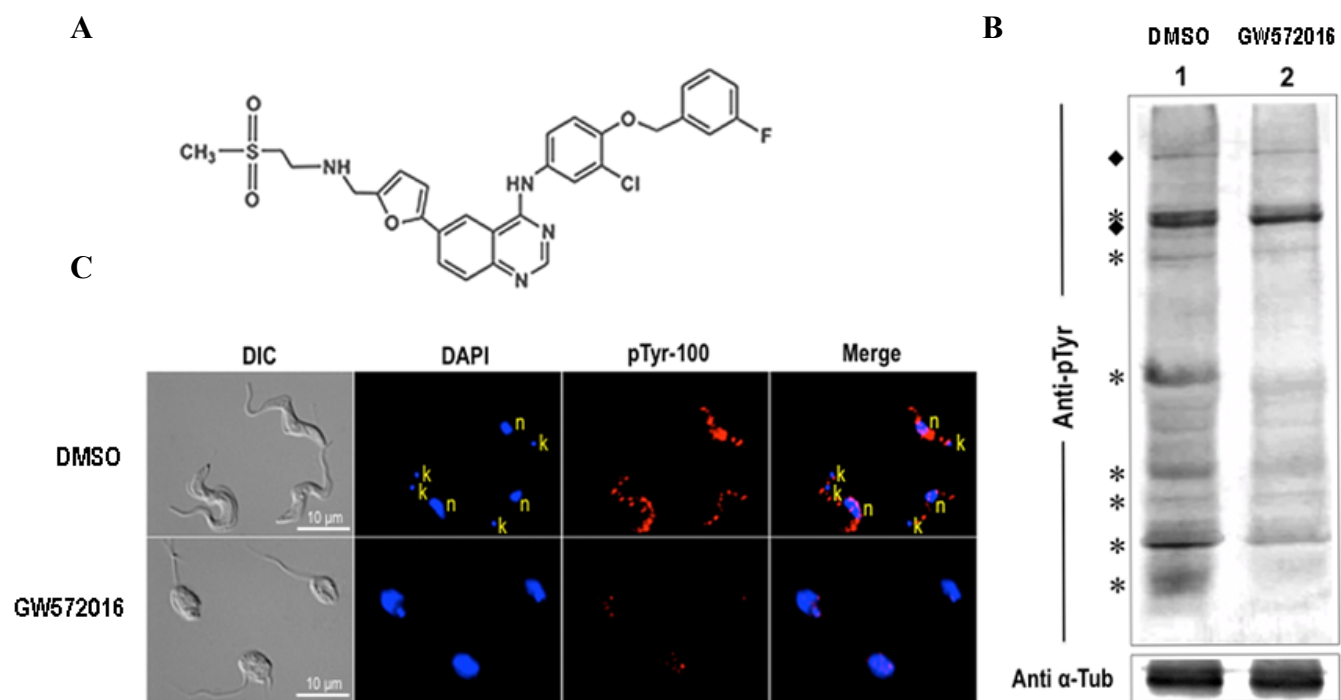
Figure 2.2: GW572016 treatment of trypanosomes diminishes binding of select proteins to P-Tyr-100 column. **(A)** A scheme for anti-phosphotyrosine antibody affinity chromatography of GW572016-susceptible tyrosine-phosphorylated proteins. **(B)** Representative silver stain gels of proteins eluted sequentially from the column with Tyrphostin A47 (lanes 2, 3), phenyl phosphate (lanes 5, 6) and 1X SDS buffer (lanes 8, 9). Lanes 1, 4, 7 present proteins eluted from sepharose CL-4B. Positions of the molecular weight markers are indicated. **(C)** Examples of Class II and Class III proteins. An asterisk (*) indicates zero spectral counts. PFK, Phosphofructokinase; BILBO1, Flagellar pocket complex protein BILBO1; PFR-1, Paraflagellar Rod protein 1.

Figure 2.2
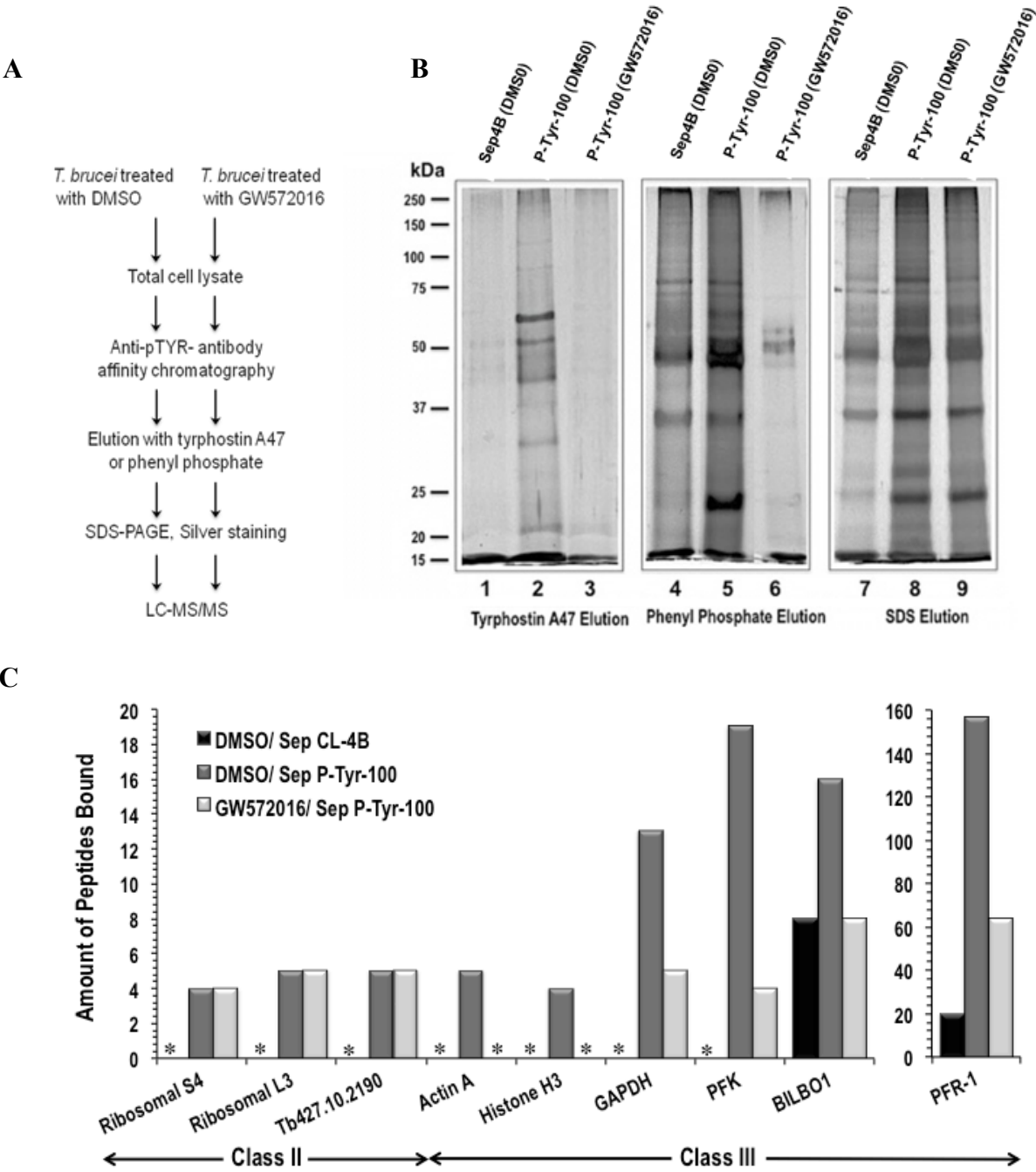
Figure 2.3: GW572016 changes morphology of the trypanosomes. (A) Differential interference contrast (DIC) microscopy and DAPI staining. Cells, at a density of 5 x 10^5/ml, were treated with GW572016 (10 µM), fixed in 4% paraformaldehyde, and stained with DAPI. DIC, DAPI, and merged images are shown. Nucleus (n) and kinetoplast (k) are labeled. Scale bar is 10 µm. **(B)** Time course showing the distribution of different cell morphologies in a population of GW572016-treated *T. brucei. T. brucei* (more than 400 cells) cell shapes were quantified after DIC microscopy, and the data expressed as percentage of the total population. Data presented are mean ± standard deviation from two separate experiments.
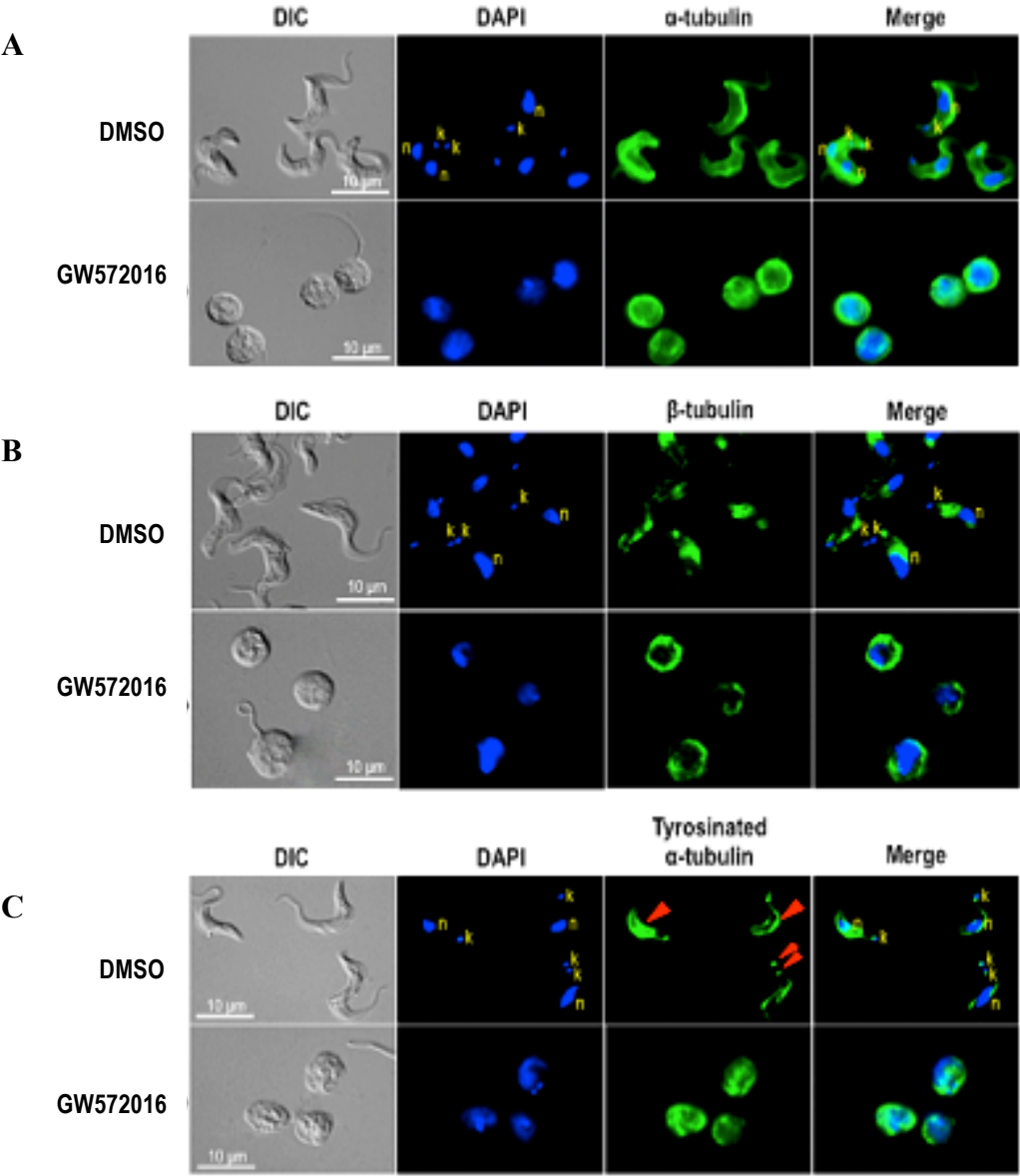
Figure 2.3
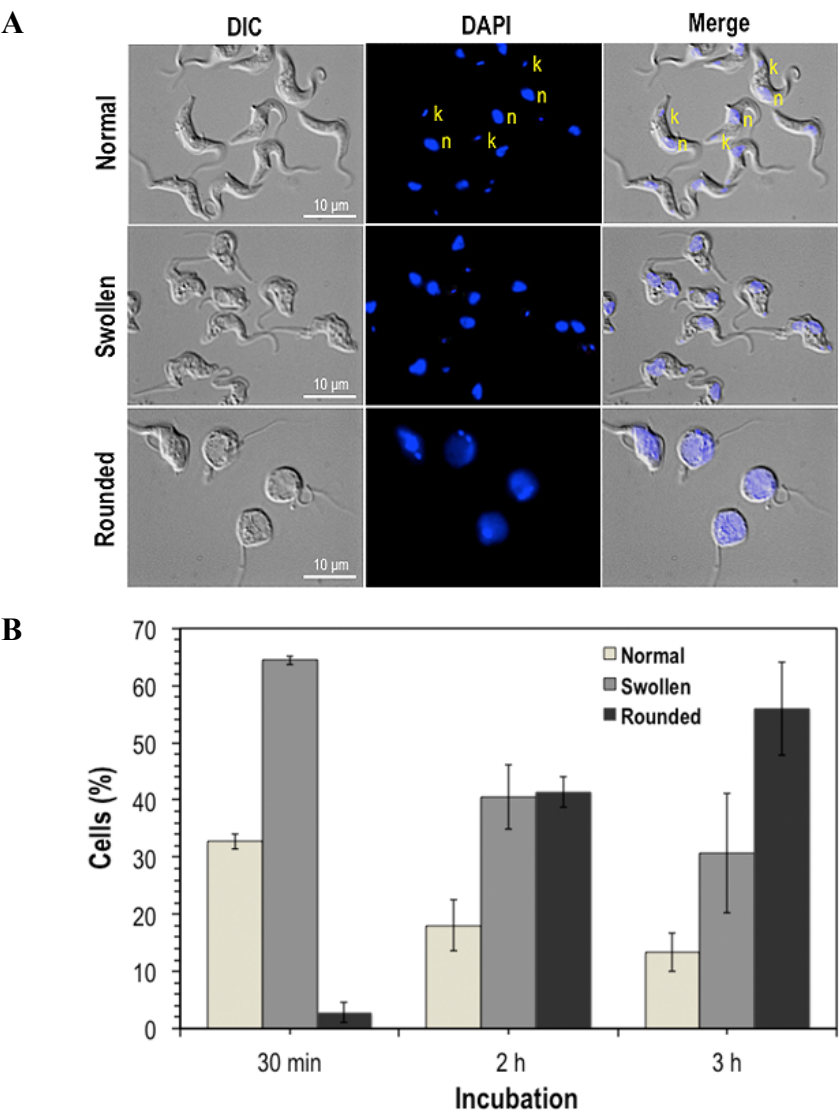
**Figure 2.4: GW572016 induces redistribution of β-tubulin and tyrosinated α-tubulin.**
Bloodstream form *T. brucei* (5×10^5/ml) were treated with either DMSO or GW572016 (10 µM) for 3 h. Cells were fixed in paraformaldehyde, permeabilized in buffered Triton-X 100 (0.1%), and stained with **(A)** KMX-1 (anti β-tubulin mouse mAb), **(B)** 12G10 (anti α-tubulin mouse mAb), or **(C)** YL1/2 (anti tyrosinated α-tubulin rat mAb). Nucleus (n) and kinetoplast (k) were stained with DAPI (blue). Appropriate secondary antibodies were used as described in *Materials and Methods*. The DIC and the merged images are also shown. Scale bar equals 10 µm in all DIC panels.

Figure 2.4

Figure 2.5: Flagellum topology is altered by GW572016 treatment of *T. brucei*. (A) Indirect immunofluorescence on DMSO (control) or 10 µM GW572016-treated *T. brucei* (5 x 10^5/ml) using L8C4 (anti-PFR 2 mouse mAb). Cells were treated for 3 h prior to fixation in paraformaldehyde and permeabilization (1% Triton X-100). A secondary anti-mouse antibody conjugated to Alexa Fluor-594 (red) was used. DAPI staining (blue) indicates the positions of nucleus (n) and kinetoplast (k). Scale bar is 10 µm. **(B)** Scanning electron micrographs (SEM) of the control and GW572016-treated *T. brucei*. Scale bar is 2 µm.
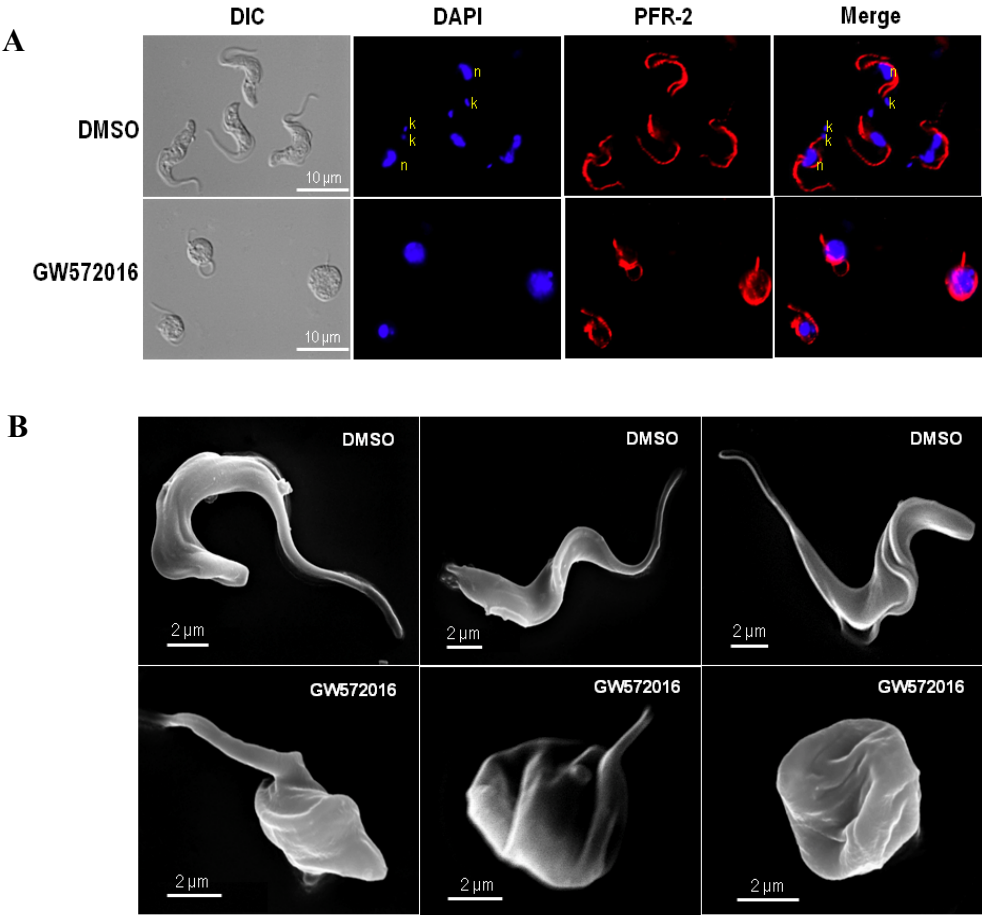
Figure 2.5

Figure 2.6: GW572016 inhibits transferrin endocytosis. Trypanosomes (5 x 10^5) were incubated with transferrin-AlexaFluor488 (Tf-Alexa488) conjugate and various concentrations of GW572016 (There was no preincubation of trypanosomes with the drug.) Propidium iodide (PI) was added as described in Materials and Methods. The Tf-Alexa488 and PI fluorescence of cellular events were determined by flow cytometry. (**A**) Representative plot of trypanosome Tf-Alexa488 fluorescence in the presence of GW572016 (dashed line) or DMSO control (solid line). (**B**) Quantification of endocytosed Tf. Median Tf-Alexa488 fluorescence of trypanosomes in the presence of 0 (DMSO only), 1 µM, 2 µM, or 3 µM GW572016. Error bars represent one standard deviation in data from three independent experiments.

Figure 2.6
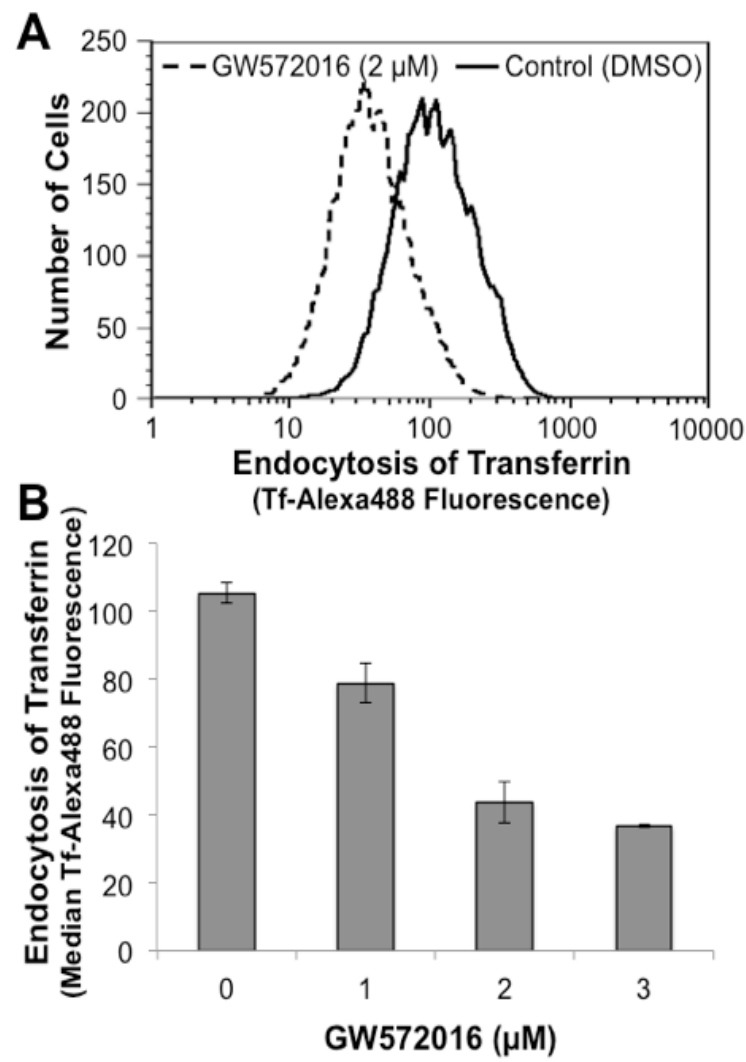
(Data from Paul Guyett)

Table 2.1: Class I proteins nonselectively bind Sepharose CL4B and an anti-pTyr affinity column. Bloodstream trypanosomes (2 x 10^8 total) were treated with either DMSO or GW572016, lysed, and adsorbed to anti-phosphotyrosine antibody column (immobilized P-Tyr-100). Sepharose CL-4B column was used as a control. Proteins were eluted sequentially from the columns with Tyrphostin A47 (200 µM), phenyl phosphate (200 mM), and 1X SDS buffer. Eluted proteins were identified by LC-MS/MS and quantitated by spectral counting. Background (proteins binding to sepharose CL4B) was removed from the list. Proteins that bound to both the Sepharose CL-4B column and the P-Tyr-100 columns in equal amounts are considered nonselective (Class I). Data presented is from a representative experiment; see *Materials and Methods* for other details of protocol.

Table 2.1: Proteins showing nonselective binding with P-Tyr-100 antibody column (Class I)

Gene ID	Protein Description	Spectral Count	
		Treatment of Cells	
		DMSO Sep CL-4B	DMSO Sep P-Tyr-100
(A) Cell Morphogenesis and Motility			
Tb427tmp.02.2970	Kinesin	5	5
Tb427tmp.244.2800	Trypanin-related protein	6	5
Tb427.01.2380	Alpha Tubulin*	31	38
Tb427tmp.01.3010	Dynein heavy chain	20	19
(B) Cellular Transport			
Tb427.10.7060	Nucleoporin interacting component (NUP93)	2	2
Tb427.10.14180	Protein transport protein Sec13	3	3
(C) Calcium Metabolism			
Tb427.06.4710	Calmodulin	8	8
(D) Protein Synthesis			
Tb427.10.560	40S ribosomal proteins S11	2	2
(E) Cellular Oxidation-Reduction			
Tb427tmp.160.4250	Tryparedoxin peroxidase*	4	4
(F) DNA/RNA/ Nucleotide Metabolism			
Tb427tmp.160.5560	Adenylosuccinate lyase	3	4
Tb427.05.4170	Histone H4A*	6	7
Tb427.02.5660	Adenylate kinase	9	9
(G) Uncharacterized			
Tb427tmp.02.1190	Hypothetical protein, conserved	12	12
Tb427.05.2950	Hypothetical protein, conserved	12	12

Indicates that more than one gene copies were found for the protein.

Table 2.2: Class II proteins: Their preferential binding to anti-pTyr Affinity column is not affected by pretreatment of *T. brucei* with GW572016. Trypanosome lysates were processed as described as described in *Legend* for Table 2.1 and the flow chart for Figure 2A. Eluted proteins were identified by LC-MS/MS and quantitated by spectral counting. Data presented is a representative experiment (see *Materials and Methods* for detailed description of protocols and criteria for listing of polypeptides).

Table 2.2: Proteins whose association with P-Tyr-100 antibody is not affected by GW572016 (Class II)

Gene ID	Protein Description	Spectral Count		
		Treatment of Cells		
		DMSO Sep CL-4B	DMSO Sep P-Tyr-100	GW572016 Sep P-Tyr-100
(A) Protein Synthesis				
Tb427.10.14600*	40S ribosomal protein S2*	0	3	5
Tb427.10.3930	40S ribosomal protein S3a	0	3	4
Tb427tmp.02.1085	40S ribosomal protein S4*	0	4	4
Tb427.04.1800	60S ribosomal protein L3, mitochondrial*	0	5	5
(B) Uncharacterized				
Tb427.06.1660	Hypothetical protein, conserved	0	4	4
Tb427.10.2190	Hypothetical protein, conserved	0	5	5

Indicates that more than one gene copies were found for the protein.

Table 2.3: Class III proteins are in a GW572016-susceptible phosphotyrosine pathway.

T. brucei lysates were processed for chromatography as described in *Materials* and *Methods* and summarized in the Legend for Table 2.1. Proteins were identified as described in Table 2.1 legend. Listed here are proteins that were eluted with Tyrphostin A47 and phenyl phosphate, from cells that had been pretreated with GW572016. Data presented is from a representative experiment as explained in *Materials* and *Methods*.

Table 2.3: Proteins in GW572016-susceptible phosphotyrosine pathway (Class III)

Tyrphostin A47 and phenyl phosphate elution

		Spectral Count		
		Treatment of Cells		
Gene ID	**Protein Description**	**DMSO Sep CL-4B**	**DMSO Sep P-Tyr-100**	**GW572016 Sep P-Tyr-100**
(A) Cell Morphogenesis and Motility				
Tb427.05.4480	Paraflagellar rod component Par4*	0	24	7
Tb427.10.10140	Paraflagellar rod component (PFC19)	0	7	3
Tb427tmp.02.2060	Flagellar radial spoke component	0	3	0
Tb427tmp.211.1470	Flagellar component, PACRGB	0	2	0
Tb427.08.6660	Paraflagellar rod component (PFC1)	3	32	16
Tb427tmp.01.5100	Paraflagellar rod component	4	33	12
Tb427tmp.01.3960	Flagellar pocket complex protein (BILBO1)	8	16	8
Tb427.03.4300	73 kDa Paraflagellar rod protein (PFR-1/PFR-C)*	20	157	64
(B) Energy Metabolism				
Tb427.03.3270	ATP-dependent phosphofructokinase (TbPFK)			
Tb427tmp.02.5500	Glucose-regulated protein 78*	0	19	4
Tb427tmp.211.3560	Glycerol kinase, glycosomal (GLK1)*	0	6	2
Tb427.06.4280	Glyceraldehyde 3-phosphate dehydrogenase, glycosomal	0	2	0
Tb427.10.5620	(GAPDH)*	0	13	5
	Fructose-bisphosphate aldolase, glycosomal (ALD)	9	31	9
(D) Uncharacterized				
Tb427.07.3740	Hypothetical protein, conserved	0	9	4
Tb427tmp.01.2390	Hypothetical protein, conserved	0	8	2
Tb427.08.4580	Hypothetical protein, conserved	0	7	0
Tb427.04.4700	Hypothetical protein, conserved	0	6	0
Tb427tmp.02.4230	Hypothetical protein, conserved	0	5	0
Tb427.10.6490	Hypothetical protein, conserved	0	4	0
Tb427.05.1230	Hypothetical protein, conserved	0	2	0
Tb427.07.4100	Hypothetical protein, conserved	0	2	0
Tb427.07.3550	Hypothetical protein, conserved	0	2	0
Tb427tmp.160.3930	Hypothetical protein, conserved	0	2	0
Tb427.07.6910	Hypothetical protein, conserved	2	9	4

Indicates that more than one gene copies were found for the protein.

Table 2.4: SDS-eluted proteins in GW572016-susceptible phosphotyrosine pathway (Class III) Trypanosome lysates were processed and proteins were identified as described in legend for Table 2.3, except that proteins were obtained with heated 1X SDS-PAGE sample buffer from the P-Tyr-100 column after the phenyl phosphate elution.

Table 2.4: Proteins in GW572016-susceptible phosphotyrosine pathway (Class III)

SDS (5%) eluate

Gene ID	Protein Description	Spectral Count		
		Treatment of Cells		
		DMSO Sep CL-4B	DMSO Sep P-Tyr-100	GW572016 Sep P-Tyr-100
(A) Cell Morphogenesis and Motility				
Tb427tmp.211.0620	Actin A*	0	5	2
Tb427tmp.211.1470	Flagellar component, PACRGB	3	8	4
Tb427.06.4670	MORN repeat-containing protein (TbMORN1)	8	23	7
(B) Organelle Biogenesis				
Tb427.02.4230	NUP-1 protein	6	18	9
(C) Energy Metabolism				
Tb427tmp.211.0540	Fructose 1,6 bisphosphate, cytosolic (FBPase)	0	2	0
Tb427.03.3270	ATP-dependent phosphofructokinase (TbPFK)	9	18	4
(D) Protein Synthesis				
Tb927.08.1110	40S ribosomal protein S9*	0	2	0
Tb427tmp.160.2550	Ribosomal protein S7	0	4	0
Tb427.10.2100	Translation elongation factor 1-alpha (EF1)*	6	16	5
(E) Protein Modification				
Tb427tmp.01.1680	Polyubiquitin	0	2	0
(F) DNA/RNA Metabolism				
Tb427.01.2430	Histone H3*	0	4	0
Tb427tmp.160.3820	Nucleolar RNA binding protein	3	6	0
(G) Uncharacterized				
Tb427.06.5070	Hypothetical protein, conserved	0	2	0
Tb427.08.8200	Hypothetical protein, conserved	0	5	0
Tb427.03.5020	Hypothetical protein, conserved	2	7	4
Tb427.01.4310	Hypothetical protein, conserved	3	50	21

* *Indicates that more than one gene copies were found for the protein.*

References

1.   Lemmon, M.A. and J. Schlessinger, *Cell signaling by receptor tyrosine kinases.* Cell, 2010. **141**(7): p. 1117-34.

2.   Lim, W.A. and T. Pawson, *Phosphotyrosine signaling: evolving a new cellular communication system.* Cell, 2010. **142**(5): p. 661-7.

3.   Parsons, M., et al., *Comparative analysis of the kinomes of three pathogenic trypanosomatids: Leishmania major, Trypanosoma brucei and Trypanosoma cruzi.* BMC Genomics, 2005. **6**: p. 127.

4.   Lochhead, P.A., et al., *dDYRK2: a novel dual-specificity tyrosine-phosphorylation-regulated kinase in Drosophila.* The Biochemical journal, 2003. **374**(Pt 2): p. 381-91.

5.   Nett, I.R., et al., *The phosphoproteome of bloodstream form Trypanosoma brucei, causative agent of African sleeping sickness.* Mol Cell Proteomics, 2009. **8**(7): p. 1527-38.

6.   Das, A., et al., *A major tyrosine-phosphorylated protein of Trypanosoma brucei is a nucleolar RNA-binding protein.* The Journal of biological chemistry, 1996. **271**(26): p. 15675-81.

7.   Parsons, M., et al., *Developmental regulation of pp44/46, tyrosine-phosphorylated proteins associated with tyrosine/serine kinase activity in Trypanosoma brucei.* Molecular and Biochemical Parasitology, 1994. **63**(1): p. 69-78.

8.   Schell, D., N.K. Borowy, and P. Overath, *Transferrin is a growth factor for the bloodstream form of Trypanosoma brucei.* Parasitology research, 1991. **77**(7): p. 558-60.

9.   Subramanya, S., et al., *Glycosylphosphatidylinositol-specific phospholipase C regulates transferrin endocytosis in the African trypanosome.* The Biochemical journal, 2009. **417**(3): p. 685-94.

10.   Subramanya, S. and K. Mensa-Wilmot, *Diacylglycerol-stimulated endocytosis of transferrin in trypanosomatids is dependent on tyrosine kinase activity.* PLoS One, 2010. **5**(1): p. e8538.

11.   Bakhiet, M., et al., *African trypanosomes activate human fetal brain cells to proliferation and IFN-gamma production.* Neuroreport, 2002. **13**(1): p. 53-6.

12.   Bellows, D.S. and M. Tyers, *Cell biology. Chemical genetics hits.* Science, 2004. **306**(5693): p. 67-8.

13. Shokat, K. and M. Velleca, *Novel chemical genetic approaches to the discovery of signal transduction inhibitors.* Drug discovery today, 2002. **7**(16): p. 872-9.

14. Katiyar, S., et al., *Lapatinib-binding protein kinases in the african trypanosome: identification of cellular targets for kinase-directed chemical scaffolds.* PLoS One, 2013. **8**(2): p. e56150.

15. Hirumi, H., J.J. Doyle, and K. Hirumi, *African trypanosomes: cultivation of animal-infective Trypanosoma brucei in vitro.* Science, 1977. **196**(4293): p. 992-4.

16. Sasse, R. and K. Gull, *Tubulin post-translational modifications and the construction of microtubular organelles in Trypanosoma brucei.* Journal of cell science, 1988. **90 (Pt 4)**: p. 577-89.

17. Armah, D.A. and K. Mensa-Wilmot, *S-myristoylation of a glycosylphosphatidylinositol-specific phospholipase C in Trypanosoma brucei.* The Journal of biological chemistry, 1999. **274**(9): p. 5931-8.

18. Rusnak, D.W., et al., *The effects of the novel, reversible epidermal growth factor receptor/ErbB-2 tyrosine kinase inhibitor, GW2016, on the growth of human normal and tumor-derived cell lines in vitro and in vivo.* Mol Cancer Ther, 2001. **1**(2): p. 85-94.

19. Xia, W., et al., *Anti-tumor activity of GW572016: a dual tyrosine kinase inhibitor blocks EGF activation of EGFR/erbB2 and downstream Erk1/2 and AKT pathways.* Oncogene, 2002. **21**(41): p. 6255-63.

20. Lackey, K.E., *Lessons from the drug discovery of lapatinib, a dual ErbB1/2 tyrosine kinase inhibitor.* Current topics in medicinal chemistry, 2006. **6**(5): p. 435-60.

21. Rush, J., et al., *Immunoaffinity profiling of tyrosine phosphorylation in cancer cells.* Nature Biotechnology, 2005. **23**(1): p. 94-101.

22. Rikova, K., et al., *Global survey of phosphotyrosine signaling identifies oncogenic kinases in lung cancer.* Cell, 2007. **131**(6): p. 1190-203.

23. Vedrenne, C., et al., *Two related subpellicular cytoskeleton-associated proteins in Trypanosoma brucei stabilize microtubules.* Molecular biology of the cell, 2002. **13**(3): p. 1058-70.

24. Schneider, A., et al., *Subpellicular and flagellar microtubules of Trypanosoma brucei brucei contain the same alpha-tubulin isoforms.* The Journal of cell biology, 1987. **104**(3): p. 431-8.

25.   Ngo, H., et al., *Double-stranded RNA induces mRNA degradation in Trypanosoma brucei.* Proceedings of the National Academy of Sciences of the United States of America, 1998. **95**(25): p. 14687-14692.

26.   Gull, K., *The cytoskeleton of trypanosomatid parasites.* Annual review of microbiology, 1999. **53**: p. 629-55.

27.   Kreitzer, G., G. Liao, and G.G. Gundersen, *Detyrosination of tubulin regulates the interaction of intermediate filaments with microtubules in vivo via a kinesin-dependent mechanism.* Molecular biology of the cell, 1999. **10**(4): p. 1105-18.

28.   Sherwin, T. and K. Gull, *Visualization of detyrosination along single microtubules reveals novel mechanisms of assembly during cytoskeletal duplication in trypanosomes.* Cell, 1989. **57**(2): p. 211-21.

29.   Kohl, L., T. Sherwin, and K. Gull, *Assembly of the paraflagellar rod and the flagellum attachment zone complex during the Trypanosoma brucei cell cycle.* The Journal of eukaryotic microbiology, 1999. **46**(2): p. 105-9.

30.   Subramanya, S. and K. Mensa-Wilmot, *Regulated cleavage of intracellular glycosylphosphatidylinositol in a trypanosome. Peroxisome-to-endoplasmic reticulum translocation of a phospholipase C.* The FEBS journal, 2006. **273**(10): p. 2110-26.

31.   Portman, N., et al., *Combining RNA Interference Mutants and Comparative Proteomics to Identify Protein Components and Dependences in a Eukaryotic Flagellum.* Journal of Biological Chemistry, 2009. **284**(9): p. 5610-5619.

32.   Bastin, P., et al., *Flagellar morphogenesis: protein targeting and assembly in the paraflagellar rod of trypanosomes.* Molecular and cellular biology, 1999. **19**(12): p. 8191-200.

33.   Wilson, M.E., et al., *Acquisition of iron from transferrin and lactoferrin by the protozoan Leishmania chagasi.* Infection and immunity, 1994. **62**(8): p. 3262-9.

34.   Steverding, D., *Bloodstream forms of Trypanosoma brucei require only small amounts of iron for growth.* Parasitology research, 1998. **84**(1): p. 59-62.

35.   Bonhivers, M., et al., *Biogenesis of the trypanosome endo-exocytotic organelle is cytoskeleton mediated.* Plos Biology, 2008. **6**(5): p. 1033-1046.

36.   Portman, N. and K. Gull, *The paraflagellar rod of kinetoplastid parasites: From structure to components and function.* International Journal for Parasitology, 2010. **40**(2): p. 135-148.

37.   Grab, D.J., et al., *The Transferrin Receptor in African Trypanosomes - Identification, Partial Characterization and Subcellular-Localization.* European Journal of Cell Biology, 1993. **62**(1): p. 114-126.

38.   Garcia-Salcedo, J.A., et al., *A differential role for actin during the life cycle of Trypanosoma brucei.* The EMBO journal, 2004. **23**(4): p. 780-9.

39.   Terman, J.R. and A. Kashina, *Post-translational modification and regulation of actin.* Current opinion in cell biology, 2013. **25**(1): p. 30-8.

CHAPTER III

A STRUCTURE-ACTIVITY-RELATIONSHIP STUDY FOR OPTIMIZATION

OF 4-ANILINOQUINAZOLINE SCAFFOLD AND DISCOVERY OF

ANTI-TRYPANOSOMAL LEADS[2]*

Abstract

New orally bioavailable drugs are immediately needed to treat Human African Trypanosomiasis (HAT), an infection caused by *Trypanosoma brucei*. The four drugs currently in use for HAT are given intravenously and have toxicity issues. The commercial drug discovery scenario for neglected diseases like HAT is less promising. To overcome this problem, an alternative use drug discovery strategy is logical that allows testing of clinically proven drugs for parasitic diseases. We have shown that the 4-anilinoquinazolines like lapatinib (GW572016) and canertinib (CI-1033) are potent antitrypanosmal compounds with GI_{50} in the low micromolar range (~1.5 µM). Further, a focused screen of nine lapatinib analogs from GlaxoSmithKline resulted in the discovery of more potent compounds with nanomolar GI_{50} (~400 nM). Inspired by this data we initiated a collaborative study to optimize the 4-anilinoquinazoline scaffold through *in vitro* drug activity assay on trypanosome growth. We hereby report the scaffold optimization strategy that that led to the development of several novel 4-anilinoquinazolines with low nanomolar GI_{50} profile (< 200 nM) against *T. brucei.*

3.1 Introduction

Parasitic diseases are a major threat to the lives and economy in the developing countries. Many such diseases have been classified as 'Neglected Tropical Diseases (NTD)' because of inadequate attention for control and prevention. It is estimated that over 1 billion people are infected by one or more NTD with many others at risk **[1]**. The pharmaceutical sector lacks interest in developing drug for NTD. To deal with this situation, a cost-effective approach is essential for identification of lead drugs.

Repurposing proven classes of molecular targets that are biologically essential in the parasite is one such approach to expedite drug discovery against these NTDs **[2]**. For example,

kinases and phosphodiesterases (PDEs) regulate many essential signaling pathways in all trypanosomatids like *Trypanosoma brucei, T. cruzi,* and *Leishmania spp.* that causes Human African Trypanosomiasis (HAT)/ Sleeping sickness, American Trypanosomiasis/ Chagas' disease, and Leishmaniasis respectively[3, 4]. Also, several kinases and PDEs in humans are established as drug targets for a variety of diseases, and large amount of information about the medicinal chemistry, toxicology, and structural biology are available. A novel antiparasitic drug discovery campaign can potentially benefit from these resources that can be extended to the identification and optimization of promising chemical scaffold. This approach has already been considered an excellent starting point for new antiparasitic lead discovery by several groups [5-9].

Nearly 50,000 people in the sub-Saharan Africa are susceptible to *T. brucei* infection annually. An infected tsetse fly serves as a transmission vector that injects the parasites into the bloodstream of human host. The parasites proliferate in the blood (early stage) and produces flu-like symptoms. Subsequently, the parasites enter the central nervous system (CNS) bypassing the blood brain barrier (late stage) and manifest more severe symptoms like sleep disruption and coma leading to death. Currently used drugs are toxic and require intravenous dosing. Therefore, new oral drugs with minimal toxicity are urgently needed that can be equally effective against both early and late stage of the disease [10].

Kinases have been targeted in drug discovery for a wide variety of human diseases including cancer [11], inflammation [12, 13], diabetes [14, 15], and CNS diseases[16]. Many tyrosine kinase inhibitors are now in the clinical use which includes lapatinib (GW572016, Tykerb, **1**), an EGFR inhibitor approved by FDA [17, 18]. There are more than 180 protein kinases expressed in *T. brucei* [19, 20], and kinases such as glycogen synthase kinase-3 [21],

phosphoinositoyl-3-kinases/TOR[7] and Aurora kinase 1[6] have already been investigated in the parasite. Protein Tyr phosphorylation in *T. brucei* has already been reported [22, 23]. However, the conventional receptor tyrosine kinases (RTKs) are absent. It is therefore believed that Tyr-phosphorylation is performed by dual-specificity kinases (*e.g.*, wee1) that can phosphorylate Ser/Thr as well as Tyr residues [4]. Recent studies indicate that enzymes with "EGFR-like" kinase domains are present in the parasite [24]. Further, inhibitors of human EGFR/HER2 such as canertinib [25], lapatinib [26], and AEE788 [27], kill *T. brucei* with GI_{50} in the low micromolar range [24].

Based on the finding that lapatinib kills *T. brucei*, we performed a focused screen of nine EGFR inhibitors from GlaxoSmithKline (**Table 3.1**). Subsequent novel lapatinib analogs were synthesized for a structure activity relationship study of a 6-phenyl 4-anilinoquinazoline scaffold. We hereby report the discovery NEU617 (**23a**), a highly selective and potent inhibitor of trypanosome replication *in vitro*.

3.2 Materials And Methods

3.2.1 Chemical synthesis

Unless otherwise noted, reagents were obtained from Sigma-Aldrich, Inc. (St. Louis, MO), or Frontier Scientific Services, Inc. (Newark, DE) and used as received. Boronic acids and aniline reagents were purchased, unless the synthesis is specifically described below. Reaction solvents were purified by passage through alumina columns on a purification system manufactured by Innovative Technology (Newburyport, MA). NMR spectra were obtained with Varian NMR systems, operating at 400 or 500 MHz for ^{1}H acquisitions as noted. LCMS analysis was performed using a Waters Alliance reverse-phase HPLC, with single-wavelength UV-visible detector and LCT Premier time-of-flight mass spectrometer (electrospray ionization). All newly

synthesized compounds were that were submitted for biological testing were deemed >95% pure by LCMS analysis (UV and ESI-MS detection) prior to submission for biological testing. Preparative LCMS was performed on a Waters FractionLynx system with a Waters MicroMass ZQ mass spectrometer (electrospray ionization) and a single-wavelength UV-visible detector, using acetonitrile/water gradients with 0.1% formic acid. Fractions were collected on the basis of triggering using UV and mass detection.

4-chloro-6-iodoquinazoline hydrochloride (13). **[40]**. Yield: 85%. ^{1}H NMR (500 MHz, DMSO-d$_6$) δ: 8.39 (d, J = 1.95 Hz, 1H), 8.29 (s, 1H), 8.13 (dd, J = 1.95, 8.30 Hz, 1H), 7.49 (d, J = 8.30 Hz, 1H). MS: m/z = 290.83 (M+H)[+].

N-(3-chloro-4-((3-fluorobenzyl)oxy)phenyl)-6-iodoquinazolin-4-amine hydrochloride (14). **[41]**. Yield: 84%. ^{1}H NMR (500 MHz, DMSO-d$_6$) δ: 11.21 (br. s., 1H), 9.16 (s, 1H), 8.92 (s, 1H), 8.34 (d, J = 8.79 Hz, 1H), 7.93 (d, J = 2.44 Hz, 1H), 7.64 - 7.68 (m, 2H), 7.46 - 7.51 (m, 1H), 7.30 - 7.37 (m, 2H), 7.20 (dt, J = 2.44, 8.79 Hz, 1H), 5.30 (s, 2H). MS: m/z = 505.85 (M+H)[+].

Libraries of **10** were synthesized by Suzuki coupling of **14** with respective boronic acid/esters following **General procedure A**. Into glass vials was combined N-(3-chloro-4-((3-fluorobenzyl)oxy)phenyl)-6-iodoquinazolin-4-amine (**14**, 100 μM), boronic acids/esters (120 μmol) and tetrakis(triphenylphosphine)palladium(0) (7 μmol). To the reaction mixture was added 1,2-dimethoxyethane (2 mL), ethanol (1.33 mL) and a 2M aqueous solution of sodium carbonate (0.301 mL, 600 μM). The vials were capped and shaken at 80 °C for 18 h. The progress of the reaction was followed by LC-MS. Reaction mixture was evaporated to dryness. Crude products were purified using flash column chromatography, or by dissolving in DMSO and purifying by reverse phase HPLC using a gradient of 30-100% acetonitrile in water containing 0.1% formic acid.

N-(3-chloro-4-((3-fluorobenzyl)oxy)phenyl)-6-(4-(morpholinosulfonyl)phenyl)quinazolin-4-amine (10a). Yield: 48.1%. ^{1}H NMR (500 MHz, DMSO-d$_6$) δ: 10.00 (s, 1H), 8.92 (d, J = 1.46 Hz, 1H), 8.64 (s, 1H), 8.28 (dd, J = 1.95, 8.79 Hz, 1H), 8.17 (d, J = 8.79 Hz, 2H), 8.04 (d, J = 2.44 Hz, 1H), 7.92 (d, J = 8.79 Hz, 3H), 7.76 (dd, J = 2.45, 8.80 Hz, 1H), 7.46 - 7.50 (m, 1H), 7.30 - 7.36 (m, 3H), 7.19 - 7.23 (m, 1H), 5.28 (s, 2H), 3.66 - 3.68 (m, 4H), 2.93 - 2.95 (m, 4H). MS: m/z = 605.2 (M+H)$^+$.

N-(3-chloro-4-((3-fluorobenzyl)oxy)phenyl)-6-(4-methylnaphthalen-1-yl)quinazolin-4-amine, (10b). Yielded 1 mg (2.6%) as a yellow film. ^{1}H NMR (400 MHz, DMSO-d$_6$) δ: 9.82 (s, 1H), 8.65 (s, 2H), 8.15 (d, J = 8.8 Hz, 1H), 8.03 (d, J = 2.2 Hz, 1H), 7.87-7.96 (m, 2H), 7.81 (d, J = 8.8 Hz, 1H), 7.71-7.76 (m, 1H), 7.63 (t, J = 8.0 Hz, 1H), 7.49-7.57 (m, 2H), 7.42-7.49 (m, 2H), 7.31 (t, J = 6.0 Hz, 2H), 7.25 (d, J = 8.8 Hz, 1H), 7.17 (t, J = 7.3 Hz, 1H), 5.24 (s, 2H), 2.74 (s, 3H). MS: m/z = 520.1 (M+H)$^+$.

4-(4-((3-chloro-4-((3-fluorobenzyl)oxy)phenyl)amino)quinazolin-6-yl)-N-ethyl-2-fluorobenzamide (10c). Yielded 1 mg (2.4%) as a yellow film. ^{1}H NMR (400 MHz, DMSO-d$_6$) δ: 9.98 (s, 1H), 8.87 (s, 1H), 8.58-8.61 (s, 1H), 8.35-8.42 (m, 1H), 8.26-8.34 (m, 1H), 8.01 (s, 1H), 7.87 (d, J = 4.4 Hz, 1H), 7.84 (m, 2H), 7.79 (d, J = 8.1 Hz, 1H), 7.70-7.76 (m, 1H), 7.47 (q, J = 7.3 Hz, 1H), 7.32 (dd, J$_A$ = 13.2 Hz, J$_B$ = 7.3 Hz, 3H),   7.18 (t, J = 8.8 Hz, 1H), 5.27 (s, 2H), 3.29 (q, J = 8.0 Hz, 2H), 1.14 (t, J = 7.0 Hz, 3H).: MS: m/z = 545.2 (M+H)$^+$.

N-(3-chloro-4-((3-fluorobenzyl)oxy)phenyl)-6-(3-(5-methyl-1,3,4-oxadiazol-2-yl)phenyl) quinazolin-4-amine (10d). Obtained 1 mg (2.5% yield) as a yellow oil. ^{1}H NMR (400 MHz, DMSO-d$_6$) δ: 9.09-10.04 (brs, 1H), 8.88 (s, 1H), 8.61 (s, 1H), 8.42 (s, 1H), 8.37 (s, 1H), 8.26 (d, J = 8.8 Hz, 1H), 8.11 (d, J = 8.1 Hz, 1H), 8.0 (m, 2H), 7.89 (d, J = 8.8 Hz, 1H), 7.72-7.81 (m,

2H), 7.43-7.51 (m, 1H), 7.28-7.36 (m, 2H), 7.14-7.22 (m, 1H) 5.26 (s, 2H), 2.65 (s, 3H). MS: m/z = 538.1 (M+H)$^+$.

3-(4-((3-chloro-4-((3-fluorobenzyl)oxy)phenyl)amino)quinazolin-6-yl)-*N*-cyclopropylbenzamide (10e).   Yielded 0.8 mg (2.0%) as a yellow film. ^{1}H NMR (400 MHz, DMSO-d$_6$) δ: 10.00 (s, 1H), 8.83 (s, 1H), 8.63 (d, J = 3.7 Hz, 1H), 8.59 (s, 1H), 8.35 (s, 1H), 8.26 (d, J = 5.1 Hz, 1H), 8.22 (s, 1H), 7.97-8.05 (m, 1H), 7.87 (t, J = 8.1Hz, 2H), 7.74 (dd, J$_A$ = 8.8 Hz, J$_B$ = 2.0 Hz, 1H), 7.63 (t, J = 7.7 Hz, 1H), 7.43-7.52 (m, 1H), 7.25-7.35 (m, 2H), 7.17 (t, J = 8.0 Hz, 1H), 5.27 (s, 2H), 2.85-2.92 (m, 1H), 0.69-0.76 (m, 2H), 0.58-0.65 (m, 2H). MS: m/z = 539.2 (M+H)$^+$.

***N*-(3-chloro-4-((3-fluorobenzyl)oxy)phenyl)-6-(quinolin-5-yl)quinazolin-4-amine   (10f).** Yielded 3.2 mg (8.4%) as a yellow solid. ^{1}H NMR (400 MHz, DMSO-d$_6$) δ: 9.81 (s, 1H), 8.98 (d, J = 2.9 Hz, 1H), 8.70 (s, 1H), 8.68 (s, 1H), 8.21-8.27 (m, 2H), 8.14 (d, J = 8.1 Hz, 1H), 8.03 (d, J = 2.2 Hz, 1H), 7.95-8.00 (m, 1H), 7.88-7.95 (m, 3H),7.68-7.96 (m, 2H), 7.53-7.59 (dd, J$_A$ = 8.4 Hz, J$_B$ = 4.0 Hz, 1H), 7.46 (q, J = 8.0 Hz, 1H), 7.22-7.33 (m, 3H), 7.17 (t, J = 8.8 Hz, 1H), 5.23 (s, 2H). MS: m/z = 508.2 (M+H)$^+$.

***N*-(3-chloro-4-((3-fluorobenzyl)oxy)phenyl)-6-(2-phenoxyphenyl)quinazolin-4-amine   (10g).** Yielded 1.4 mg (2.4%) as an orange oil. ^{1}H NMR (400 MHz, DMSO-d$_6$) δ: 9.85 (s, 1H), 8.65 (s, 1H), 8.58 (s, 1H), 8.01-8.06 (m, 2H), 7.72-7.78 (m, 2H), 7.67 (d, J = 6.6 Hz, 1H), 7.42-7.51 (m, 2H), 7.24-7.39 (m, 6H), 7.19 (t, J = 7.3 Hz, 1H), 7.00-7.09 (m, 2H), 6.94 (d, J = 8.1 Hz, 2H), 5.27 (s, 2H). MS: m/z = 548.1 (M+H)$^+$.

6-(benzo[b]thiopen-2-yl)-*N*-(3-chloro-4-((3-fluorobenzyl)oxy)phenyl)quinazolin-4-amine (10h). Obtained 5.4 mg (14% yield) as a yellow solid. ^{1}H NMR (400 MHz, DMSO-d$_6$) δ: 8.75 (s, 1H), 8.15 (t, J = 8.8 Hz, 1H), 8.03 (m, 1H), 7.96 (d, J = 8.8 Hz, 1H), 7.87 (d, J = 2.1 Hz, 2H),

7.82 (d, J = 7.3 Hz, 1H), 7.68 (s, 1H), 7.51-7.59 (m, 1H), 7.49 (s, 1H), 7.32-7.44 (m, 3H), 7.19-7.25 (m, 1H), 6.91-7.09 (m, 2H), 5.27 (s, 2H). MS: *m*/z = 512.0 (M+H)$^+$.

4-(4-((3-chloro-4-((3-fluorobenzyl)oxy)phenyl)amino)quinazolin-6-yl)phenol (10i). Yielded 1 mg (2.4%) as a yellow film. ^{1}H NMR (400 MHz, DMSO-d$_6$) δ: 10.09 (s, 1H), 8.98 (s, 1H), 8.63 (s, 2H), 8.45 (s, 1H), 8.42 (s, 1H), 8.05 (s, 1H), 7.96 (d, J = 8.8 Hz, 1H), 7.82 (d, J = 9.5 Hz, 1H), 7.43-7.51 (m, 2H), 7.27-7.36 (m, 2H), 7.14-7.22 (m, 1H), 6.66-6.72 (m, 2H), 5.27 (s, 2H). MS: *m*/z = 472.1 (M+H)$^+$.

5-(4-((3-chloro-4-((3-fluorobenzyl)oxy)phenyl)amino)quinazolin-6-yl)pyrimidine-2,4(1H,3H)-dione (10j). Yielded 2.6 mg (7.1%) as a yellow solid. ^{1}H NMR (400 MHz, DMSO-d$_6$) δ: 9.76-9.82 (brs, 1H), 8.47-8.59 (m, 2H), 8.30 (s, 1H), 8.04 (m, 2H), 7.81-7.88 (m, 1H), 7,71-7.80 (m. 2H), 7.59-7.67 (m, 1H), 7.43-7.50 (m, 1H), 7.31-7.36 (m, 1H), (m, 7.23-7.31 (m, 2H), 7.18 (t, J = 8.4 Hz, 1H), 5.26 (s, 2H). MS: *m*/z = 490.0 (M+H)$^+$.

N-(3-chloro-4-((3-fluorobenzyl)oxy)phenyl)-6-(3-(morpholinosulfonyl)phenyl)quinazolin-4-amine (10k). Yield: 30.4%. ^{1}H NMR (500 MHz, DMSO-d$_6$) δ: 10.01 (s, 1H), 8.85 (d, *J* = 1.95 Hz, 1H), 8.63 (s, 1H), 8.24 - 8.27 (m, 2H), 8.12 (t, *J* = 1.71 Hz, 1H), 8.03 (d, *J* = 2.93 Hz, 1H), 7.86 - 7.92 (m, 2H), 7.80 - 7.85 (m, 1H), 7.73 (dd, *J* = 2.44, 8.79 Hz, 1H), 7.46 - 7.52 (m, 1H), 7.30 - 7.35 (m, 3H), 7.17 - 7.22 (m, 1H), 5.28 (s, 2H), 3.66 (t, *J* = 4.90 Hz, 4H), 2.95 (t, *J* = 4.40 Hz, 4H). MS: *m*/z = 605.1 (M+H)$^+$.

N-(3-chloro-4-((3-fluorobenzyl)oxy)phenyl)-6-(4-(piperidin-1-ylsulfonyl)phenyl)quinazolin-4-amine (10l). Yield: 14.6%. ^{1}H NMR (500 MHz, DMSO-d$_6$) δ: 10.00 (s, 1H), 8.91 (d, *J* = 1.46 Hz, 1H), 8.64 (s, 1H), 8.27 (dd, *J* = 1.95, 8.30 Hz, 1H), 8.14 (d, *J* = 8.30 Hz, 2H), 8.04 (d, *J* = 2.93 Hz, 1H), 7.89 - 7.92 (m, 3H), 7.76 (dd, *J* = 2.69, 9.03 Hz, 1H), 7.46 - 7.51 (m, 1H), 7.31 -

7.36 (m, 3H), 7.20 (dt, J = 2.44, 8.55 Hz, 1H), 5.28 (s, 2H), 2.95 - 2.98 (m, 4H), 1.55 - 1.60 (m, 4H), 1.39 - 1.40 (m, 2H). MS: m/z = 603.2 (M+H)$^+$.

N-(3-chloro-4-((3-fluorobenzyl)oxy)phenyl)-6-(3-(piperidin-1-ylsulfonyl)phenyl)quinazolin-4-amine (10m). Yield: 24.8%. ^{1}H NMR (500 MHz, DMSO-d$_6$) δ: 10.01 (s, 1H), 8.84 (d, J = 1.95 Hz, 1H), 8.62 (s, 1H), 8.24 (dd, J = 1.95, 8.79 Hz, 1H), 8.21 (d, J = 7.35 Hz, 1H), 8.11 (t, J = 1.71 Hz, 1H), 8.02 (d, J = 2.44 Hz, 1H), 7.90 (d, J = 8.30 Hz, 1H), 7.82 - 7.86 (m, 1H), 7.79 - 7.81 (m, 1H), 7.72 (dd, J = 2.69, 9.03 Hz, 1H), 7.45 - 7.51 (m, 1H), 7.29 - 7.36 (m, 3H), 7.19 (dt, J = 2.44, 8.55 Hz, 1H), 5.27 (s, 2H), 2.96 (t, J = 5.4 Hz, 4Hm, 4H), 1.52 - 1.60 (m, 4H), 1.33 - 1.40 (m, 2H). MS: m/z = 603.2 (M+H)$^+$.

N-(3-chloro-4-((3-fluorobenzyl)oxy)phenyl)-6-(4-(pyrrolidin-1-ylsulfonyl)phenyl) quinazoline-4-amine (10n). Yield: 19.6%. ^{1}H NMR (500 MHz, DMSO-d$_6$) δ: 10.00 (s, 1H), 8.91 (d, J = 1.95 Hz, 1H), 8.63 (s, 1H), 8.27 (dd, J = 1.95, 8.79 Hz, 1H), 8.13 (d, J = 8.30 Hz, 2H), 8.03 (d, J = 2.44 Hz, 1H), 7.98 (d, J = 8.79 Hz, 2H), 7.90 (d, J = 8.79 Hz, 1H), 7.76 (dd, J = 2.44, 8.79 Hz, 1H), 7.45 - 7.52 (m, 1H), 7.29 - 7.36 (m, 3H), 7.20 (dt, J = 2.44, 8.55 Hz, 1H), 5.28 (s, 2H), 3.22 (t, J = 6.84 Hz, 4H), 1.66 - 1.72 (m, 4H). MS: m/z = 589.1 (M+H)$^+$.

N-(3-chloro-4-((3-fluorobenzyl)oxy)phenyl)-6-(3-(pyrrolidin-1-ylsulfonyl)phenyl) quinazolin-4-amine (10o). Yield: 28.2%. ^{1}H NMR (500 MHz, DMSO-d$_6$) δ: 10.03 (s, 1H), 8.85 (d, J = 1.46 Hz, 1H), 8.62 (s, 1H), 8.26 (dd, J = 1.95, 8.79 Hz, 1H), 8.18 - 8.23 (m, 2H), 8.03 (d, J = 2.44 Hz, 1H), 7.88 - 7.93 (m, 2H), 7.81 - 7.87 (m, 1H), 7.73 (dd, J = 2.44, 8.79 Hz, 1H), 7.45 - 7.52 (m, 1H), 7.30 - 7.37 (m, 3H), 7.20 (dt, J = 2.44, 8.55 Hz, 1H), 5.28 (s, 2H), 3.23 (t, J = 6.84 Hz, 4H), 1.68 (td, J = 3.54, 6.59 Hz, 4H). MS: m/z = 589.2 (M+H)$^+$.

N-(3-chloro-4-((3-fluorobenzyl)oxy)phenyl)-6-(4-((4-methylpiperazin-1-yl)sulfonyl) phenyl)quinazolin-4-amine (10p). Yield: 30.6%. ^{1}H NMR (500 MHz, DMSO-d$_6$) δ: 9.95 (s,

1H), 8.87 (d, J = 1.46 Hz, 1H), 8.59 (s, 1H), 8.23 (dd, J = 1.95, 8.79 Hz, 1H), 8.11 (d, J = 8.30

Hz, 2H), 7.99 (d, J = 2.44 Hz, 1H), 7.83 - 7.90 (m, 3H), 7.71 (dd, J = 2.69, 9.03 Hz, 1H), 7.40 -

7.47 (m, 1H), 7.25 - 7.32 (m, 3H), 7.15 (dt, J = 2.44, 8.55 Hz, 1H), 5.23 (s, 2H), 2.91 (br. s., 4H),

2.34 (br. s., 4H), 2.11 (s, 3H). MS: m/z = 618.2 $(M+H)^+$.

N-(3-chloro-4-((3-fluorobenzyl)oxy)phenyl)-6-(4-((4-methyl-1,4-diazepan-1-yl)sulfonyl)

phenyl)quinazolin-4-amine (10q). Yield: 42.8%. ^{1}H NMR (500 MHz, DMSO-d$_6$) δ: 10.00 (s,

1H), 8.91 (d, J = 1.95 Hz, 1H), 8.63 (s, 1H), 8.27 (dd, J = 1.95, 8.79 Hz, 1H), 8.12 (d, J = 8.80

Hz, 2H), 8.03 (d, J = 2.44 Hz, 1H), 7.96 (d, J = 8.30 Hz, 2H), 7.90 (d, J = 8.79 Hz, 1H), 7.76 (dd,

J = 2.69, 9.03 Hz, 1H), 7.45 - 7.50 (m, 1H), 7.30 - 7.36 (m, 3H), 7.20 (dt, J = 2.44, 8.55 Hz, 1H),

5.28 (s, 2H), 3.37 - 3.39 (m, 2H), 3.34 (t, J = 6.10 Hz, 3H), 2.61 - 2.64 (m, 2H), 2.54 - 2.58 (m,

2H), 2.28 (s, 3H), 1.74 - 1.80 (m, 2H). MS: m/z = 632.2 $(M+H)^+$.

N-(3-chloro-4-((3-fluorobenzyl)oxy)phenyl)-6-(4-(thiomorpholinosulfonyl)phenyl)

quinazolin-4-amine (10r).   Yield: 5.6%. ^{1}H NMR (500 MHz, DMSO-d$_6$) δ: 10.00 (s, 1H), 8.92

(d, J = 1.47 Hz, 1H), 8.64 (s, 1H), 8.28 (dd, J = 1.95, 8.79 Hz, 1H), 8.16 (d, J = 8.79 Hz, 2H),

8.04 (d, J = 2.44 Hz, 1H), 7.89 - 7.95 (m, 3H), 7.76 (dd, J = 2.45, 8.80 Hz, 1H), 7.46 - 7.52 (m,

1H), 7.30 - 7.37 (m, 3H), 7.20 (dt, J = 2.20, 8.67 Hz, 1H), 5.28 (s, 2H), 3.28 (t, J = 4.35 Hz, 4H),

2.71 (t, J = 5.35 Hz, 4H). MS: m/z = 621.2 $(M+H)^+$.

N-(3-chloro-4-((3-fluorobenzyl)oxy)phenyl)-6-(4-(piperazin-1-ylsulfonyl)phenyl)quinazolin-

4-amine (10s). To glass vials was weighed 46 mg of **14** (0.085 mmoL) and tert-butyl 4-((4-

(4,4,5,5-tetramethyl-1,3,2-dioxaborolan-2-yl)phenyl)sulfonyl)piperazine-1-carboxylate (38.4 mg

0.085 mmol) and   tetrakis(triphenylphosphine)palladium(0) (0.006 mmol).   To the reaction

mixture was added 1,2-dimethoxyethane (0.4 mL), ethanol (0.3 mL) and a 2M aqueous solution

of sodium carbonate (0.255 mL, 0.51 mmol).   The vials were capped and shaken at 85 °C for 12,

and progress of the reaction was monitored by LC-MS. The reaction mixture was evaporated to dryness, and the residue was dissolved in DMSO and purified by reverse phase HPLC using a gradient of 5-100% acetonitrile in water containing 0.1% formic acid providing the Boc-protected compound in 23.7% yield. ^{1}H NMR (500 MHz, DMSO-d$_6$) δ: 9.99 (s, 1H), 8.91 (d, J = 1.95 Hz, 1H), 8.64 (s, 1H), 8.28 (dd, J = 1.95, 8.79 Hz, 1H), 8.16 (d, J = 8.79 Hz, 2H), 8.04 (d, J = 2.44 Hz, 1H), 7.89 - 7.93 (m, 3H), 7.76 (dd, J = 2.44, 8.79 Hz, 1H), 7.46 - 7.52 (m, 1H), 7.30 - 7.36 (m, 3H), 7.20 (dt, J = 2.44, 8.79 Hz, 1H), 5.28 (s, 2H), 3.41 - 3.46 (m, 4H), 2.94 (t, J = 4.64 Hz, 4H), 1.34 (s, 9H). MS: m/z = 704.3 (M+H)$^+$. To a solution of this compound (0.015 mmol) in 0.4 mL of dichloromethane was added trifluoroacetic acid (200 μmol, 0.154 mL). The reaction mixture was stirred for 12 h at 25 °C. Volatiles were removed *in vacuo,* and the crude product was triturated with hexanes to afford a crude solid that was purified via flash column chromatography (0-10% MeOH-DCM) to afford the desired compound **10t**. Yield: 78%. ^{1}H NMR (500 MHz, DMSO-d$_6$) d: 9.01 (s, 1H), 8.80 (br. s., 1H), 8.59 (br. s., 2H), 8.39 (d, J = 7.81 Hz, 1H), 8.22 (d, J = 8.30 Hz, 2H), 7.92 - 8.03 (m, 4H), 7.72 (dd, J = 2.44, 8.79 Hz, 1H), 7.47 - 7.52 (m, 1H), 7.32 - 7.37 (m, 3H), 7.21 (dt, J = 2.20, 8.67 Hz, 1H), 5.31 (s, 2H), 3.25 (br. s., 4H), 3.18 (br. s., 4H). MS: m/z = 604.2 (M+H)$^+$.

N-(3-chloro-4-((3-fluorobenzyl)oxy)phenyl)-6-(4-(methylsulfonyl)phenyl)quinazolin-4-amine (10t). Yield: 31.8%. ^{1}H NMR (500 MHz, DMSO-d$_6$) δ: 10.00 (s, 1H), 8.92 (d, J = 1.95 Hz, 1H), 8.64 (s, 1H), 8.29 (dd, J = 1.95, 8.79 Hz, 1H), 8.14 (d, J = 8.80 Hz, 2H), 8.11 (d, J = 8.30 Hz, 2H), 8.03 (d, J = 2.44 Hz, 1H), 7.92 (d, J = 8.79 Hz, 1H), 7.76 (dd, J = 2.44, 8.79 Hz, 1H), 7.45 - 7.53 (m, 1H), 7.31 - 7.37 (m, 3H), 7.20 (dt, J = 2.20, 8.42 Hz, 1H), 5.28 (s, 2H), 3.31 (s, 3H). MS: m/z = 534.1 (M+H)$^+$.

N-(3-chloro-4-((3-fluorobenzyl)oxy)phenyl)-6-(3-(methylsulfonyl)phenyl)quinazolin-4-amine (10u). Yield: 34.9%. ^{1}H NMR (500 MHz, DMSO-d$_6$) δ: 10.02 (s, 1H), 8.88 (s, 1H), 8.63 (s, 1H), 8.38 (s, 1H), 8.30 (dd, J = 1.46, 8.79 Hz, 1H), 8.25 (d, J = 8.30 Hz, 1H), 7.99 - 8.06 (m, 2H), 7.92 (d, J = 8.79 Hz, 1H), 7.84 - 7.87 (m, 1H), 7.74 (dd, J = 2.44, 8.79 Hz, 1H), 7.45 - 7.53 (m, 1H), 7.30 - 7.36 (m, 3H), 7.20 (dt, J = 1.71, 8.67 Hz, 1H), 5.28 (s, 2H), 3.35 (s, 3H). MS: m/z = 534.2 (M+H)$^+$.

2-(4-((3-chloro-4-((3-fluorobenzyl)oxy)phenyl)amino)quinazolin-6-yl)-N,N-dimethylbenzenesulfonamide (10v). Yield: 35%. ^{1}H NMR (500 MHz, DMSO-d$_6$) δ: 9.78 (s, 1H), 8.65 (s, 1H), 8.52 (d, J = 0.98 Hz, 1H), 8.06 (d, J = 2.44 Hz, 1H), 8.01 (dd, J = 0.98, 7.81 Hz, 1H), 7.83 (dt, J = 1.46, 9.03 Hz, 1H), 7.76 - 7.81 (m, 3H), 7.72 (dt, J = 1.22, 7.69 Hz, 1H), 7.54 (dd, J = 0.98, 7.81 Hz, 1H), 7.45 - 7.50 (m, 1H), 7.30 - 7.34 (m, 2H), 7.27 (d, J = 8.79 Hz, 1H), 7.19 (dt, J = 2.44, 8.55 Hz, 1H), 5.26 (s, 2H), 2.45 (s, 6H). MS: m/z = 563.2 (M+H)$^+$.

N-(tert-butyl)-2-(4-((3-chloro-4-((3-fluorobenzyl)oxy)phenyl)amino)quinazolin-6-yl) benzenesulfonamide (10w).   Yield: 12.5%. ^{1}H NMR (500 MHz, DMSO-d$_6$) δ: 9.79 (s, 1H), 8.64 (s, 1H), 8.53 (d, J = 1.95 Hz, 1H), 8.11 (dd, J = 1.22, 8.06 Hz, 1H), 8.05 (d, J = 2.44 Hz, 1H), 7.86 (dd, J = 1.71, 8.55 Hz, 1H), 7.70 - 7.79 (m, 3H), 7.63 - 7.67 (m, 1H), 7.45 - 7.50 (m, 2H), 7.30 - 7.35 (m, 2H), 7.27 (d, J = 9.28 Hz, 1H), 7.19 (dt, J = 2.44, 8.55 Hz, 1H), 6.90 (s, 1H), 5.26 (s, 2H), 1.04 (s, 9H). MS: m/z = 591.2(M+H)$^+$.

N-(3-chloro-4-((3-fluorobenzyl)oxy)phenyl)-6-(3-morpholinophenyl)quinazolin-4-amine (23a). Yield: 38%. ^{1}H NMR (500 MHz, DMSO-d$_6$) δ: 9.90 (s, 1H), 8.76 (d, J = 1.95 Hz, 1H), 8.60 (s, 1H), 8.18 (dd, J = 1.71, 8.55 Hz, 1H), 8.04 (d, J = 2.93 Hz, 1H), 7.84 (d, J = 8.79 Hz, 1H), 7.76 (dd, J = 2.44, 8.79 Hz, 1H), 7.45 - 7.51 (m, 1H), 7.39 - 7.42 (m, 1H), 7.28 - 7.35 (m,

5H), 7.19 (dt, *J* = 2.44, 8.55 Hz, 1H), 7.03 (dd, *J* = 1.95, 8.30 Hz, 1H), 5.27 (s, 2H), 3.79 (t, *J* = 4.9 Hz, 4H), 3.24 (t, *J* = 4.86 Hz, 4H). MS: *m/z* = 541.2 (M+H)⁺.

N-(3-chloro-4-((3-fluorobenzyl)oxy)phenyl)-6-(4-morpholinophenyl)quinazolin-4-amine (23b). Yield: 35.2%. ¹H NMR (500 MHz, DMSO-d₆) δ: 9.87 (s, 1H), 8.72 (d, *J* = 1.95 Hz, 1H), 8.55 (s, 1H), 8.16 (dd, *J* = 1.95, 8.79 Hz, 1H), 8.03 (d, *J* = 2.93 Hz, 1H), 7.78 - 7.82 (m, 3H), 7.76 (dd, *J* = 2.44, 8.79 Hz, 1H), 7.45 - 7.51 (m, 1H), 7.28 - 7.35 (m, 3H), 7.19 (dt, *J* = 2.69, 8.67 Hz, 1H), 7.11 (d, *J* = 8.79 Hz, 2H), 5.27 (s, 2H), 3.76 - 3.80 (m, 4H), 3.19 - 3.23 (m, 4H). MS: *m/z* = 541.04 (M+H)⁺.

N-(3-chloro-4-((3-fluorobenzyl)oxy)phenyl)-6-(3-(morpholinomethyl)phenyl)quinazolin-4-amine (23c). Yield: 54.5%. ¹H NMR (500 MHz, DMSO-d₆) δ: 9.92 (s, 1H), 8.77 (s, 1H), 8.59 (s, 1H), 8.15 (d, *J* = 8.79 Hz, 1H), 8.03 (d, *J* = 1.95 Hz, 1H), 7.85 (d, *J* = 8.79 Hz, 1H), 7.72 - 7.80 (m, 3H), 7.43 - 7.54 (m, 2H), 7.39 (d, *J* = 7.32 Hz, 1H), 7.25 - 7.35 (m, 3H), 7.14 - 7.22 (m, 1H), 5.26 (s, 2H), 3.52-3.68 (m, 6H), 2.40 (br. s., 4H). MS: *m/z* = 554.3060 (M)⁺.

N-(3-chloro-4-((3-fluorobenzyl)oxy)phenyl)-6-(4-(morpholinomethyl)phenyl)quinazolin-4-amine (23d). Yield: 36.8%. ¹H NMR (500 MHz, DMSO-d₆) δ: 9.92 (s, 1H), 8.80 (d, *J* = 1.95 Hz, 1H), 8.60 (s, 1H), 8.20 (dd, *J* = 1.95, 8.79 Hz, 1H), 8.04 (d, *J* = 2.44 Hz, 1H), 7.84 - 7.87 (m, 3H), 7.77 (dd, *J* = 2.69, 9.03 Hz, 1H), 7.46 - 7.54 (m, 3H), 7.28 - 7.36 (m, 3H), 7.20 (dt, *J* = 1.95, 8.55 Hz, 1H), 5.28 (s, 2H), 3.61 (t, *J* = 4.64 Hz, 4H), 3.56 (s, 2H), 2.40 (br. s., 4H). MS: *m/z* = 555.2 (M+H)⁺.

(3-(4-((3-chloro-4-((3-fluorobenzyl)oxy)phenyl)amino)quinazolin-6-yl)phenyl) (morpholino)methanone (23e). Yield: 53.2%. ¹H NMR (500 MHz, DMSO-d₆) δ: 9.99 (br. s., 1H), 8.83 (d, *J* = 1.46 Hz, 1H), 8.61 (s, 1H), 8.23 (dd, *J* = 1.46, 8.79 Hz, 1H), 8.01 (d, *J* = 2.44 Hz, 1H), 7.97 (d, *J* = 7.81 Hz, 1H), 7.92 (s, 1H), 7.86 (d, *J* = 8.79 Hz, 1H), 7.73 (dd, *J* = 2.44,

8.79 Hz, 1H), 7.63 (t, J = 7.81 Hz, 1H), 7.47 (q, J = 7.65 Hz, 2H), 7.26 - 7.36 (m, 3H), 7.18 (dt, J = 2.20, 8.67 Hz, 1H), 5.26 (s, 2H), 3.20 - 3.78 (m, 8H). MS: m/z = 568.2021 (M)$^+$.

(4-(4-((3-chloro-4-((3-fluorobenzyl)oxy)phenyl)amino)quinazolin-6-yl)phenyl)(morpholino) methanone (23f). Yield: 58.9%. ^{1}H NMR (500 MHz, DMSO-d$_6$) δ: 9.93 (br. s., 1H), 8.84 (br. s., 1H), 8.60 (s, 1H), 8.21 (d, J = 8.30 Hz, 1H), 7.93 - 8.05 (m, 3H), 7.86 (d, J = 8.30 Hz, 1H), 7.76 (d, J = 7.81 Hz, 1H), 7.60 (d, J = 7.81 Hz, 2H), 7.43 - 7.51 (m, 1H), 7.26 - 7.36 (m, 3H), 7.18 (t, J = 8.06 Hz, 1H), 5.26 (s, 2H), 3.37 - 3.80 (m, 8H). MS: m/z = 568.2183 (M)$^+$.

N-(3-chloro-4-((3-fluorobenzyl)oxy)phenyl)-6-(3-(piperidin-1-yl)phenyl)quinazolin-4-amine (23g). Yield: 21%. ^{1}H NMR (500 MHz, DMSO-d$_6$) δ: 9.90 (s, 1H), 8.74 (d, J = 1.95 Hz, 1H), 8.58 (s, 1H), 8.16 (dd, J = 1.71, 8.55 Hz, 1H), 8.03 (d, J = 2.44 Hz, 1H), 7.83 (d, J = 8.79 Hz, 1H), 7.75 (dd, J = 2.44, 8.79 Hz, 1H), 7.44 - 7.51 (m, 1H), 7.27 - 7.39 (m, 5H), 7.23 (d, J = 7.81 Hz, 1H), 7.19 (dt, J = 2.44, 8.55 Hz, 1H), 7.00 (dd, J = 1.95, 8.30 Hz, 1H), 5.27 (s, 2H), 3.23 - 3.27 (m, 4H), 1.64 - 1.69 (m, 4H), 1.53 - 1.59 (m, 2H). MS: m/z = 539.16 (M+H)$^+$.

N-(3-chloro-4-((3-fluorobenzyl)oxy)phenyl)-6-(4-(piperidin-1-yl)phenyl)quinazolin-4-amine (23h). Yield: 41.4%. ^{1}H NMR (500 MHz, DMSO-d$_6$) δ: 9.87 (s, 1H), 8.69 (d, J = 0.98 Hz, 1H), 8.55 (s, 1H), 8.12 (dd, J = 1.71, 8.55 Hz, 1H), 8.03 (d, J = 2.44 Hz, 1H), 7.72 - 7.81 (m, 4H), 7.43 - 7.51 (m, 1H), 7.25 - 7.37 (m, 3H), 7.18 (dt, J = 2.44, 8.55 Hz, 1H), 7.06 (d, J = 8.79 Hz, 2H), 5.26 (s, 2H), 3.18 - 3.26 (m, 4H), 1.49 - 1.70 (m, 6H). MS: m/z = 532.3831 (M)$^+$.

N-(3-chloro-4-((3-fluorobenzyl)oxy)phenyl)-6-(3-(piperidin-1-ylmethyl)phenyl)quinazolin-4-amine (23i). Yield: 66.7%. ^{1}H NMR (500 MHz, DMSO-d$_6$) δ: 9.91 (br. s., 1H), 8.81 (d, J = 1.95 Hz, 1H), 8.60 (s, 1H), 8.19 (dd, J = 1.95, 8.79 Hz, 1H), 8.01 (d, J = 2.93 Hz, 1H), 7.87 - 7.97 (m, 3H), 7.74 (dd, J = 2.90, 9.25 Hz, 1H), 7.63 (t, J = 7.57 Hz, 1H), 7.52 (d, J = 7.32 Hz, 1H), 7.46 (dt, J = 6.35, 8.06 Hz, 1H), 7.26 - 7.35 (m, 3H), 7.17 (dt, J = 2.44, 8.55 Hz, 1H), 5.25

(s, 2H), 4.22 (br. s., 2H), 3.00 (d, J = 5.86 Hz, 4H), 1.42 - 1.77 (m, 6H). MS: m/z = 552.3265 $(M)^+$.

N-(3-chloro-4-((3-fluorobenzyl)oxy)phenyl)-6-(4-(piperidin-1-ylmethyl)phenyl)quinazolin-4-amine (23j). Yield: 52.3%. ^{1}H NMR (500 MHz, DMSO-d$_6$) δ: 9.89 (br. s., 1H), 8.80 (d, J = 1.46 Hz, 1H), 8.58 (s, 1H), 8.19 (dd, J = 1.95, 8.79 Hz, 1H), 8.01 (d, J = 2.44 Hz, 1H), 7.90 (d, J = 8.30 Hz, 2H), 7.85 (d, J = 8.79 Hz, 1H), 7.74 (dd, J = 2.44, 8.79 Hz, 1H), 7.56 (d, J = 8.30 Hz, 2H), 7.41 - 7.50 (m, 1H), 7.25 - 7.35 (m, 3H), 7.17 (dt, J = 2.20, 8.67 Hz, 1H), 5.25 (s, 2H), 3.93 (br. s., 2H), 2.74 (br. s., 4H), 1.56 - 1.69 (m, 4H), 1.45 (br. s., 2H). MS: m/z = 552.3265 $(M)^+$.

(3-(4-((3-chloro-4-((3-fluorobenzyl)oxy)phenyl)amino)quinazolin-6-yl)phenyl)(piperidin-1-yl)methanone (23k). Yield: 66.3%. ^{1}H NMR (500 MHz, DMSO-d$_6$) δ: 8.91 (s, 1H), 8.76 (br. s., 1H), 8.35 (d, J = 9.28 Hz, 1H), 7.96 - 8.00 (m, 2H), 7.87 - 7.93 (m, 2H), 7.70 (dd, J = 2.45, 8.80 Hz, 1H), 7.59 - 7.65 (m, 2H), 7.44 - 7.52 (m, 2H), 7.32 - 7.36 (m, 3H), 7.20 (dt, J = 2.44, 8.79 Hz, 1H), 5.30 (s, 2H), 3.65 (br. s., 3H), 1.41 - 1.70 (m, 7H). MS: m/z = 567.3 $(M+H)^+$.

(4-(4-((3-chloro-4-((3-fluorobenzyl)oxy)phenyl)amino)quinazolin-6-yl)phenyl)(piperidin-1-yl)methanone (23l). Yield: 73.3%. ^{1}H NMR (500 MHz, DMSO-d$_6$) δ: 9.93 (s, 1H), 8.83 (s, 1H), 8.59 (s, 1H), 8.21 (dd, J = 1.95, 8.30 Hz, 1H), 8.01 (d, J = 2.44 Hz, 1H), 7.93 (d, J = 8.30 Hz, 2H), 7.86 (d, J = 8.79 Hz, 1H), 7.74 (dd, J = 2.44, 8.79 Hz, 1H), 7.53 (d, J = 8.30 Hz, 3H), 7.43 - 7.49 (m, 1H), 7.27 - 7.34 (m, 3H), 7.17 (dt, J = 1.95, 8.55 Hz, 1H), 5.25 (s, 2H), 3.60 (br. s., 2H), 1.38 - 1.67 (m, 7H). MS: m/z = 567.3 $(M+H)^+$.

Aniline synthesis. Anilines **17** were synthesized using **General procedure B.** In a 20 mL glass vial a solution of substituted 4-nitrophenol (1.5 mmol) in 5 mL acetonitrile was combined with potassium carbonate (3 mmol) and the appropriate benzyl bromide (1.5 mmol) at 25 °C. The reaction mixture was stirred at 50 °C for 12 h. After completion of the alkylation reaction, the

reaction mixture was triturated with 10 mL of 10% MeOH/DCM and was filtered through a silica gel plug. The organic filtrate was evaporated and re-dissolved in 5 mL of MeOH:H_2O (5:1). To this solution was added Zinc (0.29 g, 4.5 mmol) followed by ammonium chloride (0.48 g, 9 mmol) at 25 °C. The temperature was raised to 50 °C and the stirring was continued 6 h. Progress of the reaction was followed by LC-MS. Upon completion of the reaction, 15 mL of DCM:MeOH (1:1) was added to the reaction mixture, inorganic residues were removed by filtration. The filtrate was evaporated and the residue was purified via flash chromatography (0-50% EtOAc/hexanes) to afford the desired substituted anilines.

4-(benzyloxy)-3-chloroaniline (17e). Yield: 24.3%. ^{1}H NMR (500 MHz, CDCl$_3$) δ: 7.47 (d, J = 7.32 Hz, 2H), 7.37 - 7.41 (m, 2H), 7.30 - 7.35 (m, 1H), 6.81 (d, J = 8.79 Hz, 1H), 6.76 (d, J = 2.93 Hz, 1H), 6.51 (dd, J = 2.69, 8.55 Hz, 1H), 5.06 (s, 2H), 3.49 (br. s., 2H). MS: m/z = 234.02 (M+H)[+].

4-((3-bromobenzyl)oxy)-3-chloroaniline (17f). Yield: 25%. ^{1}H NMR (500 MHz, CDCl$_3$) δ: 7.62 (s, 1H), 7.45 (d, J = 8.30 Hz, 1H), 7.39 (d, J = 7.81 Hz, 1H), 7.22 - 7.26 (m, 1H), 6.75 - 6.80 (m, 2H), 6.52 (dd, J = 2.93, 8.79 Hz, 1H), 5.01 (s, 2H), 3.52 (br. s., 2H). MS: m/z = 311.89 (M+H)[+].

3-chloro-4-((3-chlorobenzyl)oxy)aniline (17g). Yield: 38%. ^{1}H NMR (500 MHz, CDCl$_3$) δ: 7.47 (s, 1H), 7.29 - 7.36 (m, 3H), 6.78 (d, J = 8.30 Hz, 1H), 6.75 (d, J = 2.44 Hz, 1H), 6.50 (dd, J = 2.93, 8.79 Hz, 1H), 5.01 (s, 2H), 3.52 (br. s., 2H). MS: m/z = 267.96 (M+H)[+].

3-chloro-4-((2,3-difluorobenzyl)oxy)aniline (17h). Yield: 31%. ^{1}H NMR (500 MHz, CDCl$_3$) δ: 7.35 (t, J = 6.59 Hz, 1H), 7.07 - 7.16 (m, 2H), 6.83 (d, J = 8.79 Hz, 1H), 6.75 (d, J = 2.93 Hz, 1H), 6.52 (dd, J = 2.69, 8.55 Hz, 1H), 5.12 (s, 2H), 3.51 (br. s., 2H). MS: m/z = 270.0 (M+H)[+].

3-chloro-4-((2-fluorobenzyl)oxy)aniline (17i). Yield: 37%. ^{1}H NMR (500 MHz, CDCl$_3$) δ: 7.58 (dt, J = 1.71, 7.45 Hz, 1H), 7.27 – 7.32 (m, 1H), 7.16 (dt, J = 0.98, 7.57 Hz, 1H), 7.04 - 7.08 (m, 1H), 6.83 (d, J = 8.79 Hz, 1H), 6.75 (d, J = 2.93 Hz, 1H), 6.51 (dd, J = 2.69, 8.55 Hz, 1H), 5.12 (s, 2H), 3.50 (br. s., 2H). MS: m/z = 251.99 (M+H)$^+$.

3-chloro-4-((4-fluorobenzyl)oxy)aniline (17j). Yield: 22%. ^{1}H NMR (500 MHz, CDCl$_3$) δ: 7.40 - 7.44 (m, 2H), 7.03 - 7.10 (m, 2H), 6.78 (d, J = 8.79 Hz, 1H), 6.75 (d, J = 2.44 Hz, 1H), 6.50 (dd, J = 2.93, 8.79 Hz, 1H), 5.00 (s, 2H), 3.50 (br. s., 2H). MS: m/z = 252.0 (M+H)$^+$.

3-chloro-4-((3-methoxybenzyl)oxy)aniline (17k). Yield: %. ^{1}H NMR (500 MHz, CDCl$_3$) d: 7.27 - 7.32 (m, 1H), 7.01 - 7.05 (m, 2H), 6.86 (dd, J = 2.69, 8.06 Hz, 1H), 6.79 (d, J = 8.79 Hz, 1H), 6.74 (d, J = 2.93 Hz, 1H), 6.49 (dd, J = 2.45, 8.80 Hz, 1H), 5.04 (s, 2H), 3.83 (s, 3H), 3.44 (br. s., 2H). MS: m/z = 264.01 (M+H)$^+$.

3-chloro-4-((3-fluoro-4-(trifluoromethyl)benzyl)oxy)aniline (17l). Yield: 35.2%. ^{1}H NMR (500 MHz, CDCl$_3$) δ: 7.60 (t, J = 7.81 Hz, 1H), 7.29 - 7.36 (m, 2H), 6.77 (d, J = 4.39 Hz, 1H), 6.76 (d, J = 1.47 Hz, 1H), 6.51 (dd, J = 2.93, 8.79 Hz, 1H), 5.06 (s, 2H), 3.54 (br. s., 2H). MS: m/z = 319.93 (M+H)$^+$.

3-chloro-4-((2,3,5-trifluorobenzyl)oxy)aniline (17m). Yield: 22%. ^{1}H NMR (500 MHz, CDCl$_3$) δ: 7.13 - 7.18 (m, 1H), 6.85 - 6.93 (m, 1H), 6.81 (d, J = 8.30 Hz, 1H), 6.76 (d, J = 2.93 Hz, 1H), 6.53 (dd, J = 2.93, 8.79 Hz, 1H), 5.09 (s, 2H), 3.54 (br. s., 2H). MS: m/z = 287.96 (M+H)$^+$.

4-((3-fluorobenzyl)oxy)aniline (17n). Yield: 28%. ^{1}H NMR (500 MHz, CDCl$_3$) δ: 7.34 (m, 1H), 7.14 - 7.21 (m, 2H), 7.01 (dt, J = 2.44, 8.55 Hz, 1H), 6.81 (d, J = 8.30 Hz, 2H), 6.64 (d, J = 8.30 Hz, 2H), 4.99 (s, 2H), 3.32 (br. s., 2H). MS: m/z = 218.07 (M+H)$^+$.

4-((3-fluorobenzyl)oxy)-3-methoxyaniline (17o). Yield: 7.52%. ^{1}H NMR (500 MHz, CDCl$_3$) δ: 7.28 - 7.33 (m, 1H), 7.14 - 7.21 (m, 2H), 6.97 (dt, J = 2.20, 8.67 Hz, 1H), 6.70 (d, J = 8.30 Hz, 1H), 6.32 (d, J = 2.93 Hz, 1H), 6.16 (dd, J = 2.69, 8.55 Hz, 1H), 5.02 (s, 2H), 3.84 (s, 3H), 3.51 (br. s., 2H). MS: m/z = 248.06 (M+H)$^+$.

6-(4-(morpholinosulfonyl)phenyl)quinazolin-4(3H)-one (18). A mixture of 6-iodoquinazolin-4(3H)-one (4.5 g, 16.54 mmol), (4-(morpholinosulfonyl)phenyl)boronic acid (4.93 g, 18.20 mmol), sodium carbonate (10.52 g, 99 mmol) and tetrakis(triphenylphosphine)palladium(0) (1.338 g, 1.158 mmol) were combined in a flask, and 400 mL of 1,2-dimethoxyethane was added, with ethanol (26.7 mL) and water (33.3 ml). The reaction mixture was heated with stirring at 80 °C for 30 h. The reaction progress was monitored by LC-MS. Upon completion of the reaction, the mixture was cooled to room temperature, and the product precipitated. Solids were collected by filtration, washed with cold water and air-dried, affording **18** (5.35 g, 14.40 mmol, 87 % yield). ^{1}H NMR (500 MHz, DMSO-d$_6$) δ: 12.40 (br. s., 1H), 8.44 (d, J = 2.44 Hz, 1H), 8.22 (dd, J = 2.20, 8.55 Hz, 1H), 8.16 (d, J = 3.42 Hz, 1H), 8.07 (d, J = 8.30 Hz, 2H), 7.84 (d, J = 8.30 Hz, 2H), 7.80 (d, J = 8.79 Hz, 1H), 3.64 (t, J = 4.65 Hz, 4H), 2.91 (t, J = 4.65 Hz, 4H). MS: m/z = 372.2 (M+H)$^+$.

4-((4-(4-chloroquinazolin-6-yl)phenyl)sulfonyl)morpholine hydrochloride (19). Thionyl chloride (9.83 ml, 135 mmol) was added slowly to 1.0 g of **18** (1 g, 2.69 mmol), followed by N,N-dimethylformamide (2.085 μl, 0.027 mmol). The reaction mixture was refluxed for 36 h, monitoring reaction progress with LC-MS. The volatile components were removed via distillation, providing **19** (1.12 g, 1.683 mmol, 80% pure, 78% yield), which was used for subsequent reactions without further purification. ^{1}H NMR (500 MHz, DMSO-d$_6$) δ: 8.45 (d, J =

1.95 Hz, 1H), 8.32 (s, 1H), 8.26 (dd, *J* = 2.20, 8.55 Hz, 1H), 8.07 (d, *J* = 8.79 Hz, 2H), 7.79 - 7.86 (m, 3H), 3.65 (t, *J* = 4.60 Hz, 4H), 2.92 (t, *J* = 4.65 Hz, 4H). MS: *m*/z = 390.04 (M+H)$^+$.

6-(4-(morpholinosulfonyl)phenyl)-N-arylquinazolin-4-amineshydrochloride **20** were synthesized following **General procedure C**. To a solution of **19** (100 µmol) in N,N-dimethylformamide (0.5 mL) was added aryl amine (110 µmol) and the mixture was heated on a shaker plate at 80 °C for 12 h. After cooling the reaction mixture to room temperature, 0.5 mL of isopropanol was added. The resulting yellowish precipitate was filtered and washed with 2mL of isopropanol, affording the amines **20**.

6-(4-(morpholinosulfonyl)phenyl)-N-phenylquinazolin-4-amine hydrochloride. (20a). Yield: 50.8%. ^{1}H NMR (500 MHz, DMSO-d$_6$) δ: 11.51 (br. s., 1H), 9.20 (s, 1H), 8.93 (s, 1H), 8.50 (d, *J* = 8.79 Hz, 1H), 8.21 (d, *J* = 8.30 Hz, 2H), 8.01 (d, *J* = 8.30 Hz, 1H), 7.95 (d, *J* = 8.30 Hz, 2H), 7.75 (d, *J* = 8.30 Hz, 2H), 7.51 - 7.55 (m, 2H), 7.34 - 7.37 (m, 1H), 3.65 - 3.67 (br. m, 4H), 2.92 - 2.95 (br. m., 4H). MS: *m*/z = 447.2 (M+H)$^+$.

6-(4-(morpholinosulfonyl)phenyl)-N-(p-tolyl)quinazolin-4-amine hydrochloride (20b). Yield: 54.9%. ^{1}H NMR (500 MHz, DMSO-d$_6$) δ: 11.62 (br. s., 1H), 9.24 (s, 1H), 8.93 (s, 1H), 8.51 (d, *J* = 8.30 Hz, 1H), 8.22 (d, *J* = 8.30 Hz, 3H), 8.03 (d, *J* = 8.79 Hz, 1H), 7.95 (d, *J* = 8.79 Hz, 2H), 7.63 (d, *J* = 7.81 Hz, 2H), 7.34 (d, *J* = 7.81 Hz, 2H), 3.67 (t, *J* = 4.4 Hz, 4H), 2.95 (t, *J* = 4.4 Hz, 4H), 2.38 (s, 3H). MS: *m*/z = 496.2 (M+H)$^+$.

2-chloro-4-((6-(4-(morpholinosulfonyl)phenyl)quinazolin-4-yl)amino)phenol hydrochloride (20c). Yield: 52.7%. ^{1}H NMR (500 MHz, DMSO-d$_6$) δ: 11.60 (br. s., 1H), 10.55 (br. s., 1H), 9.22 (s, 1H), 8.96 (s, 1H), 8.51 (dd, *J* = 1.47, 8.79 Hz, 1H), 8.22 (d, *J* = 8.30 Hz, 2H), 8.02 (d, *J* = 8.79 Hz, 1H), 7.95 (d, *J* = 8.30 Hz, 2H), 7.81 (d, *J* = 2.93 Hz, 1H), 7.52 (dd, *J* = 2.44, 8.79 Hz,

1H), 7.12 (d, J = 8.79 Hz, 1H), 3.7 (t, J = 4.40 Hz, 4H), 2.95 (t, J = 4.4 Hz, 4H). MS: m/z = 497.2 (M+H)$^+$.

N-(3-chloro-4-methoxyphenyl)-6-(4-(morpholinosulfonyl)phenyl)quinazolin-4-amine hydrochloride (20d). Yield: 43.4%. ^{1}H NMR (500 MHz, DMSO-d$_6$) δ: 11.34 (br. s., 1H), 9.14 (s, 1H), 8.94 (s, 1H), 8.49 (d, J = 8.79 Hz, 1H), 8.20 (d, J = 8.79 Hz, 2H), 8.00 (d, J = 8.79 Hz, 1H), 7.96 (d, J = 8.30 Hz, 2H), 7.93 (d, J = 2.44 Hz, 1H), 7.70 (dd, J = 2.44, 8.79 Hz, 1H), 7.31 (d, J = 9.28 Hz, 1H), 3.93 (s, 3H), 3.67 (t, J = 4.6 Hz, 4H), 2.95 (t, J = 4.6 Hz, 4H). MS: m/z = 511.1 (M+H)$^+$.

N-(4-(benzyloxy)-3-chlorophenyl)-6-(4-(morpholinosulfonyl)phenyl)quinazolin-4-amine hydrochloride (20e). Yield: 70.1%. ^{1}H NMR (500 MHz, DMSO-d$_6$) δ: 11.49 (br. s., 1H), 9.18 (s, 1H), 8.95 (s, 1H), 8.50 (dd, J = 1.71, 8.55 Hz, 1H), 8.20 - 8.22 (m, 2H), 8.01 (d, J = 8.79 Hz, 1H), 7.93 - 7.96 (m, 3H), 7.68 (dd, J = 2.69, 9.03 Hz, 1H), 7.51 - 7.53 (m, 2H), 7.35 - 7.46 (m, 4H), 5.30 (s, 2H), 3.66 - 3.68 (t, J = 4.9 Hz, 4H), 2.5 (t, J = 4.4 Hz, 4H). MS: m/z = 587.2 (M+H)$^+$.

N-(4-((3-bromobenzyl)oxy)-3-chlorophenyl)-6-(4-(morpholinosulfonyl)phenyl)quinazolin-4-amine hydrochloride (20f). Yield: 51.6%. ^{1}H NMR (500 MHz, DMSO-d$_6$) δ: 11.45 (br. s., 1H), 9.17 (s, 1H), 8.95 (s, 1H), 8.50 (d, J = 8.79 Hz, 1H), 8.21 (d, J = 8.79 Hz, 2H), 8.01 (d, J = 8.30 Hz, 1H), 7.94 - 7.97 (m, 3H), 7.72 (s, 1H), 7.69 (dd, J = 2.69, 9.03 Hz, 1H), 7.58 (d, J = 7.81 Hz, 1H), 7.52 (d, J = 7.81 Hz, 1H), 7.37 - 7.43 (m, 2H), 5.31 (s, 2H), 3.67 (t, J = 4.4 Hz, 4H), 2.95 (t, J = 4.35 Hz, 4H). MS: m/z = 665.1 (M+H)$^+$.

N-(3-chloro-4-((3-chlorobenzyl)oxy)phenyl)-6-(4-(morpholinosulfonyl)phenyl)quinazolin-4-amine hydrochloride (20g). Yield: 49.1%. ^{1}H NMR (500 MHz, DMSO-d$_6$) δ: 11.54 (br. s., 1H), 9.19 (br. s., 1H), 8.96 (br. s., 1H), 8.50 (d, J = 8.79 Hz, 1H), 8.21 (d, J = 8.30 Hz, 2H), 7.98 -

8.08 (m, 1H), 7.94 - 7.96 (m, 3H), 7.69 (dd, J = 2.44, 8.79 Hz, 1H), 7.58 (br. s., 1H), 7.37 - 7.50 (m, 4H), 5.31 (br. s., 2H), 3.67 (br. s., 4H), 2.95 (br. s., 4H). MS: m/z = 621.1 (M+H)$^+$.

N-(3-chloro-4-((2,3-difluorobenzyl)oxy)phenyl)-6-(4-(morpholinosulfonyl)phenyl) quinazolin-4-amine hydrochloride (20h). Yield: 53.3%. ^{1}H NMR (500 MHz, DMSO-d$_6$) δ: 11.58 (br. s., 1H), 9.22 (s, 1H), 8.97 (s, 1H), 8.51 (dd, J = 1.46, 8.79 Hz, 1H), 8.22 (d, J = 8.30 Hz, 2H), 8.03 (d, J = 8.79 Hz, 1H), 7.93 - 7.97 (m, 3H), 7.73 (dd, J = 2.44, 8.79 Hz, 1H), 7.43 - 7.53 (m, 3H), 7.28 - 7.34 (m, 1H), 5.38 (s, 2H), 3.67 (t, J = 4.4 Hz, 4H), 2.95 (t, J = 4.6 Hz, 4H). MS: m/z = 623.2 (M+H)$^+$.

N-(3-chloro-4-((2-fluorobenzyl)oxy)phenyl)-6-(4-(morpholinosulfonyl)phenyl)quinazolin-4-amine hydrochloride (20i). Yield: 41.2%. ^{1}H NMR (500 MHz, DMSO-d$_6$) δ: 11.32 (br. s., 1H), 9.12 (br. s., 1H), 8.93 (br. s., 1H), 8.47 (d, J = 8.79 Hz, 1H), 8.18 (d, J = 8.30 Hz, 2H), 7.98 (d, J = 8.79 Hz, 1H), 7.92 - 7.96 (m, 3H), 7.70 (dd, J = 2.44, 8.79 Hz, 1H), 7.60 - 7.63 (m, 1H), 7.43 - 7.46 (m, 2H), 7.25 - 7.32 (m, 2H), 5.31 (s, 2H), 3.65 (t, J = 4.6 Hz, 4H), 2.93 (t, J = 4.6 Hz, 4H). MS: m/z = 605.2 (M+H)$^+$.

N-(3-chloro-4-((4-fluorobenzyl)oxy)phenyl)-6-(4-(morpholinosulfonyl)phenyl)quinazolin-4-amine hydrochloride (20j). Yield: 67.1%. ^{1}H NMR (500 MHz, DMSO-d$_6$) δ: 11.66 (br. s., 1H), 9.24 (br. s., 1H), 8.97 (s, 1H), 8.52 (d, J = 8.79 Hz, 1H), 8.23 (d, J = 8.30 Hz, 2H), 8.03 (d, J = 8.79 Hz, 1H), 7.94 - 7.96 (m, 3H), 7.70 (dd, J = 2.44, 8.79 Hz, 1H), 7.55 - 7.58 (m, 2H), 7.41 (d, J = 8.79 Hz, 1H), 7.26 - 7.30 (m, 2H), 5.28 (s, 2H), 3.7 (t, J = 4.9 Hz, 4H), 2.95 (t, J = 4.6 Hz, 4H). MS: m/z = 605.2 (M+H)$^+$.

N-(3-chloro-4-((3-methoxybenzyl)oxy)phenyl)-6-(4-(morpholinosulfonyl)phenyl)quinazolin-4-amine hydrochloride (20k). Yield: 43.1%. ^{1}H NMR (500 MHz, DMSO-d$_6$) δ: 11.40 (br. s., 1H), 9.15 (s, 1H), 8.94 (s, 1H), 8.49 (d, J = 8.30 Hz, 1H), 8.20 (d, J = 8.30 Hz, 2H), 8.00 (d, J =

8.79 Hz, 1H), 7.93 - 7.97 (m, 3H), 7.68 (dd, *J* = 2.44, 8.79 Hz, 1H), 7.33 - 7.39 (m, 2H), 7.06 - 7.08 (m, 2H), 6.91 - 6.96 (m, 1H), 5.27 (s, 2H), 3.78 (s, 3H), 3.67 (t, *J* = 4.9 Hz, 4H), 2.95 (t, *J* = 4.4 Hz, 4H). MS: *m*/z = 617.2 (M+H)$^+$.

N-(3-chloro-4-((3-fluoro-4-(trifluoromethyl)benzyl)oxy)phenyl)-6-(4-(morpholinosulfonyl) phenyl)quinazolin-4-amine hydrochloride (20l). Yield: 40.9%. ^{1}H NMR (500 MHz, DMSO-d$_6$) δ: 11.74 (br. s., 1H), 9.29 (s, 1H), 8.98 (s, 1H), 8.52 (dd, *J* = 1.46, 8.79 Hz, 1H), 8.24 (d, *J* = 8.79 Hz, 2H), 8.05 (d, *J* = 8.79 Hz, 1H), 7.99 (d, *J* = 2.44 Hz, 1H), 7.95 (d, *J* = 8.30 Hz, 2H), 7.89 (t, *J* = 7.81 Hz, 1H), 7.72 (dd, *J* = 2.44, 8.79 Hz, 1H), 7.63 (d, *J* = 11.23 Hz, 1H), 7.55 (d, *J* = 7.81 Hz, 1H), 7.38 (d, *J* = 8.79 Hz, 1H), 5.43 (s, 2H), 3.67 (t, *J* = 4.4 Hz, 4H), 2.95 (t, *J* = 4.4 Hz, 4H). MS: *m*/z = 673.2 (M+H)$^+$.

N-(3-chloro-4-((2,3,5-trifluorobenzyl)oxy)phenyl)-6-(4-(morpholinosulfonyl)phenyl) quinazolin-4-amine hydrochloride (20m). Yield: 42%. ^{1}H NMR (500 MHz, DMSO-d$_6$) δ: 11.49 (br. s., 1H), 9.19 (s, 1H), 8.96 (s, 1H), 8.51 (d, *J* = 9.77 Hz, 1H), 8.21 (d, *J* = 8.30 Hz, 2H), 8.02 (d, *J* = 8.79 Hz, 1H), 7.95 - 7.98 (m, 3H), 7.73 (dd, *J* = 2.69, 9.03 Hz, 1H), 7.56- 7.65 (m, 1H), 7.48 (d, *J* = 8.79 Hz, 1H), 7.34 - 7.36 (m, 1H), 5.38 (s, 2H), 3.67 (t, *J* = 4.9 Hz, 4H), 2.95 (t, *J* = 4.4 Hz, 4H). MS: *m*/z = 641.1 (M+H)$^+$.

N-(4-((3-fluorobenzyl)oxy)phenyl)-6-(4-(morpholinosulfonyl)phenyl)quinazolin-4-amine (20n). Yield: 45.8%. ^{1}H NMR (500 MHz, DMSO-d$_6$) δ: 11.40 (br. s., 1H), 9.15 (s, 1H), 8.88 (s, 1H), 8.49 (d, *J* = 8.79 Hz, 1H), 8.20 (d, *J* = 8.79 Hz, 2H), 7.92 - 8.02 (m, 3H), 7.65 (d, *J* = 9.30 Hz, 2H), 7.45 - 7.51 (m, 1H), 7.31 - 7.35 (m, 2H), 7.16 - 7.22 (m, 3H), 5.21 (s, 2H), 3.67 (t, *J* = 4.4 Hz, 4H), 2.95 (t, *J* = 4.4 Hz, 4H). MS: *m*/z = 571.2 (M+H)$^+$.

N-(4-((3-fluorobenzyl)oxy)-3-methoxyphenyl)-6-(4-(morpholinosulfonyl)phenyl)quinazolin-4-amine (20o). Yield: 18%. ^{1}H NMR (500 MHz, DMSO-d$_6$) δ: 11.32 (br. s., 1H), 9.14 (s, 1H),

8.90 (s, 1H), 8.49 (d, J = 8.30 Hz, 1H), 8.20 (d, J = 8.79 Hz, 2H), 7.99 (d, J = 8.79 Hz, 1H), 7.96 (d, J = 8.30 Hz, 2H), 7.45 - 7.50 (m, 1H), 7.41 (d, J = 2.44 Hz, 1H), 7.28 - 7.34 (m, 3H), 7.15 - 7.22 (m, 2H), 5.19 (s, 2H), 3.84 (s, 3H), 3.67 (t, J = 4.9 Hz, 4H), 2.95 (t, J = 4.4 Hz, 4H). MS: m/z = 601.1 (M+H)$^{+}$.

3.2.2 Trypanosome growth inhibition assay

Bloodstream *T. brucei brucei* Lister 427 cells were cultured in HMI-9 medium [42].The growth inhibition assays were performed as described [24]. The mean GI_{50} and standard deviation in the tables are calculated from two different experiments performed in duplicates.

3.2.3 HepG2 cell toxicity assay

The 384 well MTT cytotoxicity assay is a modification of the MTT method described by Ferrari *et al* [43], optimized for 384 well throughput, with modifications described in detail in the Supporting Information. The 50% inhibitory concentrations (IC_{50}) were generated for each toxicity dose response test using GraphPad Prism (GraphPad Software Inc., San Diego, CA) using the nonlinear regression (sigmoidal dose-response/variable slope) equation.

3.3 Results

We screened nine quinazoline-based EGFR inhibitors (**1-9**, **Table 3.1**) [18,28-30], received from GlaxoSmithKline, against *T brucei brucei* Lister 427 growth and observed a 10-fold range in potency (**Table 3.1**) despite limited scope in variation of the R^1 "tail" region of the scaffold. Also, lapatinib (**9,** 1.54 μM) demonstrated four-fold more potency against *T. brucei* as compared to a HepG2 hepatocarcinoma cell line in terms of GI_{50} [31]. The immediate goals of our subsequent optimization efforts are twofold; (i) improve the potency of this chemotype for inhibition of *T. brucei* replication, and (ii) increase the selectivity ratio over HepG2.

94

Noting the effect of subtle tail-group changes on parasite growth inhibition, we first focused our attention on broader exploration of replacements for the furan-derived tail. This was achieved by a broad diversity scan utilizing Suzuki chemistry methodology using boronic acids or esters to enumerate a virtual library of lapatinib analogs (**10**, **Scheme 1**). The structures in this virtual library were clustered based on a maximum dissimilarity algorithm, and cluster centers were selected for synthesis (PipelinePilot, Scitegic, Inc).

In anticipation of the parallel synthesis, we prepared the iodoquinazoline **14** by the route shown in **Scheme 1.** Treatment of the commercially available anthranilic acid **11** with formamide proceeded in 70% yield, followed by chlorination with thionyl chloride to provide the chloroquinazoline **13** in 85% yield. This template was reacted with the requisite aniline (**17,** **Scheme 2**), which was prepared by a sequence of alkylation of the nitrophenol **15** with 3-fluorobenzyl bromide followed by nitro group reduction. With the required template **14** in hand, we smoothly prepared ten analogs (**10a-k**) from the selected boronates using standard Suzuki reaction conditions. The structures and biological activities for these compounds are summarized in **Table 3.2**. From this series of analogs we identified **NEU369 (10a)**, which was approximately equipotent to lapatinib against *T brucei* cells. Further testing of this compound and its analogs showed that, unlike lapatinib, it did not inhibit HepG2 cell growth ($EC_{50} > 15$ μM) (**Table 3.3**).

Scheme 1. Synthesis of lapatinib analogs 10.[a]
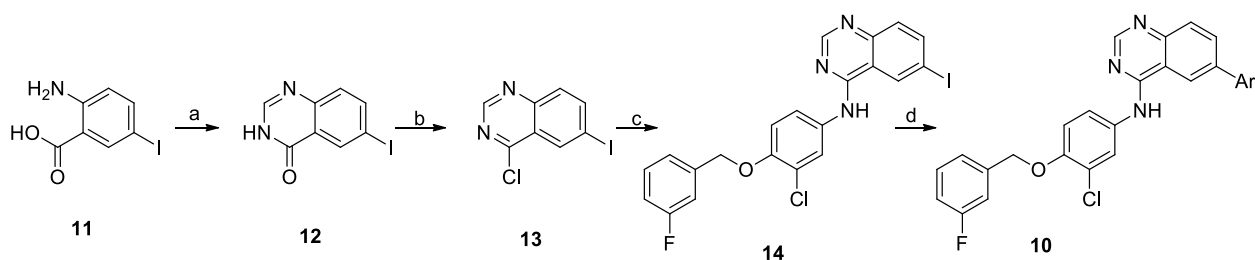
[a]Reagents and conditions: (a) formamide, 170 °C, 4h, 70%; (b) thionyl chloride, DMF, 80 °C,

12h, 85%; (c) 3-chloro-4-((3-fluorobenzyl)oxy)aniline, 2-propanol, 80 °C, 12h, 85%; (d) Ar-B(OH)$_2$, Pd(PPh$_3$)$_4$, 2M Na$_2$CO$_3$, DME, EtOH, 80 °C, 12h.

Scheme 2. Synthesis of requisite aniline intermediates 17.[a]
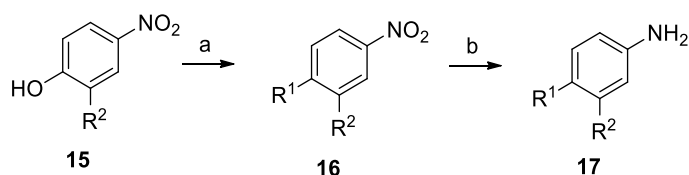
[a]Reagents and conditions: (a) alkyl halide, K$_2$CO$_3$, acetonitrile, 50 °C, 12h; (b) Zn, NH$_4$Cl, MeOH, H$_2$O, 25-50 °C, 6h.

Keeping the newly identified tail group present in **10a (Table 3.3)**, we turned our attention to exploration of the aniline head group region of the molecule. Preparation of the requisite chloroquinazoline **19 (Scheme 3)** was achieved by treatment of **12** with the required boronic acid using Suzuki conditions, followed by chlorination with thionyl chloride. This intermediate was reacted with a range of anilines (**Scheme 2**) to provide analogs **20 (Table 3.3)**.

This library was designed to explore the role of halogen substitutions on the terminal benzyl substituent (R^1) headgroup, testing positional isomers of fluoro substitutions and other potential halogen replacements such as methoxy and trifluoromethyl groups. These modifications produced insignificant changes in activity of the compounds against *T. brucei*. We prepared a few analogs to assess functional group tolerance at the R^2 position of the head group, replacing the chlorine atom of lapatinib with hydrogen and methoxy groups; these changes also resulted in very modest alterations in anti-trypanosomal activity. Interestingly, truncation of the molecule (**20a**) gave potency approximately equal to **10a**, translating to a slightly improved

ligand efficiency value (LE of **10a**=0.14; **20a**=0.18) [**32**]. Importantly, HepG2 cell toxicity was unaffected by any of these modifications.

Scheme 3. Synthesis of head group expansion set 20.[a]
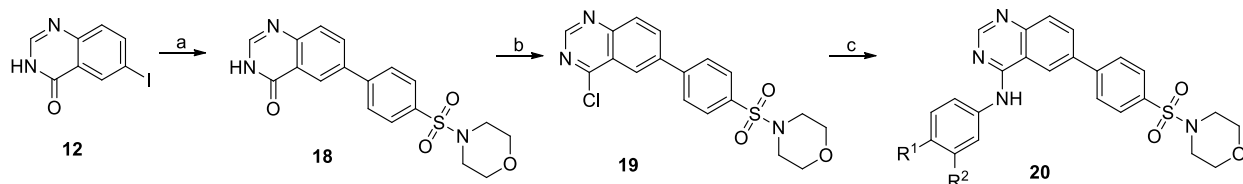
[a]Reagents and conditions: (a) (4-(morpholinosulfonyl)phenyl)boronic acid, Pd(PPh$_3$)$_4$, 2M Na$_2$CO$_3$, DME, EtOH, 80 °C, 30h, 85%; (b) thionyl chloride, DMF, 80 °C, 36h, 66%; (c) Ar-NH$_2$, 2-propanol, 80 °C, 12h.

For the next round of analogs, we turned our attention back to further refinement of the tail group region of lapatinib, performing focused modifications of the 6-aryl position of the quinazoline ring that were designed to evaluate steric requirements, as well as the required adornment of polarity in this region of the inhibitor. These compounds (**10k-x**) were accessed from the corresponding boronic acids using the route shown in **Scheme 1**. The larger sulfonamide side chains showed some modest preference for *meta*-substitution (**Table 3.4**, entries 1-6), though the methyl sulfones (entries 11-12) showed preference for *para*-substituents. Comparing the sulfonamide substituents, morpholine was preferred over the other heterocyclics tested.

Scheme 4. Synthesis of analogs 23.[a]
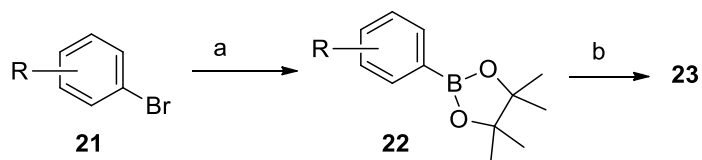
A more systematic evaluation of linker and regiochemistry is shown in **Table 3.5**. Compounds were synthesized from **14** by reaction with the appropriate boronate ester **22**. In the case of the morpholinosulfonamides (entries 1-8), *meta-* substitution is always better than para; the most potent analog, **NEU617, (23a)**, is directly linked to the aromatic ring. For piperidinosulfonamides (entries 9-16), the meta preference is less consistent, and none of these analogs show as potent growth inhibition as **23a**. When the tail contains a morpholine (entries 1-8), the linker has little impact on potency (except for **23a**, a clear outlier); all *meta*-substituted analogs are otherwise approximately equipotent. In cases where the morpholine moiety is at the *para*-position there is little difference resulting from linker variation.

With piperidine-substitution (entries 9-16), it appears that a modest preference exists for the *meta*-substituted amide, with a 6.7-fold loss of activity when moved to the *para* position (compare entries 13 and 14), though the importance of positional substitution is otherwise less for other examples, within ~2-fold in activity.

3.4 Discussion

Discovery of the 4-Anilinoquinazoline Scaffold for Anti-Trypanosome Lead Drugs

Large compound libraries have been screened in the cell culture systems to discover new anti-trypanosomal leads in the past **[33]**. Targeting essential metabolic pathways in the parasite which have significantly diverged from human is a better way to complement the lead discovery approaches against parasitic diseases like HAT. This can be achieved by the use of a select group of existing compounds (focused screen) as a starting point that has already been tested for other

human diseases (alternative use drug discovery). The use of focused screen and alternative use drug discovery strategy reduces the labor, cost and time involved in the process of lead discovery.

Transferrin (Tf, a growth factor) endocytosis is an important cellular pathway in *T. brucei* for iron uptake from the host blood [34]. Our lab has shown that receptor-mediated endocytosis of Tf in the African trypanosome is stimulated by diacylglycerol (DAG) [35]. In most eukaryotes, a Ser/Thr kinase protein kinase C that binds to the lipid with its C1-domain is responsible for amplifying the DAG mediated signaling pathways. However, the DAG signaling pathways have not been studied in trypanosomes. We adopted a chemical biology approach to understand the pathway linking DAG and Tf endocytosis in the trypanosome. We found that the DAG-stimulated endocytosis of Tf was not blocked on by a Ser/Thr protein kinase inhibitor, but by a Tyr kinase inhibitor Tyrphostin A47 [36]. We also recently found that lapatinib, a Tyr kinase inhibitor and an FDA approved anti-cancer drug, blocked transferrin endocytosis in *T. brucei* [37].

Based on this finding we believed that kinase inhibitor drugs that have been approved for human diseases could be further tested for anti-trypanosomal drug discovery. In a focused screen of ten compounds derived from the 4-anilinoquinazoline scaffold, it was found nine compounds including lapatinib killed *T. brucei* at low micromolar concentrations [24]. We hereby describe the subsequent scaffold optimization study that followed these results and led to the discovery of more potent trypanocidal compounds based on established human EGFR inhibitor chemotypes.

We have accelerated our anti-trypanosomal discovery program by eliminating the need to perform high-throughput screens. Indeed, in only a few optimization cycles we have attained good potency that has enabled the identification of these compounds as a lead series for
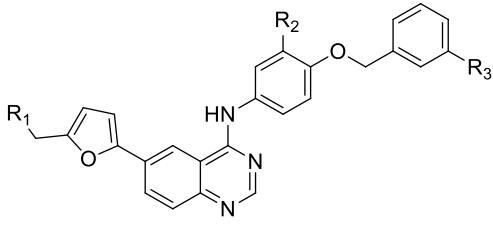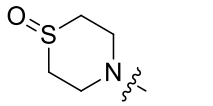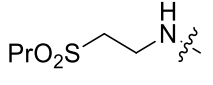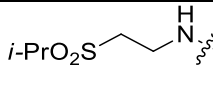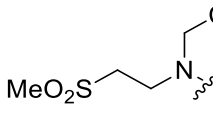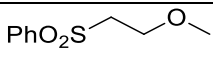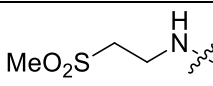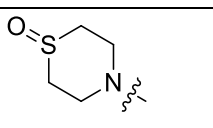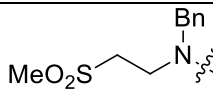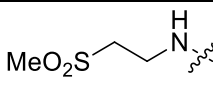
trypanosomiasis. Additional work is needed, however, particularly towards optimizing **23a** to improve predicted central nervous system exposure. A recent report by Wager *et al.* described an analysis that correlated compound properties to CNS exposure using data for both experimental and marketed drugs,[38] and devised a scoring paradigm for prediction of CNS exposure [**39**]. This protocol, termed multi-parameter optimization, or MPO, allows prediction of likely CNS exposure for a given compound based on how closely it meets desired property ranges for MW, cLogP, LogD, pKa, and TPSA (**Table 3.6**), with a maximal MPO score of 6.0, and compounds >4.0 predicted to be CNS-penetrant. As shown in **Table 3.6**, compound **23a** has significant shortcomings in terms of properties that have been shown relevant to CNS activity, particularly due to high calculated lipophilicity (cLogP, cLogD=7.1) and molecular weight (541 Da). Future efforts will be focused on reduction of molecular size and lipophilicity to improve the likelihood of CNS penetration, a pivotal requirement for any new therapeutic for HAT.

We have developed a potent anti-trypanosomal growth inhibitor (**23a**) based on the 6-furanyl 4-anilinoquinazoline scaffold of lapatinib, which displays good selectivity over HepG2 cells. However, further optimization and animal studies will be required to explore the therapeutic efficacy of this scaffold. This study extrapolates our understanding of DAG signaling pathways in trypanosomes for anti-trypanosome lead drugs development, and at the same time represents the phosphotyrosine signaling in trypanosomes for anti-parasite drug discovery.
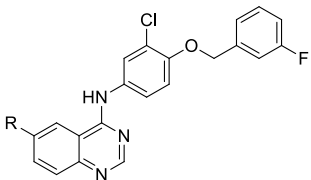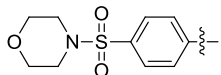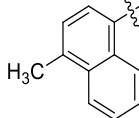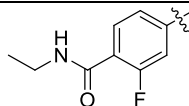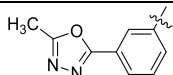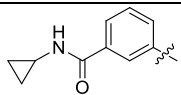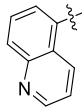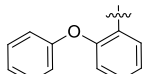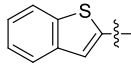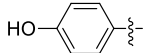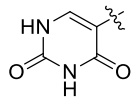
TABLES

Table 3.1: Initial screening data of lapatinib analogs.

Compd	GSK Number	R$_1$	R$_2$	R$_3$	TbbGI$_{50}$ (μM)[a,b]
1	GW58337A	(O=S-thiomorpholine-N)	Cl	H	0.41
2	GW601906A	PrO$_2$S-CH$_2$CH$_2$-NH	Cl	F	0.43
3	GW633460A	i-PrO$_2$S-CH$_2$CH$_2$-NH	Cl	F	0.48
4	GW616030X	MeO$_2$S-CH$_2$CH$_2$-N(CH$_2$CN)	Cl	F	0.52
5	GW615311X	PhO$_2$S-CH$_2$CH$_2$-O-CH$_3$	Cl	F	0.55
6	GW580496A	MeO$_2$S-CH$_2$CH$_2$-NH	Br	H	0.56
7	GW576924A	(O=S-thiomorpholine-N)	F	F	0.60
8	GW616907X	MeO$_2$S-CH$_2$CH$_2$-N(Bn)	Cl	F	1.51
9	lapatinib	MeO$_2$S-CH$_2$CH$_2$-NH	Cl	F	1.54
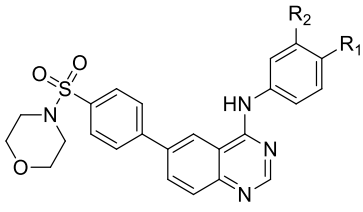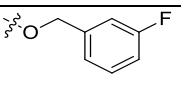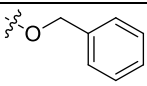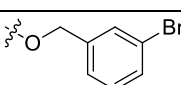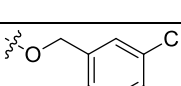
[a.] All GI$_{50}$ values are ± 7%. [b] Concentration giving 50% inhibition of growth of *T brucei brucei* Lister 427 cells
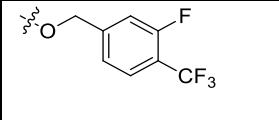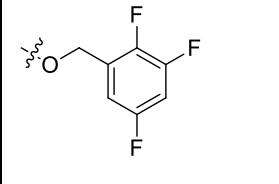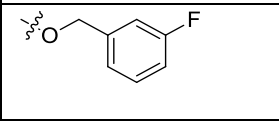
Table 3.2: *T. brucei* growth inhibition data of diverse analogs of lapatinib 10a-10k.

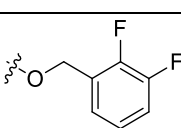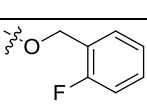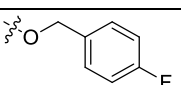| Compd	R_1	TbbGI$_{50}$ (μM)[a,b]
10a		1.39
10b		2.27
10c		3.85
10d		4.21
10e		4.50
10f		4.53
10g		5.3
10h		5.98
10i		6.45
10j		22.63

[a.] All GI$_{50}$ values are ± 7%. [b] Concentration giving 50% inhibition of growth of *T brucei brucei* Lister 427 cells
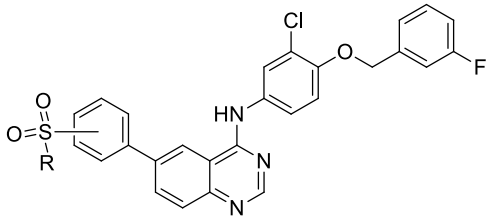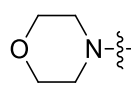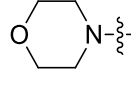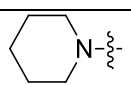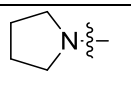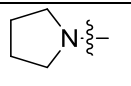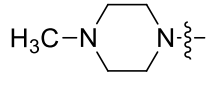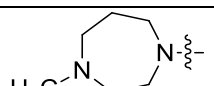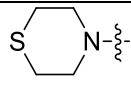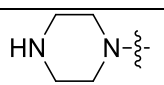
Table 3.3: *T. brucei* **growth inhibition data for headgroup variations of 10a.**

Compd	R₁	R₂	Tbb GI$_{50}$ (μM)[a,b]	HepG2 IC$_{50}$ (μM)
10a	(3-fluorobenzyloxy)	Cl	1.39	>15
20a	H	H	1.44	> 3
20b	CH$_3$	H	1.15	> 15
20c	OH	Cl	1.06	> 15
20d	OCH$_3$	Cl	0.82	> 15
20e	(benzyloxy)	Cl	1.35	> 15
20f	(3-bromobenzyloxy)	Cl	0.68	> 15
20g	(3-chlorobenzyloxy)	Cl	0.66	> 15
20h	(2,3-difluorobenzyloxy)	Cl	0.82	>15
20i	(2-fluorobenzyloxy)	Cl	1.65	> 15
20j	(4-fluorobenzyloxy)	Cl	1.34	> 15
20k	(3-methoxybenzyloxy)	Cl	1.43	> 15

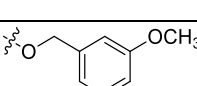|				
20l		Cl	0.54	> 15
20m		Cl	1.12	> 3
20n		H	0.65	> 15
20o		OCH$_3$	1.88	> 15

[a.] All GI$_{50}$ values are ± 7%. [b] Concentration giving 50% inhibition of growth of *T brucei brucei* Lister 427 cells
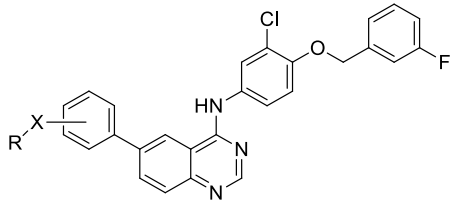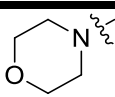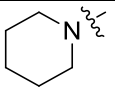
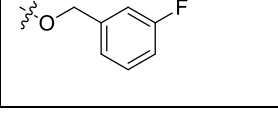**Table 3.4:** *T. brucei* and HepG2 growth inhibition data for focused analogs of 10a.

Entry	Compd	position	R₁	Tbb GI$_{50}$ (μM)[a,b]	HepG2 IC$_{50}$ (μM)
1	**10a**	*p*	morpholine N	1.39	>15
2	**10k**	*m*	morpholine N	0.33	> 15
3	**10l**	*p*	piperidine N	0.32	> 15
4	**10m**	*m*	piperidine N	0.46	>15
5	**10n**	*p*	pyrrolidine N	0.35	> 15
6	**10o**	*m*	pyrrolidine N	0.25	> 15
7	**10p**	*p*	H_3C-N piperazine N	0.53	> 15
8	**10q**	*p*	H_3C-N homopiperazine N	0.81	1.81
9	**10r**	*p*	thiomorpholine N	0.47	> 15
10	**10s**	*p*	HN piperazine N	0.28	3.32
11	**10t**	*p*	CH_3	0.90	> 15
12	**10u**	*m*	CH_3	3.21	> 15

| 13 | **10v** | *o* | N(CH$_3$)$_2$ | 1.04 | > 15 |
| 14 | **10w** | *o* | NHC(CH$_3$)$_3$ | 4.66 | nd[c] |

[a.] All GI$_{50}$ values are ± 7%. [b] Concentration giving 50% inhibition of growth of *T brucei brucei* Lister 427 cells. [c]Not determined.

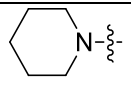**Table 3.5: Growth inhibitory potency of regiochemical and linker analogs of 10.**

Entry	Compd	R	Regio	X	Tbb GI$_{50}$ (μM)[a,b]	HepG2 IC$_{50}$ (μM)
1	**23a**		m	--	0.042	>20
2	**23b**		p	--	1.91	9.6
3	**23c**		m	CH$_2$	0.36	nd[c]
4	**23d**		p	CH$_2$	0.99	12.9
5	**23e**		m	C=O	0.55	nd
6	**23f**		p	C=O	1.21	nd
7	**10k**		m	SO$_2$	0.33	>20
8	**10a**		p	SO$_2$	1.39	>20
9	**23g**		m	--	0.76	>15
10	**23h**		p	--	0.38	nd
11	**23i**		m	CH$_2$	0.65	nd
12	**23j**		p	CH$_2$	1.5	nd
13	**23k**		m	C=O	0.14	>6
14	**23l**		p	C=O	0.94	nd
15	**10m**		m	SO$_2$	0.46	>20
16	**10l**		p	SO$_2$	0.32	>20

[a.] All GI$_{50}$ values are ± 7%. [b] Concentration giving 50% inhibition of growth of *T brucei brucei* Lister 427 cells. [c]Not determined.

Table 3.6: Desirable ranges for CNS penetration and the MPO scoring for 23a.

Prop	Targeted Value	Properties of 23a	MPO Score
cLogP	≤ 3	7.1	0
cLogD	≤ 2	7.1	0
TPSA	$40 < X \leq 90$	59.5	1.00
MW	≤ 360	541	0
HBD	≤ 0.5	1	0.8
pKa	≤ 8	3.05	1.0
		MPO score	**2.8**

References

1.   www.unitingtocombatntds.org,

2.   Pollastri, M. P.; Campbell, R. K. *Target repurposing for neglected diseases.* Future Med Chem 2011, 3, 1307-1315.

3.   Gould, M. K.; de Koning, H. P. *Cyclic-nucleotide signalling in protozoa.* FEMS Microbiol Rev 2011, 35, 515-541.

4.   Parsons, M.; Worthey, E. A.; Ward, P. N.; Mottram, J. C. *Comparative analysis of the kinomes of three pathogenic trypanosomatids: Leishmania major, Trypanosoma brucei and Trypanosoma cruzi.* BMC Genomics 2005, 6, 127.

5.   Bland, N. D.; Wang, C.; Tallman, C.; Gustafson, A. E.; Wang, Z.; Ashton, T. D.; Ochiana, S. O.; McAllister, G.; Cotter, K.; Fang, A. P.; Gechijian, L.; Garceau, N.; Gangurde, R.; Ortenberg, R.; Ondrechen, M. J.; Campbell, R. K.; Pollastri, M. P. *Pharmacological validation of Trypanosoma brucei phosphodiesterases B1 and B2 as druggable targets for African sleeping sickness.* J Med Chem 2011, 54, 8188-8194.

6.   Ochiana, S. O.; Pandarinath, V.; Wang, Z.; Kapoor, R.; Ondrechen, M. J.; Ruben, L.; Pollastri, M. P. *The human Aurora kinase inhibitor danusertib is a lead compound for anti-trypanosomal drug discovery via target repurposing.* Eur J Med Chem 2012.

7.   Diaz-Gonzalez, R.; Kuhlmann, F. M.; Galan-Rodriguez, C.; Madeira da Silva, L.; Saldivia, M.; Karver, C. E.; Rodriguez, A.; Beverley, S. M.; Navarro, M.; Pollastri, M. P. *The susceptibility of trypanosomatid pathogens to PI3/mTOR kinase inhibitors affords a new opportunity for drug repurposing.* PLoS Negl Trop Dis 2011, 5, e1297.

8.   de Koning, H. P.; Gould, M. K.; Sterk, G. J.; Tenor, H.; Kunz, S.; Luginbuehl, E.; Seebeck, T. *Pharmacological validation of Trypanosoma brucei phosphodiesterases as novel drug targets.* J Infect Dis 2012, 206, 229-237.

9.   Beghyn, T. B.; Charton, J.; Leroux, F.; Laconde, G.; Bourin, A.; Cos, P.; Maes, L.; Deprez, B. *Drug to genome to drug: discovery of new antiplasmodial compounds.* J Med 2011, 54, 3222-3240.

10.   Nwaka, S.; Hudson, A. *Innovative lead discovery strategies for tropical diseases.* Nat Rev Drug Discov 2006, 5, 941-955.

11.   Chahrour, O.; Cairns, D.; Omran, Z. *Small molecule kinase inhibitors as anti-cancer therapeutics.* Mini Rev Med Chem 2012, 12, 399-411.

12.   Page, T. H.; Smolinska, M.; Gillespie, J.; Urbaniak, A. M.; Foxwell, B. M. *Tyrosine kinases and inflammatory signalling.* Curr Mol Med 2009, 9, 69-85.

109

13. Ito, K.; Caramori, G.; Adcock, I. M. *Therapeutic Potential of Phosphatidylinositol 3-Kinase Inhibitors in Inflammatory Respiratory Disease.* J Pharmacol Exp Therap 2007, 321, 1-8.

14. Louvet, C.; Szot, G. L.; Lang, J.; Lee, M. R.; Martinier, N.; Bollag, G.; Zhu, S.; Weiss, A.; Bluestone, J. *A. Tyrosine kinase inhibitors reverse type 1 diabetes in nonobese diabetic mice.* Proc Natl Acad Sci U S A 2008.

15. Wagman, A. S.; Johnson, K. W.; Bussiere, D. E. *Discovery and development of GSK3 inhibitors for the treatment of type 2 diabetes.* Curr Pharm Des 2004, 10, 1105-1137.

16. Chico, L. K.; Van Eldik, L. J.; Watterson, D. M. *Targeting protein kinases in central nervous system disorders.* Nat Rev Drug Discov 2009, 8, 892-909.

17. Natoli, C. *Tyrosine Kinase Inhibitors.* Current Cancer Drug Targets 2010, 10, 462.

18. Lackey, K. E. *Lessons from the drug discovery of lapatinib, a dual ErbB1/2 tyrosine kinase inhibitor.* Curr Top Med Chem 2006, 6, 435-460.

19. Johannessen, L. E.; Ringerike, T.; Molnes, J.; Madshus, I. H. *Epidermal growth factor receptor efficiently activates mitogen-activated protein kinase in HeLa cells and Hep2 cells conditionally defective in clathrin-dependent endocytosis.* Exp Cell Res 2000, 260, 136-145.

20. Naula, C.; Parsons, M.; Mottram, J. C. *Protein kinases as drug targets in trypanosomes and Leishmania.* Biochim Biophys Acta 2005.

21. Oduor, R. O.; Ojo, K. K.; Williams, G. P.; Bertelli, F.; Mills, J.; Maes, L.; Pryde, D. C.; Parkinson, T.; Van Voorhis, W. C.; Holler, T. P. *Trypanosoma brucei Glycogen Synthase Kinase-3, A Target for Anti-Trypanosomal Drug Development: A Public-Private Partnership to Identify Novel Leads.* PLoS Negl Trop Dis 2011, 5, 1017.

22. Nett, I. R.; Martin, D. M.; Miranda-Saavedra, D.; Lamont, D.; Barber, J. D.; Mehlert, A.; Ferguson, M. A. *The phosphoproteome of bloodstream form trypanonosoma brucei, causative agent of African sleeping sickness.* Mol Cell Proteomics 2009.

23. Nett, I. R.; Davidson, L.; Lamont, D.; Ferguson, M. A. *Identification and specific localization of tyrosine-phosphorylated proteins in Trypanosoma brucei.* Eukaryot Cell 2009, 8, 617-626.

24. Katiyar, S.; Kufareva, I.; Behera, R.; Thomas, SM.; Ogata, Y.; Pollastri, M.; Abagyan, R.; Mensa-Wilmot, K. *Lapatinib-Binding Protein Kinases in the African Trypanosome: Identification of Cellular Targets for Kinase-Directed Chemical Scaffolds.* PLoS ONE 2013, 8(2):e56150.

25. Slichenmyer, W. J.; Elliott, W. L.; Fry, D. W. *CI-1033, a pan-erbB tyrosine kinase inhibitor.* Semin Oncol 2001, 28, 80-85.

26. Xia, W.; Mullin, R. J.; Keith, B. R.; Liu, L. H.; Ma, H.; Rusnak, D. W.; Owens, G.; Alligood, K. J.; Spector, N. L. *Anti-tumor activity of GW572016: a dual tyrosine kinase inhibitor blocks EGF activation of EGFR/erbB2 and downstream Erk1/2 and AKT pathways.* Oncogene 2002, 21, 6255-6263.

27. Traxler, P.; Allegrini, P. R.; Brandt, R.; Brueggen, J.; Cozens, R.; Fabbro, D.; Grosios, K.; Lane, H. A.; McSheehy, P.; Mestan, J.; Meyer, T.; Tang, C.; Wartmann, M.; Wood, J.; Caravatti, G. *AEE788: a dual family epidermal growth factor receptor/ErbB2 and vascular endothelial growth factor receptor tyrosine kinase inhibitor with antitumor and antiangiogenic activity.* Cancer Res 2004, 64, 4931-4941.

28. Rusnak, D. W.; Lackey, K.; Affleck, K.; Wood, E. R.; Alligood, K. J.; Rhodes, N.; Keith, B. R.; Murray, D. M.; Knight, W. B.; Mullin, R. J.; Gilmer, T. M. *The effects of the novel, reversible epidermal growth factor receptor/ErbB-2 tyrosine kinase inhibitor, GW2016, on the growth of human normal and tumor-derived cell lines in vitro and in vivo.* Mol Cancer Ther 2001, 1, 85-94.

29. Petrov, K. G.; Zhang, Y. M.; Carter, M.; Cockerill, G. S.; Dickerson, S.; Gauthier, C. A.; Guo, Y.; Mook, R. A., Jr.; Rusnak, D. W.; Walker, A. L.; Wood, E. R.; Lackey, K. E. *Optimization and SAR for dual ErbB-1/ErbB-2 tyrosine kinase inhibition in the 6-furanylquinazoline series.* Bioorg Med Chem Lett 2006, 16, 4686-4691.

30. Rusnak, D. W.; Affleck, K.; Cockerill, S. G.; Stubberfield, C.; Harris, R.; Page, M.; Smith, K. J.; Guntrip, S. B.; Carter, M. C.; Shaw, R. J.; Jowett, A.; Stables, J.; Topley, P.; Wood, E. R.; Brignola, P. S.; Kadwell, S. H.; Reep, B. R.; Mullin, R. J.; Alligood, K. J.; Keith, B. R.; Crosby, R. M.; Murray, D. M.; Knight, W. B.; Gilmer, T. M.; Lackey, K. *The characterization of novel, dual ErbB-2/EGFR, tyrosine kinase inhibitors: potential therapy for cancer.* Cancer Res 2001, 61, 7196-7203.

31. Cai, X.; Zhai, H.-X.; Wang, J.; Forrester, J.; Qu, H.; Yin, L.; Lai, C.-J.; Bao, R.; Qian, C. *Discovery of 7-(4-(3-Ethynylphenylamino)-7-methoxyquinazolin-6-yloxy)-N-hydroxyheptanamide (CUDC-101) as a Potent Multi-Acting HDAC, EGFR, and HER2 Inhibitor for the Treatment of Cancer.* J Med Chem 2010, 53, 2000-2009.

32. Hopkins, A. L.; Groom, C. R.; Alex, A. *Ligand efficiency: a useful metric for lead selection.* Drug Discov Today 2004, 9, 430-431.

33. Mackey, Z. B.; Baca, A. M.; Mallari, J. P.; Apsel, B.; Shelat, A.; Hansell, E. J.; Chiang, P. K.; Wolff, B.; Guy, K. R.; Williams, J.; McKerrow, J. H. *Discovery of trypanocidal compounds by whole cell HTS of Trypanosoma brucei.* Chem Biol Drug Des 2006, 67, 355-363.

34.   Steverding, D. *The transferrin receptor of Trypanosoma brucei.* Parasitol Int 2000, 48, 191-198.

35.   Subramanya, S.; Hardin, C. F.; Steverding, D.; Mensa-Wilmot, K. *Glycosylphosphatidylinositol-specific phospholipase C regulates transferrin endocytosis in the African trypanosome.* Biochem J 2009, 417, 685-694.

36.   Subramanya, S.; Mensa-Wilmot, K. *Diacylglycerol-stimulated endocytosis of transferrin in trypanosomatids is dependent on tyrosine kinase activity.* PLoS ONE 2010, 5, e8538.

37.   Behera, R.; Guyett, P.; Thomas, S.; Katiyar, S.; Ogata, Y.; Mensa-Wilmot, K.,unpublished results

38.   Wager, T. T.; Chandrasekaran, R. Y.; Hou, X.; Troutman, M. D.; Verhoest, P. R.; Villalobos, A.; Will, Y. *Defining Desirable Central Nervous System Drug Space through the Alignment of Molecular Properties, in Vitro ADME, and Safety Attributes.* ACS Chem Neurosci 2010, 1, 420-434.

39.   Wager, T. T.; Hou, X.; Verhoest, P. R.; Villalobos, A. Moving beyond Rules: The *Development of a Central Nervous System Multiparameter Optimization (CNS MPO) Approach To Enable Alignment of Druglike Properties.* ACS Chem Neurosci 2010, 1, 435-449.

40.   Iino, T.; Sasaki, Y.; Bamba, M.; Mitsuya, M.; Ohno, A.; Kamata, K.; Hosaka, H.; Maruki, H.; Futamura, M.; Yoshimoto, R.; Ohyama, S.; Sasaki, K.; Chiba, M.; Ohtake, N.; Nagata, Y.; Eiki, J.-i.; Nishimura, T. *Discovery and structure–activity relationships of a novel class of quinazoline glucokinase activators.* Bioorg Med Chem Lett 2009, 19, 5531-5538.

41.   Mahboobi, S.; Sellmer, A.; Winkler, M.; Eichhorn, E.; Pongratz, H.; Ciossek, T.; Baer, T.; Maier, T.; Beckers, T. *Novel Chimeric Histone Deacetylase Inhibitors: A Series of Lapatinib Hybrides as Potent Inhibitors of Epidermal Growth Factor Receptor (EGFR), Human Epidermal Growth Factor Receptor 2 (HER2), and Histone Deacetylase Activity.* J Med Chem 2010, 53, 8546-8555.

42.   Hirumi, H.; Hirumi, K. *Axenic culture of African trypanosome bloodstream forms.* Parasitol.Today. 1994, 10, 80-84.

43.   Ferrari, M.; Fornasiero, M. C.; Isetta, A. M. *MTT colorimetric assay for testing macrophage cytotoxic activity in vitro.* J Immunol Methods 1990, 131, 165-172.

CHAPTER IV

THERAPEUTIC EFFICACY OF GW572016, CI-1033, NEU617, AND AEE788

IN A MOUSE MODEL OF ACUTE HUMAN AFRICAN TRYPANOSOMIASIS[3]

Abstract

Human African Trypanosomiasis (HAT) is a life threatening neglected tropical disease caused by *Trypanosoma brucei*. We need new orally bioavailable drugs as emerging resistance and toxic side effects of current therapies pose a limit to treatment choices. Drug development against neglected diseases in general faces numerous setbacks because of which an alternative drug discovery strategy ("Piggy-back" approach) is appropriate. Phosphotyrosine signaling in the parasite is unique, biologically essential, and divergent from the system found in the mammalian host; this situation makes the pathway an attractive target for chemotherapeutic intervention. Studies on tyrosine kinase inhibitors in humans have led to the development of small molecules that can be tested on trypanosomes. Here we test the potential of 4-anilinoquinazoline and pyrrolopyrimidine scaffolds for antitrypanosome lead drug discovery. GW572016, CI-1033, NEU617, and AEE788 were tested on axenically culture bloodstream trypanosome. The efficacy of the drugs on mice infected with *T. brucei* was also investigated. All four compounds actively inhibited replication of *T. brucei* in the culture at low micromolar to nanomolar concentration. For *in vivo* studies, the compounds were tested in a mouse model of acute HAT by intraperitoneal or oral administration. In all cases, drug treatment controlled infection and extended the mean survival of mice as compared to the control mice that were treated with vehicle. Oral administration of GW572016 and AEE788 was better at controlling. With NEU617, the intraperitoneal route was more efficacious compared to the oral route. CI-1033 produced a similar effect irrespective of the dosing route. We conclude that both 4-anilinoquinazoline and pyrrolopyrimidine are promising scaffolds that can be optimized as orally active antitrypanosome lead drugs in a lead optimization campaign.

4.1 Introduction

Millions of people in the Saharan sub-continent are potentially at risk of contracting Human African Trypanosomiasis (HAT), also known as sleeping sickness. HAT is a parasitic disease caused by *Trypanosoma brucei*, transmitted by the sand fly (Glossina spp.). The disease develops in two clinically distinct forms; acute form disease is caused by *T. b. rhodesiense* that is more prevalent in East and Southern Africa whereas infection with *T. b. gambiense* leads to a chronic form that is endemic in West and Central Africa **[1, 2]**. The parasites replicate in the blood during the early (hemolymphatic) stage and subsequently progress to the central nervous system (encephalitic stage) by crossing the blood brain barrier **[3]**.The disease, when untreated in early stage, might lead to death as most of the drugs fail to cross the blood brain barrier in the late stage.

The choices of drug for treatment of HAT are limited. All four (suramin, pentamidine, melarsoprol, and eflornithine) drugs are given by injection and that requires hospitalization. Because it is a disease that is prevalent among poor and rural communities, pharmaceutical companies lack interest in developing drugs for HAT, considering it financially unprofitable. Over the years HAT has emerged as one of the most neglected diseases of the tropics as defined by the World Health Organization **[4, 5]**. We critically need novel orally active drugs with improved therapeutic index. An 'Alternative use drug discovery' strategy can overcome the obstacles in conventional drug discovery by adopting proven drugs and facilitating discovery of "lead candidates" for further optimization.

The tyrosine kinase signaling pathway is an unexplored area in the African trypanosome. Unlike the mammalian system, the human type receptor tyrosine kinases and phosphorylated tyrosine binding domains are absent. However, presence of phosphotyrosine proteins has been

reported **[6-8].** That indicates that a deeply diverged phosphotyrosine signaling pathway might exist in the parasite. Tyrphostin A47, a tyrosine kinase inhibitor, prevents transferrin endocytosis and kills the parasite **[9]**. Following upon these results, we hypothesize that targeted inhibition of the phosphotyrosine pathway with chemical compounds will be biologically detrimental for the parasite. 4-Anilinoquinazoline and pyrrolopyrimidine are important classes of ATP-mimicking tyrosine kinase inhibitors **[10-13]**. Because of their strong selectivity and potency, many of them (GW572016, Erlotinib, Gefitinib etc.) are already in use or in clinical trials (CI-1033, AEE788) against proliferative diseases like cancer **[14-17]**.

In the current study we investigated GW572016, CI-1033 and AEE788 and a new 4-anilinoquinaoline NEU617 as antitrypanosome agents. The compounds inhibited growth of *T. brucei* in culture at low micromolar to nanomolar range of concentrations. When tested *in vivo* in a mouse model of acute HAT to access the curative efficacy, all of them demonstrated good activity depending on the route of administration. GW572016 could control parasitemia and cured infection in 25% of the animals. CI-1033 and AEE788 checked parasitemia and improved the mean survival of infected mice by 4 days and 5 days respectively when given orally. NEU617, when given intraperitoneally (IP), helped mice survive a level of parasitemia that killed the untreated mice. The study shows that 4-anilinoquionazoline and pyrrolopyrimidine are very good scaffolds for lead drug discovery against HAT. Oral bioavailability of the compounds makes them especially suitable for a lead optimization campaign.

4.2 Materials And Methods

4.2.1 Materials

Dimethyl Sulfoxide (DMSO) was purchased from Fisher Scientific. N-methyl-2- pyrrolidone and

polyethylene glycol 300 were from Fluka (Sigma-Aldrich). The components for preparation of HMI-9 medium were previously described **[18, 19]**.

4.2.2 Test compounds and preparation

GW572016 (Lapatinib), CI-1033 (Canertinib) and AEE788 were gifts from GlaxoSmithKline (Durham, NC), Pfizer (New London, CT), Novartis (Vienna, Austria) respectively. NEU617 was synthesized in the laboratory of Dr. M.P. Pollastri **[20]**. All compounds were dissolved in DMSO as 10 mM stocks and stored at -20°C in small aliquots in order to avoid repeated freezing and thawing. The final concentration of DMSO in all experiments was <0.5%. For *in vivo* studies, compounds were reconstituted in two different solvents based on the route of administration; (i) DMSO for intraperitoneal (I.P.) administration, or (ii) N-methyl-2-pyrrolidone and polyethylene glycol 300 (1:9, v/v) for oral (P.O.) dosing. The drugs were prepared fresh daily and the concentration was adjusted so that the animals received less than 200 µl of solvent/dose/animal.

4.2.3 Structures of test compounds

GW572016 (Lapatinib), CI-1033 (Canertinib), and AEE788 are small molecule tyrosine kinase inhibitors (mammalian) developed by GlaxoSmithKline, Novartis, and Pfizer respectively. Both GW572016 and CI-1033 share a 4-anilinoquinazoline scaffold. AEE788 is a pyrrolopyrimidine derivative. These compounds are well studied for development as anti-cancer drugs *in vitro* and *in vivo* **[21-25]**. NEU617 is a novel 4-anilinoquinazoline. The chemical structures of these compounds are shown **(Fig. 4.1)**.

4.2.4 Trypanosome culture

The bloodstream form *Trypanosoma brucei brucei* CA427 strain (gift from Dr. C.C.

Wang, UCSF, CA) was used for both in vitro and in vivo experiments. Parasites were routinely cultured in the HMI-9 medium containing 10% FBS, 10% serum plus (heat inactivated), and antibiotic/ antimycotic solution with a final concentration of 100 I.U. penicillin/mL, 100 μg/mL streptomycin, 0.25 μg/mL Amphotericin B. The culture was maintained in log growth phase under standard conditions (5% CO_2 and 37°C) and sub-cultured every 2-3 days interval.

4.2.5 Mice

Swiss Webster (female) mice, age 8-10 weeks, were purchased from Harlan Laboratories and housed in a micro-isolator with four animals per group under standard conditions. The animals were infected following an acclimatization period of 7 days at the facility. All experiments were conducted as per the protocol approved by the Institutional Animal Care and Use Committee (IACUC) at the University of Georgia, Athens. The animals were checked least daily during the course of an experiment.

4.2.6 In vitro assay

The standard growth inhibition assay was performed following a 48 h incubation protocol **[13]**. All compounds were tested initially at 400 nM and 4 μM to define the range of concentrations for subsequent assays. *T. brucei,* from a mid log phase culture, were harvested by centrifuging at 3000 RPM for 10 min, diluted in pre-warmed fresh HMI-9 medium, and added at 2×10^3 cells/ml/well in 24-wells plates. DMSO or drugs (2 μl) were added from appropriate stocks to the final concentrations with DMSO less than 0.5%. After 48 h incubation under standard culturing conditions, cell density in each well was determined with a hemocytometer. The growth inhibition was plotted, and GI_{50} for each drug was calculated from the equation derived from the plot. Standard deviation was reported from two independent experiments with double replicates.

118

4.2.7 Drug efficacy in mouse a model of acute HAT

Log phase CA427 *T. brucei* were washed twice in 1X bicine-buffered saline with glucose (50 mM Bicine, 50 mM NaCl, 5 mM KCl, and 1% w/v glucose), pelleted (3000 RPM for 10 min), and resuspended at 10^4 cells/ml of BSG. Each mouse was inoculated intraperitoneally with 10^3 cells with 26G ½ ″ needle (day 0). The animals were randomly assigned to different groups (four mice per group). Prior to infecting the animals, body weights were recorded and tails marked. Drug treatment was initiated one-day post infection and continued as mentioned. Control group received the vehicle. Animals in the treatment groups were given calculated amounts of drugs based on their body weights (see Table 1). Parasitemia was monitored daily for 14 days, by collecting 2 µl of blood (tail prick) in 18 µl of 0.85% ammonium chloride (NH_4Cl) (1:10 dilution). The parasites were counted with a hemocytometer. Further dilutions were made with BBG when the parasitemia was higher than 10^6/ml. If no parasite was detected after 14 days, parasitemia was determined thrice a week for next 30 days. Animals surviving with no detectable parasitemia 30 days post death of the last control mouse were considered cured. Animals showing distress at any stage of the experiment was euthanized and considered dead. The graphs were plotted with graphpad prizm software (La Jolla, CA).

4.3 Results

4.3.1 Effects of drugs on axenically cultured trypanosomes

It has been reported that Tyrophostin A47, a tyrosine kinase inhibitor, kills *T. brucei* **[9]**. We investigated the effect of three tyrosine kinase inhibitors namely GW572016, CI-1033 and AEE788 on blood stream form trypanosomes *in vitro*. All compounds inhibited growth of *T. brucei* in a concentration dependent manner. The GI_{50} (concentration that inhibits *T. brucei* growth by 50%) values were 1.5 µM for GW572016, 2.0 µM for CI-1033 and 2.5 µM AEE788

(Fig. 4. 2.A, B, D). NEU617 was significantly more potent with a GI_{50} value of 0.04 **(Fig. 4.2.C)**.

4.3.2 Efficacy of drugs in a mouse model of acute HAT

All four compounds were tested in mice infected with CA427 strain *T. brucei*. The drugs were administered in two different routes (IP and PO) in separate experiments as mentioned in materials and methods. Parasites were usually detected in blood as early as 2 days post infection and the parasitemia peaked at a level of 10^8-10^9 between day 5-7 days. The untreated animals failed to control infection and died by day 8. Animals in distress were euthanized at any stage of the experiment. The mean survival time for the control group was 4-5 days **(Fig. 4.3. 4.4, 4.5, 4.6)**. GW572016 is an orally bioavailable drug **[21]**. When the drug was administered IP, the treated animals outlived the control and the increase in mean survival was 1.25 days **(Fig. 4.3.E)**. Better results were obtained in animals treated orally with GW572016 when compared to those receiving IP injection. GW572016 achieved 25% cure by oral administration where the infection was controlled **(Fig. 4.3.D)**. The mean survival period of remaining animals in the group was extended by 3.2 days as a result of GWGW572016 treatment **(Fig. 4.3.F)**. The onset of parasitemia was delayed in mice treated by IP dosing route **(Fig. 4.3.A)**. However, the treatment could not eliminate the infection and the animals died by day 7 (Fig 4.3.C). In the group that received treatment orally the parasitemia was comparable with the control group. Drug treated animals could survive a parasitemia as high as 10^9 **(Fig 4.3.B)**.

Similar data were obtained when CI-1033 was given IP or orally. The treatment prolonged the life span of the animals compared to the control **(Fig. 4.4.C, D)**; the mean survival increased by 1.5 days (IP dosing) or 5 days (oral dosing) compared to the control group **(Fig. 4.4.E, F)**. In both situations parasites were detected one day later, and the level of parasites in the

120

blood in the treated group remained lower than the control initially **(Fig. 4.4.A, B)**. Also, the parasitemia developed at a slower rate and the drugged animals could withstand a higher level of infection.

The efficacy of NEU617, when given IP, was better compared to the oral route. The animals survived longer when it was given by IP; the mean survival increased by 4.25 days (compared to 1.5 days when given PO) **(Fig. 4.5.C, D, E, and F)**. The treated group had a lower parasitemia when compared to the control group **(Fig. 4.5.A, B)**. When NEU617 was given IP, the trypanosomes were detected one day later than the control where as both groups showed parasites on the same day in the oral dosing experiment.

Efficacy of AEE788 was improved by oral administration. The animal survival was prolonged in the group by oral route with an extension of mean survival by 5 days than the control **(Fig. 4.6.D, F)**. However, the animals died around the same time as the control when AEE788 was given IP, and the mean survival was relatively similar **(Fig. 4.6.C, E)**. AEE788 showed good activity at controlling the infection by IP route initially and the animals died with low level of parasitemia **(Fig. 4.6.A)**. The treated animals could tolerate higher parasitemia than the control mice by oral dosing. We noticed a second wave of parasitemia that killed the animals **(Fig. 4.6.B)**.

4.4 Discussion

Few drugs are available for treating human African Trypanosomiasis and they are not orally administered. Discovery of new drugs against *T. brucei* is a priority of WHO since pharmaceutical companies are less concerned in investing in drug discovery programs for parasitic diseases **[26]**. An "alternative use drug discovery" strategy is one good approach that

121

can be used to find new drugs especially if these compounds have been used in phase I human trials.

Our interest for investigating protein tyrosine kinase inhibitors (PTKIs) as potential drug candidates for HAT is logical. First, tyrosine kinase activity inhibitors block transferrin endocytosis which is essential pathway for uptake of extracellular iron in *T. brucei* [9]. Second, orally bioavailable tyrosine kinase inhibitors are available that have been tested in mice [21-25]. To determine the effect on bloodstream form *T. brucei,* we tested two 4-anilinoquinazolines (GW572016 and CI-1033) and a pyrrolopyrimidine (AEE788) **(Fig. 4.1)**. All three drugs inhibited replication of cultured *T. brucei* at low micromolar concentrations (GI50 value of $\leq$ 3.0 μM) **(Fig. 4.2)**. It is important to mention here that not all the PTKIs that we tested are active against *T. brucei*. Target profiling has shown that GW572016, CI-1033, and AEE788 bind essential protein kinases in *T. brucei* [13]. Considering the fact that these drugs are optimized against human targets it is less likely that they will be concurrently optimized against trypanosome PTKs. In an initial attempt to optimize 4-anilinoquinazoline scaffold for anti-trypanosome drug discovery NEU617 was developed [20]. *In vitro* NEU617 was potent at low nanomolar concentration (GI$_{50}$ 42 nM) **(Fig. 4.2.C)**.
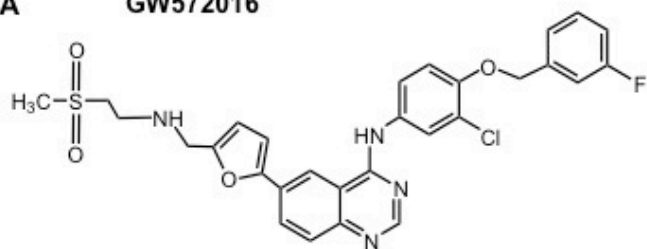
We tested these compounds in animal models of acute HAT to find out whether they might be lead drugs against HAT. Better results were obtained when GW572016, CI-1033, and AEE788 were given orally **(Fig. 4.3.D, 4.4.D, 4.6.C)**. This finding further suggests that both 4-anilinoquinazoline and pyrrolopyrimidine scaffolds can be improved in future to discover novel orally bioavailable drugs for HAT. Also, it was found that the animals when received these drugs intraperitoneally the animals died with a low level of parasites which implies that these drug could be toxic. In a separate experiment, toxicity of AEE788 was confirmed at 30 mg/kg of IP

injection. NEU617, however, had a better activity by IP dosing (Fig. 4.5.B, D, F). This could be due to either low absorption from digestive tract or binding of drug by plasma proteins. NEU617 had no toxicity issue at the dose rate of 10 mg/kg.

To summarize, parasitemia was controlled and an increase in the mean survival was noticed following treatment with GW572016/ CI-1033/AEE788 (PO) or NEU617 (IP). Also, the drug treatment made the animals more resistant to higher parasite load that the control group failed to withstand. The drugs were well tolerated at the dose mentioned earlier with no sign of toxicity or adverse effect during the entire course of treatment. We conclude that the 4-anilinoquinazoline and pyrrolopyrimidine are good scaffolds for developing orally available drugs against HAT.

Figure 4.1: Chemical structures of GW572016, CI-1033, NEU617 and AEE788.
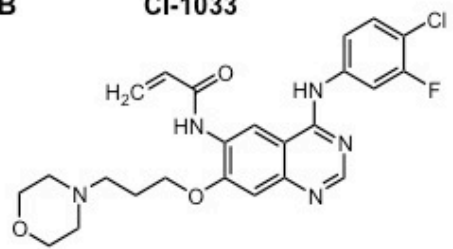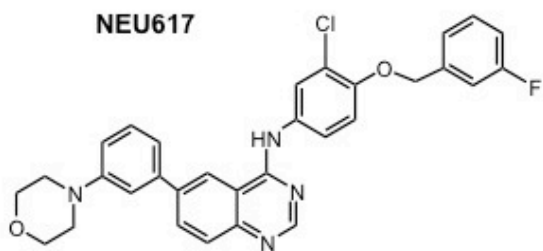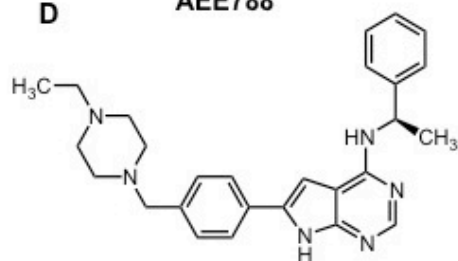
Figure 4.2: GW572016, CI-1033, NEU617 and AEE788 inhibit *T. brucei* growth *in vitro*.

Bloodstream *T. brucei* (initial cell density of 2 x 10^3 cells/ ml) were cultured in 24-well plates for 48 h with either DMSO (0 μM control) or different concentrations of drug. Trypanosome density following incubation was determined with a hemocytometer. The mean parasite density ± standard deviation obtained from two independent experiments in duplicate was plotted in the graphs. An (*) indicates no live cells were detected.

Figure 4.2
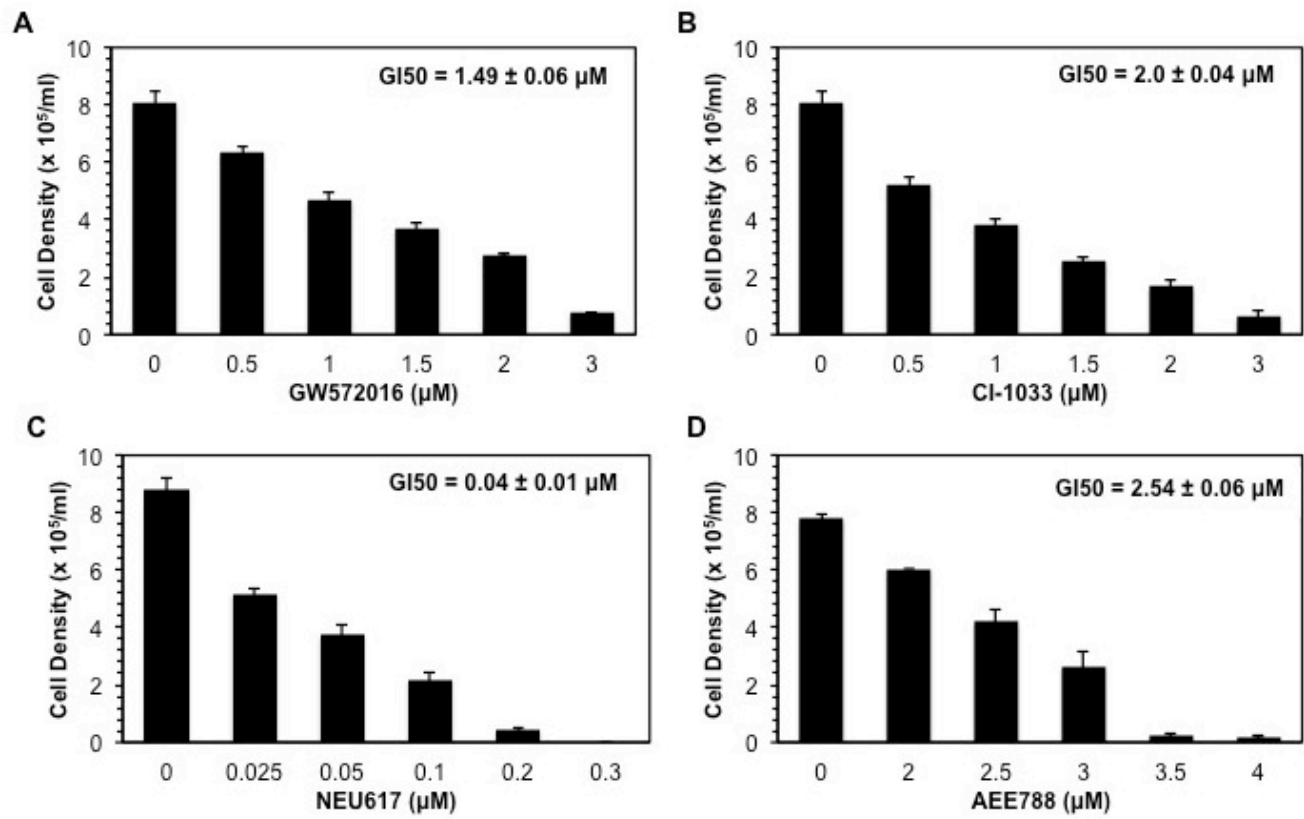
Figure 4.3: Assessment of GW572016 in a mouse model of acute HAT. (A, B) Parasitemia following GW572016 treatment. Animals were infected with 1000 *T. brucei* CA427 parasites (day 0). Parasitemia was determined by collecting 2 µl of blood by tail prick into 18 µl of 0.85% ammonium chloride, and counted with a hemocytometer. The parasitemia was determined every 24 h. U: Untreated group, and T: Treated group. **(C, D) Animal survival post infection.** Animals were treated from day 1 with 100 mg/kg GW572016 once daily. The control group received only the vehicle. (PO: Oral gavage, and IP: Intraperitoneal injection). (E, F) **Mean survival.** The average number of days that treated animals survived (cured not included) was calculated and plotted as the mean survival. The standard deviation in the mean survival in the group is presented. * Indicates that a mouse was cured.

Figure 4.3
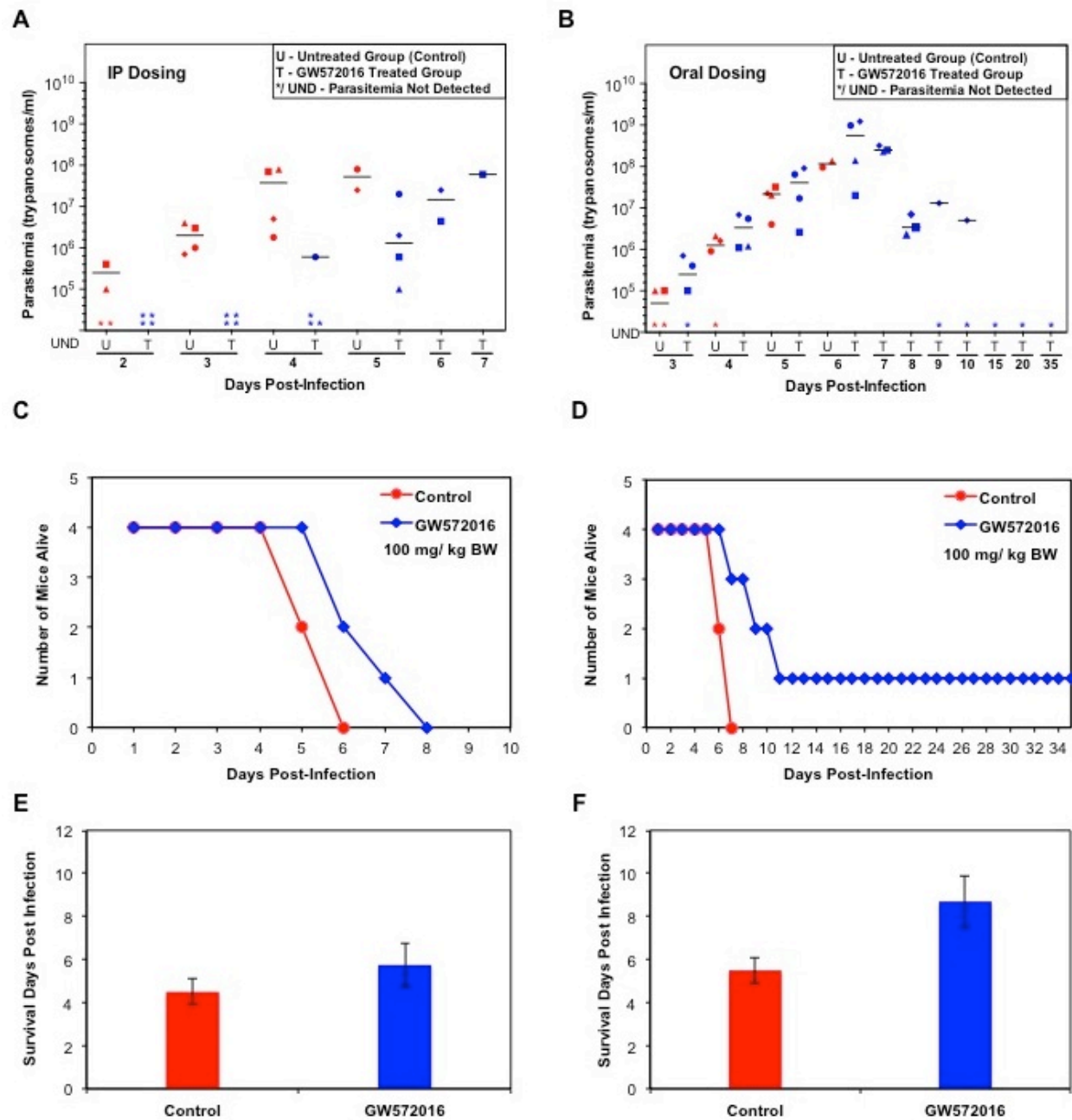
Figure 4.4: Assessment of CI-1033 in a mouse model of acute HAT. (A, B) Parasitemia following CI-1033 treatment. Parasitemia was determined once daily with a hemocytometer. U: Untreated group and T: Treated group. **(C, D) Animal survival post infection.** Animals were dosed with 30 mg/kg CI-1033once daily in the treated group where as control group received the vehicle. (PO: Oral gavage, and IP: Intraperitoneal injection). **(E, F) Mean survival.** Average survival days ± standard deviation in the group was plotted.

Figure 4.4
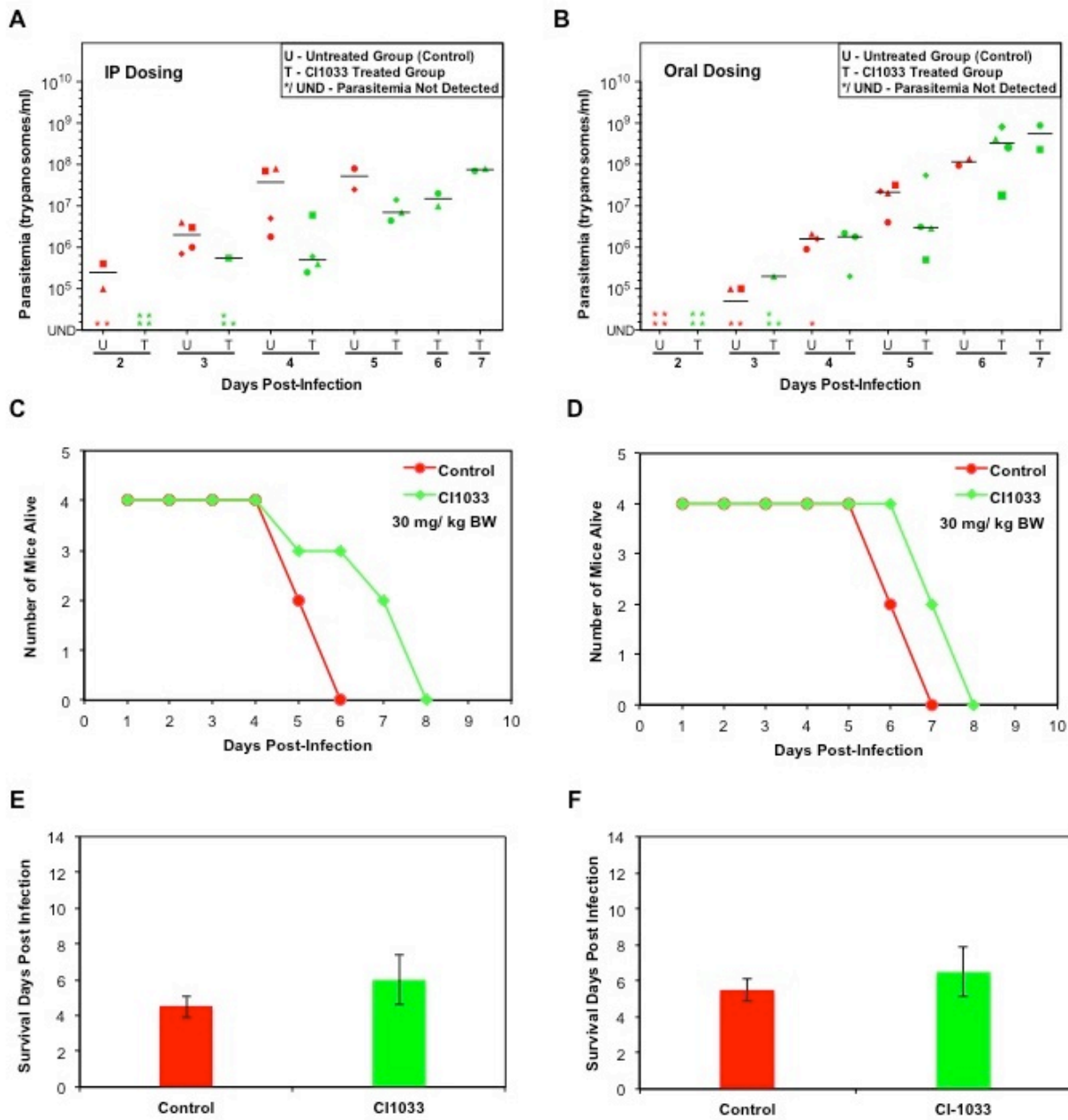
Figure 4.5: Assessment of NEU617 in a mouse model of acute HAT: (A, B) Parasitemia following NEU617 treatment. Parasitemia was determined as described and graphs were plotted. U: Untreated group and T: Treated group. **(C, D) Animal survival post infection.** The animals were treated with10 mg/kg NEU617 twice daily (20 mg/ kg BW total). The control group received the vehicle only. (PO: Oral gavage and IP: Intraperitoneal injection). **(E, F) Mean survival.** Average survival days ± standard deviation in the group was plotted.

Figure 4.5
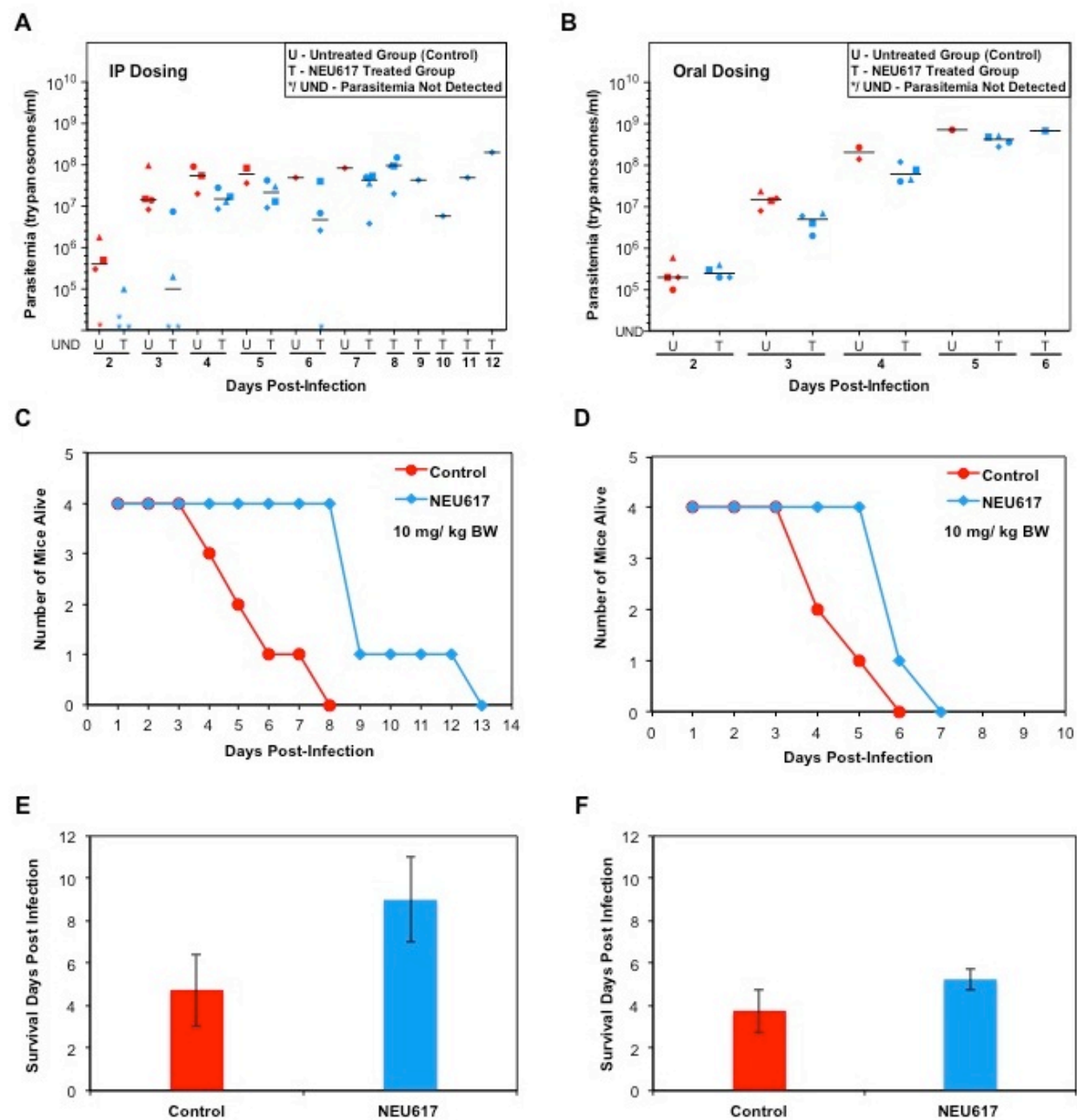
Figure 4.6: Assessment of AEE788 in a mouse model of acute HAT. (A, B) Parasitemia following AEE788 treatment. Parasitemia in the blood was determined with a hemocytometer and graphs were plotted. U: Untreated group and T: Treated group. **(C, D) Animal survival post infection.** The animals were treated with 30 mg/kg NEU617 once daily. The control group received the vehicle only. (PO: Oral gavage, and IP: Intraperitoneal injection). **(E, F) Mean survival.** Average survival days ± standard deviation in the group was plotted.
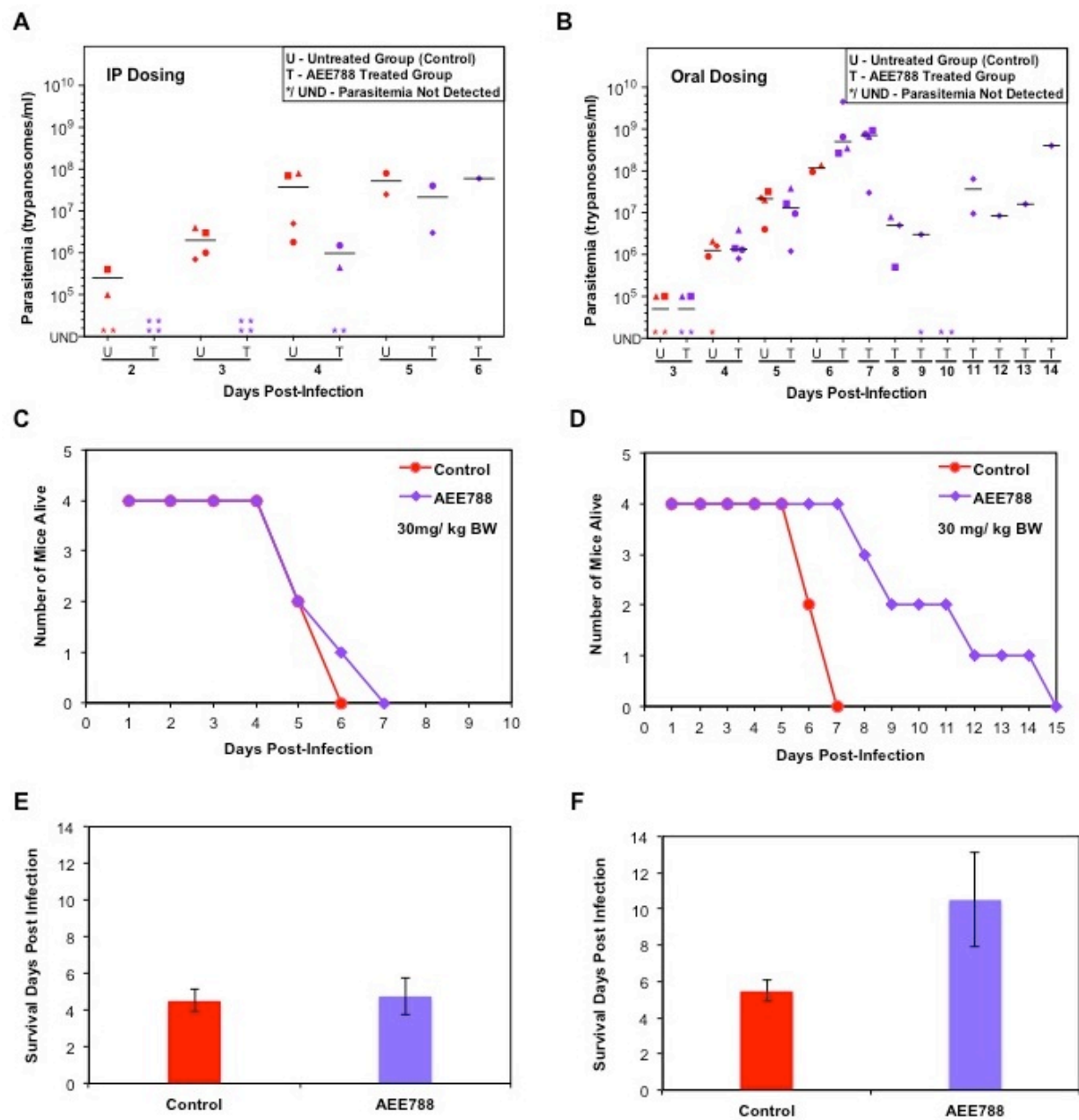
Figure 4.6

References

1.   Barrett, M.P., et al., *Human African trypanosomiasis: pharmacological re-engagement with a neglected disease.* British Journal of Pharmacology, 2007. **152**(8): p. 1155-1171.

2.   Kennedy, P.G., *Human African trypanosomiasis of the CNS: current issues and challenges.* J Clin Invest, 2004. **113**(4): p. 496-504.

3.   Simarro, P.P., J. Jannin, and P. Cattand, *Eliminating human African trypanosomiasis: where do we stand and what comes next?* PLoS Med, 2008. **5**(2): p. e55.

4.   O'Connell, D., *Neglected Diseases.* Nature, 2007. **449**(7159): p. 157-157.

5.   Yamey, G. and P. Hotez, *Neglected tropical diseases.* Br Med J, 2007. **335**(7614): p. 269-70.

6.   Parsons, M., et al., *Trypanosoma congolense: developmental regulation of protein kinases and tyrosine phosphorylation during the life cycle.* Exp Parasitol, 1995. **80**(3): p. 507-14.

7.   Wheeler-Alm, E. and S.Z. Shapiro, *Glycosome-associated tyrosine-phosphorylated protein in Trypanosoma brucei.* Trop Med Parasitol, 1993. **44**(4): p. 281-4.

8.   Nett, I.R., et al., *The phosphoproteome of bloodstream form Trypanosoma brucei, causative agent of African sleeping sickness.* Mol Cell Proteomics, 2009. **8**(7): p. 1527-38.

9.   Subramanya, S. and K. Mensa-Wilmot, *Diacylglycerol-stimulated endocytosis of transferrin in trypanosomatids is dependent on tyrosine kinase activity.* PLoS One, 2010. **5**(1): p. e8538.

10.   Ellis, A.G., et al., *Preclinical analysis of the analinoquinazoline AG1478, a specific small molecule inhibitor of EGF receptor tyrosine kinase.* Biochem Pharmacol, 2006. **71**(10): p. 1422-34.

11.   Levitzki, A. and A. Gazit, *Tyrosine kinase inhibition: an approach to drug development.* Science, 1995. **267**(5205): p. 1782-8.

12.   Levitzki, A. and E. Mishani, *Tyrphostins and other tyrosine kinase inhibitors.* Annu Rev Biochem, 2006. **75**: p. 93-109.

13.   Katiyar, S., et al., *Lapatinib-binding protein kinases in the african trypanosome: identification of cellular targets for kinase-directed chemical scaffolds.* PLoS One, 2013. **8**(2): p. e56150.

14.   Tiseo, M., M. Loprevite, and A. Ardizzoni, *Epidermal growth factor receptor inhibitors: a new prospective in the treatment of lung cancer.* Curr Med Chem Anticancer Agents, 2004. **4**(2): p. 139-48.

15.   Cockerill, G.S. and K.E. Lackey, *Small molecule inhibitors of the class 1 receptor tyrosine kinase family.* Curr Top Med Chem, 2002. **2**(9): p. 1001-10.

16.   Reardon, D.A., et al., *Phase I study of AEE788, a novel multitarget inhibitor of ErbB- and VEGF-receptor-family tyrosine kinases, in recurrent glioblastoma patients.* Cancer chemotherapy and pharmacology, 2012. **69**(6): p. 1507-18.

17.   Campos, S., et al., *Multicenter, randomized phase II trial of oral CI-1033 for previously treated advanced ovarian cancer.* Journal of clinical oncology : official journal of the American Society of Clinical Oncology, 2005. **23**(24): p. 5597-604.

18.   Hirumi, H., J.J. Doyle, and K. Hirumi, *African trypanosomes: cultivation of animal-infective Trypanosoma brucei in vitro.* Science, 1977. **196**(4293): p. 992-4.

19.   Hirumi, H. and K. Hirumi, *In vitro cultivation of Trypanosoma congolense bloodstream forms in the absence of feeder cell layers.* Parasitology, 1991. **102 Pt 2**: p. 225-36.

20.   Patel, G., Karver, CE., Behera,R., Guyett, P., Sullenberger, C., Edwards, P., Roncal, NE., Mensa-Wilmot, K., Pollastri, MP., *Kinase scaffold repurposing for neglected disease drug discovery: Discovery of an efficacious, lapatanib-derived lead compound for trypanosomiasis.* J Med Chem, 2013.

21.   Xia, W., et al., *Anti-tumor activity of GW572016: a dual tyrosine kinase inhibitor blocks EGF activation of EGFR/erbB2 and downstream Erk1/2 and AKT pathways.* Oncogene, 2002. **21**(41): p. 6255-63.

22.   Christensen, J.G., et al., *Plasma vascular endothelial growth factor and interleukin-8 as biomarkers of antitumor efficacy of a prototypical erbB family tyrosine kinase inhibitor.* Molecular cancer therapeutics, 2005. **4**(6): p. 938-47.

23.   Nyati, M.K., et al., *Radiosensitization by pan ErbB inhibitor CI-1033 in vitro and in vivo.* Clinical cancer research : an official journal of the American Association for Cancer Research, 2004. **10**(2): p. 691-700.

24.   Rusnak, D.W., et al., *The effects of the novel, reversible epidermal growth factor receptor/ErbB-2 tyrosine kinase inhibitor, GW2016, on the growth of human normal and tumor-derived cell lines in vitro and in vivo.* Mol Cancer Ther, 2001. **1**(2): p. 85-94.

25.   Traxler, P., et al., *AEE788: a dual family epidermal growth factor receptor/ErbB2 and vascular endothelial growth factor receptor tyrosine kinase inhibitor with antitumor and antiangiogenic activity.* Cancer research, 2004. **64**(14): p. 4931-41.

26.   Fairlamb, A.H., *Future prospects for the chemotherapy of human trypanosomiasis. 1. Novel approaches to the chemotherapy of trypanosomiasis.* Trans R Soc Trop Med Hyg, 1990. **84**(5): p. 613-7.

CHAPTER V

CONCLUSION AND FUTURE DIRECTION

Human African trypanosomiasis (HAT) is a life-threatening neglected tropical disease caused by *Trypanosoma brucei* [1, 2]. Drugs available for treatment of HAT are toxic and given parenterally [3-5]; safer orally active drugs are immediately needed. To foster drug discovery process, it is valuable to study essential pathways in *T. brucei* that can be exploited for chemotherapy.

Phosphotyrosine signaling in trypanosomes is divergent; mammalian type receptor tyrosine kinases and phosphotyrosine binding domains (*e.g.* SH2 and PTB) are absent in the genome [6]. Tyrosine phosphorylated proteins are detected by western blotting and mass spectrometry analysis [7-9]. It is therefore implicated that tyrosine phosphorylation might be carried out by dual specificity kinases in the parasite. Tyrosine kinase activity regulates transferrin endocytosis, a mechanism for internalization of extracellular iron, in bloodstream form *T. brucei* [10]. Further, Tyrphostin A47, a tyrosine kinase inhibitor, reduces transferrin endocytosis and kills the parasite [10]. It can be inferred from this data that phosphotyrosine signaling is essential for trypanosomes, and the pathway can be targeted for drug intervention. The tools and techniques for studying this pathway in trypanosomes are not optimized yet.

We hereby report the use of a chemical biology strategy to investigate phosphotyrosine signaling in bloodstream *T. brucei*. In the search for anti-trypanosomal tyrosine kinase inhibitors, we recognized the potential of 4-anilinoquinazoline scaffold that we further optimized in a

138

structure-activity relationship study. Finally, we tested several potent tyrosine kinase inhibitors in a mouse model of acute human African trypanosomiasis.

4-Anilinoquinazoline drugs are in clinical use for cancer (*e.g.* lapatinib, gefitinib, erlotinib) **[11-15]**. To begin with, we performed a "focused screen" of ten 4-anilinoquinazoline derivatives against *T. brucei* and observed that the compounds inhibited growth at low micromolar concentration. GW572016 (lapatinib) had a GI_{50} (the concentration that inhibits parasite growth by 50%) of 1.5 μM and was selectively toxic against *T. brucei* in comparison to human HeLa cells.

We used GW572016 as a chemical tool and found that the drug inhibited tyrosine phosphorylation of select trypanosome proteins. Recent work in our lab has identified four GW572016 binding protein kinases (TbLBPK1-4) as possible targets **[16]**. The pathways downstream of these kinases are unknown. One possible way of discovering these pathways is by looking into potential effector proteins as those whose apparent tyrosine phosphorylation was inhibited by GW572016. By adapting an affinity chromatography /mass spectrometry approach we identified 39 effector proteins. Predicted functions of these proteins include (i) cytoskeleton (*e.g.* tubulin), (ii) cell morphology and flagellum biogenesis (*e.g.* PFR-1/PFR-C), (iii) endocytosis (*e.g.* actin A), (iv) glycolysis (*e.g.* phosphofructokinase) and (v) protein synthesis (*e.g.* ribosomal protein S7). We further investigated the effects of GW572016 on three pathways, namely cell morphology, flagellum biogenesis, and endocytosis.

When incubated with the drug, the morphology of trypanosomes changed from "long slender" to "round". *T. brucei* is a polarized cell and the shape is maintained with the assistance of subpellicular microtubules. We therefore studied the effect of GW572016 on cellular distribution of tubulins by fluorescence microscopy. The localization of β-tubulin changed from

the area between the nucleus and the kinetoplast in untreated cells to the cell periphery in round trypanosomes. The distribution pattern of α-tubulin remained unaltered. Tyrosinated α-tubulin is normally present in the basal body, emergent flagellum, and at the cell posterior. In GW572016-treated cells, tyrosinated α-tubulin was found throughout the cytoplasm. Related data were obtained for the paraflagellar rod (PFR); it was localized at the periphery of round cells instead of spanning the length of the flagellum. Scanning electron microscopy revealed that the flagellum is retracted into the round cell body. We conclude that the phosphotyrosine signaling regulate at least (i) trypanosome morphology, (ii) flagellum topology, (iii) distribution of tyrosinated α-tubulin, and (iv) localization of β-tubulin *in vivo*.

A "piggy back" drug discovery strategy **[27]** employs clinically proven drugs for testing against other diseases. Such an alternative approach could be useful to expedite drug discovery against neglected diseases. From the focused screen mentioned above, we realized that 4-anilinoquinazoline is a promising scaffold for antitrypanosome drug discovery. Nine compounds used in an initial screen displayed a 10 fold range of potency in terms of GI_{50} in trypanosomes. Inspired by this data we designed a project (in collaboration with medicinal chemists) to further optimize the 4-anilinoquinazoline scaffold against trypanosome replication. This study led to the discovery of several 4-anilinoquinazolines with low nanomolar GI_{50} profile (< 200 nM) against *T. brucei*.

Finally, we tested therapeutic potential of three 4-anilinoquinazolines (GW572016, CI-1033, and NEU617) **[17, 18]** and one pyrrolopyrimidine derivative (AEE788) **[19]** in an animal model of acute human African trypanosomiasis. The compounds were administered by two routes (oral and intraperitoneal) in separate experiments. It was observed that drug treatment, in all cases, controlled the infection and extended the mean survival of mice as compared to the

control mice. Both GW572016 and AEE788 gave better results when administered by the oral route. However, with NEU617, the intraperitoneal route was more efficacious. A similar effect irrespective of the dosing route was noticed with CI-1033. This study showed that both 4-anilinoquinazoline and pyrrolopyrimidine are promising scaffolds that can be optimized as orally active antitrypanosome lead drugs in a lead optimization campaign.

The current work addresses two independent but related aspect of research on trypanosomes; first, a chemical tool driven exploration of *T. brucei* biology; and second, a drug discovery initiative for identification of potential leads. Considering the fact that phosphotyrosine signaling is not well explored in any trypanosomatid, our findings provide a foundation for further investigation. Recent work in our lab has already reported kinases which could be potentially mediating tyrosine phosphorylation in *T. brucei* [16]. However, the substrates of these kinases are unknown. Further, biochemical characterization [20, 21] and genetic validation experiments [22, 23] are needed to reveal the real potential of these kinases as drug targets. Depending on how essential these kinases are in the phosphotyrosine signaling pathway, structure based inhibitors can be designed to improve selectivity and potency. Following upon the target kinases, we identified the potential downstream effector proteins and their associated cellular pathways. Subsequently, we can test which of these candidate proteins are in fact tyrosine-phosphorylated. To figure out this, an affinity chromatography/ mass-spectrometry experiment can be designed after phosphotyrosine enrichment (phosphotyrosine proteins are low abundant) [24]. The drug discovery project can be expanded in future by testing 4-anilinoquinazoline class of compounds in animal models of late stage *T. brucei* disease [25, 26]. Also, the study of pharmacokinetics of these drugs will provide an insight of their availability after oral administration, rate of elimination, and central nervous system (CNS)

exposure, which will be important for control of "late stage" disease. This will help to develop a

safe and effective dosing concentration, and reduce toxicity issues.

References

1.   Hotez, P.J., et al., *Control of neglected tropical diseases.* The New England journal of medicine, 2007. 357(10): p. 1018-27.

2.   O'Connell, D., *Neglected Diseases.* Nature, 2007. 449(7159): p. 157-157.

3.   Burchmore, R.J., et al., *Chemotherapy of human African trypanosomiasis.* Curr Pharm Des, 2002. 8(4): p. 256-67.

4.   Docampo, R. and S.N. Moreno, *Current chemotherapy of human African trypanosomiasis.* Parasitol Res, 2003. 90 Supp 1: p. S10-3.

5.   Fairlamb, A.H., *Chemotherapy of human African trypanosomiasis: current and future prospects.* Trends Parasitol, 2003. 19(11): p. 488-94.

6.   Parsons, M., et al., *Comparative analysis of the kinomes of three pathogenic trypanosomatids: Leishmania major, Trypanosoma brucei and Trypanosoma cruzi.* BMC Genomics, 2005. 6: p. 127.

7.   Parsons, M., et al., *Trypanosoma congolense: developmental regulation of protein kinases and tyrosine phosphorylation during the life cycle.* Exp Parasitol, 1995. 80(3): p. 507-14.

8.   Wheeler-Alm, E. and S.Z. Shapiro, *Evidence of tyrosine kinase activity in the protozoan parasite Trypanosoma brucei.* J Protozool, 1992. 39(3): p. 413-6.

9.   Nett, I.R.E., et al., *Identification and Specific Localization of Tyrosine-Phosphorylated Proteins in Trypanosoma brucei.* Eukaryotic Cell, 2009. 8(4): p. 617-626.

10.   Subramanya, S. and K. Mensa-Wilmot, *Diacylglycerol-stimulated endocytosis of transferrin in trypanosomatids is dependent on tyrosine kinase activity.* PLoS One, 2010. 5(1): p. e8538.

11.   Tiseo, M., M. Loprevite, and A. Ardizzoni, *Epidermal growth factor receptor inhibitors: a new prospective in the treatment of lung cancer.* Curr Med Chem Anticancer Agents, 2004. 4(2): p. 139-48.

12.   Cockerill, G.S. and K.E. Lackey, *Small molecule inhibitors of the class 1 receptor tyrosine kinase family.* Curr Top Med Chem, 2002. 2(9): p. 1001-10.

13.   Cohen, M.H., et al., *FDA drug approval summary: Erlotinib (Tarceva (R)) tablets.* Oncologist, 2005. 10(7): p. 461-466.

14. Cohen, M.H., et al., *FDA drug approval summary: Gefitinib (ZD1839) (Iressa (R)) tablets.* Oncologist, 2003. 8(4): p. 303-306.

15. Lackey, K.E., *Lessons from the drug discovery of lapatinib, a dual ErbB1/2 tyrosine kinase inhibitor.* Curr Top Med Chem, 2006. 6(5): p. 435-60.

16. Katiyar, S., et al., *Lapatinib-binding protein kinases in the african trypanosome: identification of cellular targets for kinase-directed chemical scaffolds.* PLoS One, 2013. 8(2): p. e56150.

17. Nyati, M.K., et al., *Radiosensitization by pan ErbB inhibitor CI-1033 in vitro and in vivo.* Clinical cancer research : an official journal of the American Association for Cancer Research, 2004. 10(2): p. 691-700.

18. Campos, S., et al., *Multicenter, randomized phase II trial of oral CI-1033 for previously treated advanced ovarian cancer.* Journal of clinical oncology : official journal of the American Society of Clinical Oncology, 2005. 23(24): p. 5597-604.

19. Traxler, P., et al., *AEE788: a dual family epidermal growth factor receptor/ErbB2 and vascular endothelial growth factor receptor tyrosine kinase inhibitor with antitumor and antiangiogenic activity.* Cancer research, 2004. 64(14): p. 4931-41.

20. de Souza Leite, M., et al., *Trypanosoma brucei brucei: biochemical characterization of ecto-nucleoside triphosphate diphosphohydrolase activities.* Exp Parasitol, 2007. 115(4): p. 315-23.

21. Das, A., et al., *Biochemical characterization of Trypanosoma brucei RNA polymerase II.* Molecular and Biochemical Parasitology, 2006. 150(2): p. 201-210.

22. Caceres, A.J., P.A.M. Michels, and V. Hannaert, *Genetic validation of aldolase and glyceraldehyde-3-phosphate dehydrogenase as drug targets in Trypanosoma brucei.* Molecular and Biochemical Parasitology, 2010. 169(1): p. 50-54.

23. Gupta, S., et al., *Glucose-6-phosphate dehydrogenase of trypanosomatids: characterization, target validation, and drug discovery.* Mol Biol Int, 2011. 2011: p. 135701.

24. Rush, J., et al., *Immunoaffinity profiling of tyrosine phosphorylation in cancer cells.* Nature Biotechnology, 2005. 23(1): p. 94-101.

25. Jacobs, R.T., et al., *SCYX-7158, an orally-active benzoxaborole for the treatment of stage 2 human African trypanosomiasis.* Plos Neglected Tropical Diseases, 2011. 5(6).

26. Nare, B., et al., *Discovery of novel orally bioavailable oxaborole 6-carboxamides that demonstrate cure in a murine model of late-stage central nervous system African trypanosomiasis.* Antimicrobial Agents and Chemotherapy, 2010. 54(10): p. 4379-4388.

27. Nwaka, S. et al., *Innovative lead discovery strategies for tropical diseases.* Nature

Review Drug Discovery, 2006. 5. p 941-955.